REGIONAL GEOLOGY AND GROUNDWATER CONTROLS OF NATURAL SLOPE STABILITY

by

P.B. Fransham
B.Sc. (Sir George Williams) 1971
M.Sc. (McGill University) 1973

A thesis submitted to
the Faculty of Graduate Studies and Research
in partial fulfillment
of the requirements of the degree of
Doctor of Philosophy
(Civil Engineering)

Department of Civil Engineering and Applied Mechanics
McGill University
Montreal, Canada

October, 1978

REGIONAL GEOLOGY AND GROUNDWATER CONTROLS OF NATURAL SLOPE STABILITY

ABSTRACT

A study into the geological and groundwater controls of sensitive clay slope stability in the Ottawa Valley was carried out with the objective of establishing a field orientated method for regional slope stability mapping of sensitive clays. The research program consisted of a field, laboratory and numerical study of the regional geology, stratigraphy, mechanical behaviour and groundwater regime.

Stability calculations were performed on forty-six different site geologies using pore pressure distributions obtained from finite element simulations. A series of graphs show the effect of the degree of slope submergence, of the depth to bedrock, of the nature of the surficial layer, of a lower piezometric level in the bedrock, and of the number of soil layers on the calculated factor of safety. These graphs show that the factor of safety can vary by as much as 60 percent depending on the site geology.

Peter B. Fransham
Ph.D. Thesis
Department of Civil Engineering

RÉSUMÉ

Une étude des contrôles géologiques et de l'eau souterraine sur la stabilité des pentes d'argile sensible dans la Vallée de l'Outaouais a été entreprise dans le but d'établir une méthode d'identification sur terrain de la stabilité des pentes à l'échelle régionale. Le programme de recherche a consisté à observer sur terrain, en laboratoire et par analyse numérique la géologie régionale, la stratigraphie, le comportement mécanique et l'eau souterraine.

Des facteurs de stabilité ont été calculés pour quarante-six pentes de géologie différente en utilisant les différentes pressions interstielles obtenues par la méthode d'éléments finis. Une série de diagrammes sont présentés; ceux-ci montrent l'effet du pourcentage de la pente qui est inondée, de la profondeur du banc rocheux, de la composition de la couche superficielle, du niveau piézomètre qui est bas dans le banc rocheux et du nombre des couches de sol sur le facteur de sécurité qui est obtenu. Ces diagrammes démontrent que le facteur de sécurité peut varier par autant que 60 pour cent dépendant de la géologie locale.

PREFACE

The following are the principal accomplishments of the thesis and what may be considered as original contributions to the understanding of sensitive clay slope instability.

1) The thesis topic in itself is somewhat original in that it is an application of geological and geotechnical science to the problem of predicting slope instability in sensitive clays.

2) The results of the field and laboratory investigation into the behaviour of the sensitive clay yielded some interesting results. On the basis of samples from two borings, separated by a hundred meters, it would appear that the sensitive clay behaviour is essentially independent of the stratigraphy and is controlled largely by the effective overburden stresses. While further research is required to prove or disprove this finding, it can be considered as a working hypothesis for the present time.

3) The bedrock control of the groundwater regime in the Ottawa Valley has been common knowledge to area geotechnical engineers. However, the fact that the flow regime is different in the massive gneisses than in the fractured limestones has been identified in this research.

4) This thesis represents the first time that a transient finite element model has been applied to clay slopes of the Ottawa Valley. The results of the modelling indicate that the finite element method can be successfully used to predict pore pressure distributions.

5) The finite element method was also used to show how the geology influences the pore pressure distribution. While a similar study has already dealt with the Rocky Mountains, this is the first time that such a study has been concluded for the Ottawa Valley.

6) A series of graphs were produced which show the influence of the geology and groundwater on the stability of natural sensitive clay slopes. These graphs have led to the development of a slope stability mapping method that can be applied to sensitive clay slopes in the Ottawa Valley. By using the above mentioned graphs and surficial geology maps, it is now possible to estimate in the field the factor of safety of natural sensitive clay slopes within 10 to 15%.

Most of the research for this thesis was carried out while the author was employed by the Geological Survey of Canada. The information was collected under project number 740052. The project was given the cooperation of other government agencies and personnel too numerous to mention here. I would like to thank the Geological Survey for the opportunity to complete this thesis and my colleagues N.R. Gadd and D. Proudfoot for their assistance in the fields of stratigraphic interpretation and computer methods respectively. All of the drilling was carried out by the Department of Public Works. Furthermore, all of the soil testing was performed by the technical staff of DPW under the author's supervision and direction. The computer facilities at the Department of Energy, Mines and Resources were used for the finite element and slope stability analyses.

I would also like to thank Dr. R.N. Yong for his assistance during my years at McGill University and the Geological Survey. Finally, I would like to thank my wife Lise for the hours that she spent drafting, typing and proofreading the manuscript.

TABLE OF CONTENTS

	Page
ABSTRACT	ii
RESUME	iii
PREFACE	iv
TABLE OF CONTENTS	vi
LIST OF FIGURES	x
LIST OF PLATES	xiv
LIST OF TABLES	xv
LIST OF SYMBOLS	xvi
1 - INTRODUCTION AND PROBLEM STATEMENT	
1.1 Definition of the Problem	1
1.2 Objectives and Scope	4
1.3 Literature Review	9
1.3a Geology and Stratigraphy of Sensitive Clays	9
1.3b Groundwater Movement in Sensitive Clay Slopes	11
1.3c Slope Stability and Mechanical Properties	13
2 - GEOLOGY AND STRATIGRAPHY OF SENSITIVE CLAYS	
2.1 Introduction	16
2.2 Distribution of Sensitive Clays	17
2.3 Stratigraphy of Sensitive Clays	20
2.3a Varved Clay	22
2.3b Deepwater Marine Facies	24
2.3c Prograding Delta Facies	26
2.3d Shoaling Prograding Delta Facies	28
2.3e Fluvial Sand	30

		Page
2.4	Summary of Index Property Tests	30
2.5	Geological History of the Ottawa Valley	34
2.6	Summary	37
3 -	MECHANICAL AND CHEMICAL PROPERTIES	
3.1	Introduction	39
3.2	Undrained Strength Tests	43
3.3	Consolidation Behaviour	46
3.4	Triaxial Testing	52
3.5	Chemistry and Mineralogy of Sensitive Clay Deposits	60
3.6	Summary	66
4 -	GROUNDWATER INVESTIGATIONS	
4.1	General	69
4.2	Field Investigation	71
4.2a	Site Locations	71
4.2b	Intrumentation	78
4.3	Results of Field Monitoring of Pore Pressures	80
4.3a	Site P1	80
4.3b	Site P2	85
4.3c	Site P3	88
4.4	Numerical Analysis of Groundwater Flow	92
4.4a	Equations of Saturated and Unsaturated Flow	92
4.4b	Finite Element Formulation	100
4.4c	Climatic Conditions	110
4.4d	Saturated-Unsaturated Hydraulic Conductivities	114

		Page
4.5	Calibration of the Finite Element Method	121
4.6	Finite Element Modelling of Slopes	133
4.6a	General	133
4.6b	Depth to Bedrock	137
4.6c	Number of Soil Layers	144
4.6d	Depth of Submergence	146
4.6e	Bedrock Sink Term	152
4.6f	Nature of the Surficial Layer	156
4.7	Summary and Conclusions	158
5 -	SLOPE STABILITY OF SENSITIVE CLAY SLOPES	
5.1	General	162
5.2	Slope Stability Theory	162
5.3	Stability Calculations	169
5.4	Results of Stability Analyses	172
5.4a	General	172
5.4b	Depth of Submergence	174
5.4c	Depth to Bedrock	177
5.4d	Number of Soil Layers	182
5.4e	Bedrock Sink Term	184
5.4f	Nature of the Surficial Layer	186
5.4g	Proposed Stability Mapping Method	187
5.5	Verification of Stability Mapping Method	189
5.6	Summary	196
6 -	SUMMARY AND CONCLUSIONS	
6.1	General	199
6.2	Geology and Stratigraphy	200
6.3	Mechanical Behaviour	200
6.4	Groundwater Investigations	202
6.5	Stability Calculations	205
6.6	Recommendations for Further Research	207

		Page
REFERENCES		209
VOLUME 2		
APPENDIX A	SUMMARY OF LABORATORY TEST DATA	A-1 to A-27
APPENDIX B	PIEZOMETER INSTALLATION PROCEDURES	B-1 to B-6
APPENDIX C	COMPLETION OF FINITE ELEMENT FORMULATION	C-1 to C-5
APPENDIX D	STATISTICS FROM FINITE ELEMENT ANALYSES	D-1 to D-145
APPENDIX E	FLOW NETS AND CRITICAL CIRCLES FOR FORTY-SIX MODELS	E-1 to E-49

LIST OF FIGURES

Figure		Page
1.1	Stable vs failed slopes in marine clay	2
1.2	Flow chart of thesis organization	6
1.3	Neoclassical groundwater flow	12
2.1	Distribution of sensitive clays and associated landslides	18
2.2	Air photograph of landslide scars in the banks of an abandoned river channel	19
2.3	Stratigraphic column	21
3.1	Location of borehole 76-1	41
3.2	Site profile and borehole locations	42
3.3	Geotechnical profile - borehcle 76-1-1	44
3.4	Geotechnical profile - borehole 76-1-2	45
3.5	Consolidation results - borehole 76-1-1	48
3.6	Consolidation results - borehole 76-1-2	49
3.7	Geochemical data - borehole 76-1-2	64
4.1	Flow diagram for chapter 4	72
4.2	Two typical slope sections	74
4.3	Location of instrumented slopes	75
4.4a	Site P1 - profile & mean heads	76
4.4b	Site P2 - profile & mean heads	77
4.4c	Site P3 - profile & mean heads	79
4.5	Piezometer design	81
4.6	Pore pressure vs depth - site P1	84
4.7	Pore pressure vs depth - site P2	86

Figure		Page
4.8	Pore pressure vs depth - site P3	90
4.9	Location map & pore pressure vs depth data for Hull site	91
4.10	Flow through a soil element	94
4.11	(a) Pressure head variation with moisture content; and (b) Hydraulic conductivity versus moisture content.	99
4.12	A - Triangular element B - Flow region associated with node n	104
4.13	Surface pressure head vs relative humidity	112
4.14	Unsaturated hydraulic conductivity vs moisture content	118
4.15	Pressure head vs moisture content	120
4.16	Mesh and boundary conditions for site P1	123
4.17	Comparison of measured and calculated pressure heads; site P1; crest	126
4.18	Comparison of measured and calculated pressure heads; site P1; mid-slope	127
4.19	Comparison of measured and calculated pressure heads; site P1; toe	128
4.20	Regression analysis of calculated and measured pressure heads	132
4.21	Finite element mesh	135
4.22	Pressure head vs depth; crest - no submergence; sand at surface	139
4.23	Pressure head vs depth; toe - no submergence; sand at surface	140
4.24	Pressure head vs depth; crest - no submergence; clay at surface	141

Figure		Page
4.25	Pressure head vs depth; toe - no submergence; clay at surface	142
4.26	Pressure head vs depth; crest; no submergence; bedrock elevation: 5 meters; sand at surface	147
4.27	Pressure head vs depth; toe; no submergence; bedrock elevation: 5 meters; sand at surface	148
4.28	Pressure head vs depth; crest; model A; bedrock elevation: 5 meters; sand at surface	150
4.29	Pressure head vs depth; toe; model A; bedrock elevation: 5 meters; sand at surface	151
4.30	Pressure head vs depth; crest; models G & H; bedrock elevation: 5 meters; sand at surface	154
4.31	Pressure head vs depth; toe; models G & H; bedrock elevation: 5 meters; sand at surface	155
5.1	Forces acting for the method of slices applied to a circular and composite sliding surface	165
5.2	Location of trial circle centres and elevations at which radii are tangent	170
5.3	Factor of safety vs % of slope submerged	175
5.4	Factor of safety vs depth to bedrock for different depths of submergence; sand at surface	178
5.5	Factor of safety vs depth to bedrock for different depths of submergence; clay at surface	179
5.6	Factor of safety vs no. of soil layers for different depths of submergence	183

Figure		Page
5.7	Factor of safety vs % of slope submerged and bedrock sink term	185
5.8	Failed vs unfailed slopes in relation to a factor of safety of 1.0	188
5.9	Profile of South Nation River	191
5.10	Factor of safety vs ru parameter	195

LIST OF PLATES

Plate		Page
2.1	Varved clay	23
2.2	Close-up of varved clay	23
2.3	Deepwater marine clay	25
2.4	Close-up of the above plate showing an ice rafted pebble and the characteristic black mottling	25
2.5	Prodelta clay	27
2.6	Close-up of prodelta clay showing black mottling and the red-grey banding	27
2.7	Shoaling prograding delta clay	29
2.8	Close-up of section of core shown in plate 2.7	29
2.9	Fluvial sand	31

LIST OF TABLES

Table		Page
2.1	Summary of mean index property tests for all four soil units	32
4.1	Summary of piezometer monitoring, Hammond, site P1	83
4.2	Summary of piezometer monitoring, Casselman, site P2	87
4.3	Climatic data and moisture balance for Ottawa	115
4.4	Hydraulic conductivities for the different soil layers	117
4.5	Combination of geological factors modelled.	136
5.1	Summary of factors of safety for different geological settings	173
5.2	Recommended minimum values of static factor of safety	194

LIST OF SYMBOLS

* Symbols used for slope stability equations.

$A(\psi)$		quasilinear operator
b		geometric coefficient
	*	breadth of slice
C		quasilinear operator
c		geometric coefficient
c'	*	cohesion
$c(\psi)$		specific moisture capacity
E_L, E_R	*	resultant of the total horizontal forces on the left and right sides of the n-th slice
e		element number
F	*	factor of safety
f	*	perpendicular offset of the normal force from the centre of rotation
h		total head
	*	height of slice
i		1, 2, 3 reference to Cartesian coordinate
K_i		hydraulic conductivity
K_{ij}		hydraulic conductivity tensor
K^r		relative hydraulic conductivity
M		molecular weight (equation 4.39)
		mass storage
M_{in}		mass input
M_{out}		mass output
m		series of points; i.e. m = 1,2,3...N

N		number of nodal points
n		series of points; i.e. n = 1,2,3...N
p		water pressure
	*	total normal stress
p'	*	effective normal stress
Q_L, Q_R	*	resultants of the horizontal and vertical forces on the left and right hand sides of the n-th slice
R		residual
		universal gas constant (equation 4.39)
	*	radius
r		relative humidity
S		sink term used to simulate uptake of water by plants
	*	shear strength
S_m	*	shear strength mobilized
S_s		specific storage
S_ω		degree of saturation
T		temperature
t		time
u	*	pore pressure
V_{x_i}		flow velocity
V		flow region
V_n		flow region associated with element n
W	*	weight of the slice
W_i		weighting function
X_L, X_R	*	resultants of the vertical shear forces on the left and right sides of the n-th slice
x	*	horizontal distance of the slice from the centre of rotation
x_i		vector of Cartesian coordinate

β		unity in saturated zone; zero in unsaturated zone
θ		volumetric moisture content
ϕ'	*	angle of internal friction
ϕ_m		angle of internal friction mobilized
ψ		pressure head
ψ_s		minimum pressure head at surface
δ		Kronecker's delta
ξ		linear independent coordinate functions
Γ^e		prescribed flux boundary
η		porosity
γ	*	unit weight of water
σ_n	*	total normal stress
ℓ		corners of triangle
	*	length of arc along the base of a slice
α		average angle between the tangent to the base of the slice and the horizontal
Δ		area of triangle

1 - INTRODUCTION AND PROBLEM STATEMENT

1.1 Definition of the Problem

Portions of the Ottawa - St. Lawrence - Lac St. Jean lowlands are covered with a layer of sensitive marine clay and these marine clays are particularly susceptible to slope failures. Many cases of unpredicted instability can be found in the literature (see Mitchell and Markell, 1974) and illustrate the magnitude of the problem. Recognition of the potential for instability in sensitive clay slopes has prompted all levels of government to attempt to map on a regional basis the stability of sensitive clay slopes and restrict development in those regions where the risk of failure is high.

There have been essentially two approaches to stability mapping. The first is based on a simple slope height-slope angle relationship. The geometry of a number of failed and unfailed slopes are plotted on an inclination-height diagram and a line separating the failed and unfailed slopes is drawn. Figure 1.1 is an example of one such study and indicates readily the limitation of the method. Of the eleven apparently stable slopes, three have a slope geometry that lies above the line. Zoning restrictions are based on whether or not a slope is stable. If by virtue of the height-inclination diagram, a slope is deemed unstable, a set-back distance is determined from a method proposed by Mitchell and Markell (1974). However, in actual fact, a slope may be stable even though it is above the line in figure 1.1 and undue restrictions may be placed on the land; thus its full potential is not realized.

FIG 1.1 STABLE vs FAILED SLOPES IN MARINE CLAY

(After Wong,1975)

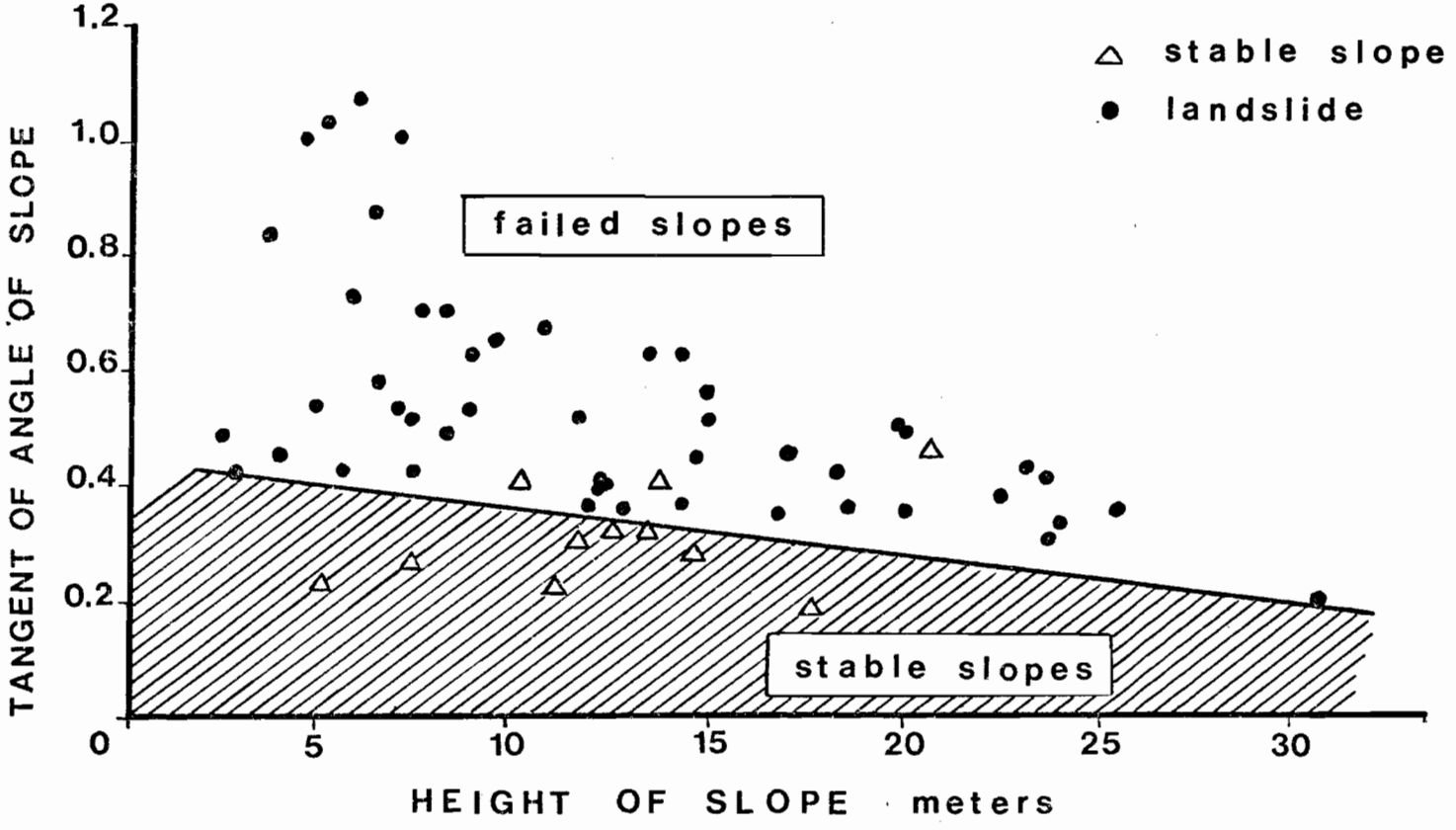

NOTE
number of stable slopes plotted : 11

The second approach has been to survey the slopes in a given area, assume a set of strength parameters and groundwater conditions, and then perform stability analyses using an appropriate stability model (Klugman and Chung, 1976). The problem with this method is that it does not take into account the regional variation in geology, strength parameters and groundwater conditions. Therefore, factors of safety less than one are commonly obtained for stable slopes. Slopes have been classified according to their factor of safety and guidelines given for the scope of the geotechnical investigation that would be required before any construction takes place. There are two main problems associated with a study of this nature. The first is that engineers are likely to be skeptical of the reliability of the safety factor since certain slopes are standing with factors of safety less than one. Secondly, detailed geotechnical investigations may be unnecessarily performed on certain slopes, thereby increasing the cost of the proposed project.

Although these two approaches to regional slope stability mapping do yield a general impression of the relative stability of slopes, they do lack the accuracy that is needed for rational land-use planning. However, these methods will continue to be used due to the general low cost of the investigation. Most project budgets would not allow for the drilling, sampling, testing and analyses that would be required if a detailed slope stability analysis were to be performed on every slope.

The question therefore arises as to how to combine the accuracy of a detailed analysis with the simplicity and low cost of the above mentioned approaches. The answer lies

partially in another question: what factors are required for a stability analysis and how can they be mapped on a regional scale? Duncan and Buchignani (1975) have outlined the requirements for a detailed stability analysis as being: site geology; strength parameters for each of the soil layers; and an estimate of the pore pressures along a potential failure plane. Peck (1975) and La Rochelle (1975) have stated that an understanding of the local and regional geomorphology is a prerequisite to a stability analysis. Techniques for mapping the distribution of the different soil layers and their stratigraphy have been well established by the geological profession. Mapping of the strength parameters and groundwater regime is generally more complex due to the three dimensional nature of the problem. Undrained shear strength varies depending on the nature of the surficial layer, the thickness of the dessicated crust and the geologic history. Pore pressures have been shown to depend on the permeability contrasts between the various soil layers (Hodge and Freeze, 1977); therefore, mapping of pore pressure distributions are dependent on the local and regional geology. Variations in strength parameters and groundwater conditions can be accounted for by using a probabilistic approach to slope stability (Alonso, 1976; Yong et al., 1977). But, on a regional scale, the limits and nature of the strength-groundwater variations must be established before a risk analysis can be performed with any degree of confidence.

1.2 Objectives and Scope

The objective of this thesis is to establish a rational approach to regional slope stability mapping. In the previous section, it was shown that the stability of

natural slopes is dependent on: the site geology; the strength parameters for the component soils; and the prevailing groundwater conditions. The thesis will therefore investigate on a regional scale the interrelationships between these factors and establish the geologic and groundwater controls of slope stability. In the final analysis, this thesis will provide the engineer with the geologic base on which judgements regarding the stability of sensitive clay slopes can be made. To achieve the stated objective, a four-part research program was initiated, consisting of: 1) a field, office, and literature study of the regional geology and stratigraphy; 2) a field and laboratory investigation of the physical, mechanical, and porewater chemistry of the sensitive clays; 3) a field and numerical study of the regional and local groundwater regime; and 4) stability analyses of slopes of different geology and pore pressure conditions. Figure 1.2 shows the overall organization of the thesis, the components of each of the four parts, and the relationship of each part to the objective of understanding the geological controls of slope stability. Continuity between the parts of the research is maintained by virtue that the conclusions of one part are in most cases a prerequisite to the development of the subsequent parts.

The areal extent of the study consisted of the Ottawa Valley. Physiographic boundaries between the Ottawa Valley Basin and the St. Lawrence Valley Basin created an Ottawa Valley embayment of the Champlain Sea, which constituted a partially restricted marine basin. Since time was not sufficient to evaluate the geological controls of landslides in the entire region inundated by the Champlain Sea, it was felt that the Ottawa Valley Basin provided a well defined area that could be studied in detail.

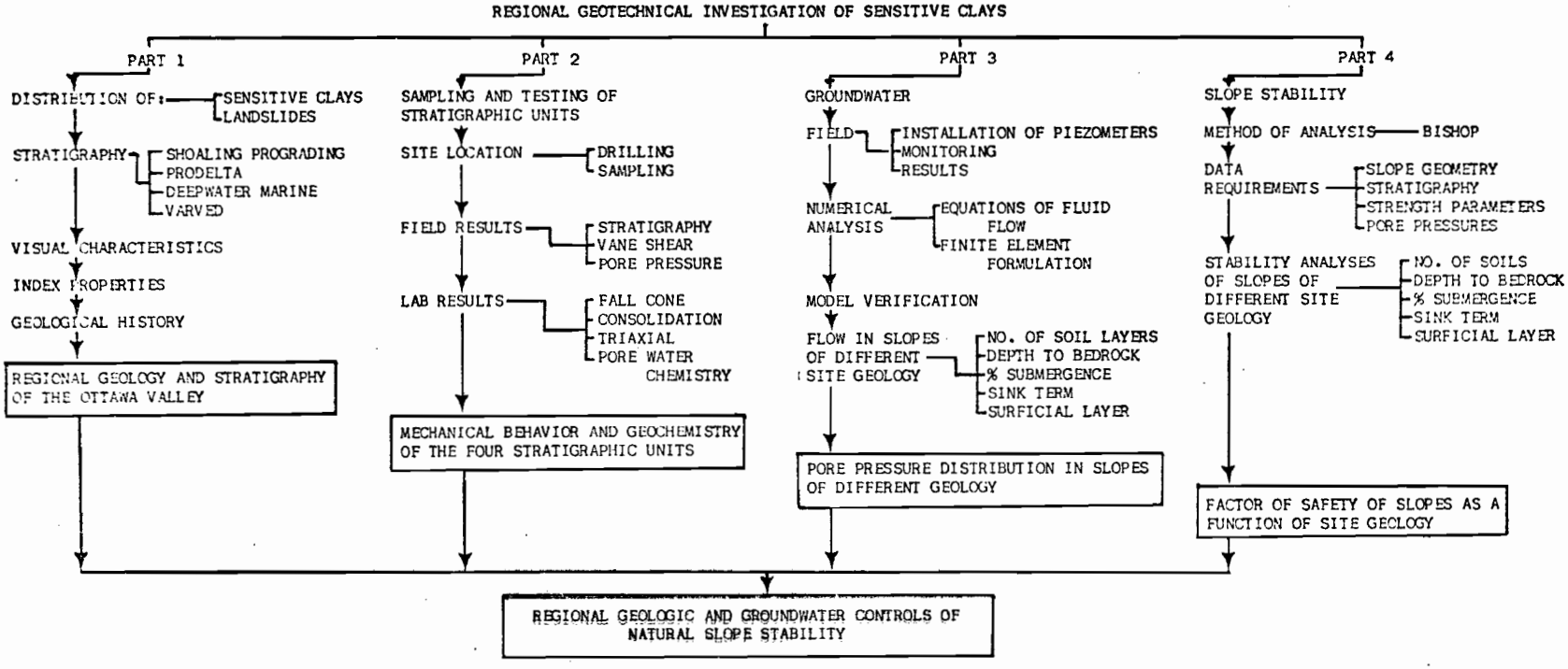

FIGURE 1.2 FLOW CHART OF THESIS ORGANIZATION

The geological framework for the thesis is given in Part 1. Included in the discussion are: an overview of the distribution of the sensitive clays and associated landslides; a detailed description of the visual and physical properties of the four stratigraphic units; and a geological history of the region based on the interpretation of the depositional environments and the regional geomorphology. The surficial mapping and stratigraphic studies cover the area bounded by the marine limit to the north and west and a large end moraine to the south and east. The marine limit represents the maximum elevation of marine transgression. At elevations greater than the limit, there are no Champlain Sea clays; hence no landslides in sensitive clays. The end moraine represented a convenient break in the clay deposits and separated the sensitive clays of the Ottawa Valley from those of the St. Lawrence lowlands.

The objective of Part 2 was to obtain samples of the sensitive clay and to relate the results of field vane tests, triaxial tests, consolidation tests, and porewater chemistry to the stratigraphy and overburden stresses. After careful study of existing borehole information and geological maps, a site was chosen for the field investigation and for the recovery of good quality tube samples for laboratory testing. The field component consisted of two borings, separated by 100 meters, at which shelby tube samples were taken, vane shear tests performed and ten piezometers installed. Ten Osterberg tube samples were obtained from borings placed adjacent to the initial holes. Thirty-eight consolidated undrained triaxial tests were performed on the clay from the Osterberg tubes, along with ten consolidation tests. In addition to the above tests, porewater chemistry was determined on samples from one of the boreholes.

An understanding of the groundwater system is essential to the evaluation of the stability of natural slopes (Hodge and Freeze, 1977). The research into the geological controls of the groundwater regime consisted of a field and numerical component. Three sites were instrumented with piezometers and monitored over a period from early spring to late summer. Two of the sites were in essentially the same geological setting, while the third differed from the other two and was in a different geological setting. The field data, coupled with the results obtained from a literature search have been used to evaluate the general groundwater system for the Ottawa Valley. Extrapolation of the field data to sites of different geological settings was performed by means of a transient finite element model developed by Neuman et al. (1974). After a comparison check of the finite element method with one of the field sites, which showed that the model was capable of simulating reasonably well the pore pressure distribution in slopes, the pore pressures in forty-six models of different site geology were calculated. Different geological factors investigated are: depth to bedrock; number of soil layers; depth of submergence; nature of the surficial layer; and a lower piezometric level in the bedrock aquifer. The different site geologies that were modelled are consistent with the stratigraphy of the sensitive clays of the Ottawa Valley and therefore give an indication of the geologic control of the pore pressure distribution.

Part 4 is an amalgamation of the stratigraphy, strength parameters, and pore pressure distributions in the forty-six models into an investigation of the geological controls of slope stability. Stability analyses were performed using the Bishop method and factors of safety were calculated for each of the forty-six different models. It

has therefore been possible to determine the extent to which the stability of natural slopes is affected by certain differences in site geology.

1.3 Literature Review

A review of some of the more pertinent literature is given here to serve as background information on the geology, mechanical behaviour and groundwater flow in sensitive clays. This review is an integral part of the thesis in that it demonstrates the results of previous research and how the thesis relates to and expands upon the existing knowledge.

There exists a considerable volume of published and unpublished research on sensitive clays. A comprehensive bibliography on the subject has been compiled by A.E. Thurston (1976) of the Ontario Ministry of Natural Resources. The number of references is well over one thousand, which makes the process of doing a complete literature search somewhat difficult. Certain articles can be considered as summaries and states of the art, thereby condensing the relevant aspects of several papers into one concise report. Those papers that were deemed important to the discussion of the geological controls of slope stability are reviewed here as background information.

1.3a Geology and Stratigraphy of Sensitive Clays

A series of seventeen maps showing the distribution of the sensitive clay deposits and associated landslides for the Ottawa Valley has been compiled by Fransham et al. (1976). A simplified legend was used for the compilation and consists of four map units. The sensitive clay deposits

have been grouped into a single map unit; hence, the surficial expression of the sensitive clay can be readily seen. In addition to the distribution of the clay deposits are all those landslides that could be identified on air photographs.

The stratigraphy and geologic history of the region has been studied for many years by Gadd (1963, 1975, 1977). Initially, the only stratigraphic sections available for analysis were road cuts and river banks. No stratigraphic drilling had been performed and a complete stratigraphic column was not available. The preliminary stratigraphic interpretation was that there were two clay deposits: a lower marine clay overlain by a freshwater clay. The two clay theory became the basis for geological controls of landslides (Sangrey and Paul, 1971) and for the interpretation of porewater chemistry profiles (Torrance, 1975). Evolution of this original hypothesis has occurred during the past three years. An extensive program of stratigraphic drilling was carried out by the Geological Survey of Canada and has led to the subdivision of the marine clay into four distinct units (Fransham and Gadd, 1977; Gadd, 1977), and a trend away from the two layer theory. Gadd (1975) has shown that in certain localities there is a layer of freshwater clay overlying the marine clay, but the freshwater clay is generally restricted to the bottoms of abandoned river channels. Gadd (1975) also presented evidence that the location of the ancient channels was controlled by bedrock faults. Maps showing the bedrock geology for the Ottawa region have been prepared by Wilson (1941) and have remained essentially unmodified since their publication.

1.3b Groundwater Movement in Sensitive Clay Slopes

There have been several groundwater investigations in the Ottawa Valley. Most of the previous studies have been associated with a larger investigation and the reporting of the groundwater regime has been limited. Crawford and Eden (1967) have shown that a general case of downdrainage in sensitive clay slopes was present at two sites. The Green Creek site east of Ottawa had stronger downward gradients than the Breckenridge site north west of Ottawa. Similar downdrainage conditions were reported by Jarrett and Eden (1970) for the Orleans, Ontario, area with the exception that there were artesian pressures near the Ottawa River suggesting that the rivers are the ultimate groundwater discharge zones. Chagnon (1975) has shown that no artesian pressures were present at the toe of a slope in Hull, Quebec. Scott et al. (1976) indicate that the artesian pressures are dissipated in the toe area when the depth of river erosion intersects the bedrock surface. It is evident from the literature that there is the possibility that artesian pressures may occur near the toe and downdrainage conditions near the crest. This kind of flow pattern can be anticipated by considering the neoclassical flow theory as outlined by Patton and Hendron (1974) and is illustrated in figure 1.3. The crest of the slope is a groundwater recharge zone, hence there is decreasing head with depth. Artesian pressures at the toe indicated a groundwater discharge zone and water levels increase with depth. The neoclassical flow theory is only generally applicable for homogeneous and isotropic soils of infinite extent. Where a permeable bedrock aquifer is present (Chagnon, 1975; Jarrett and Eden, 1970), modification to the flow regime will have to account for anisotropy.

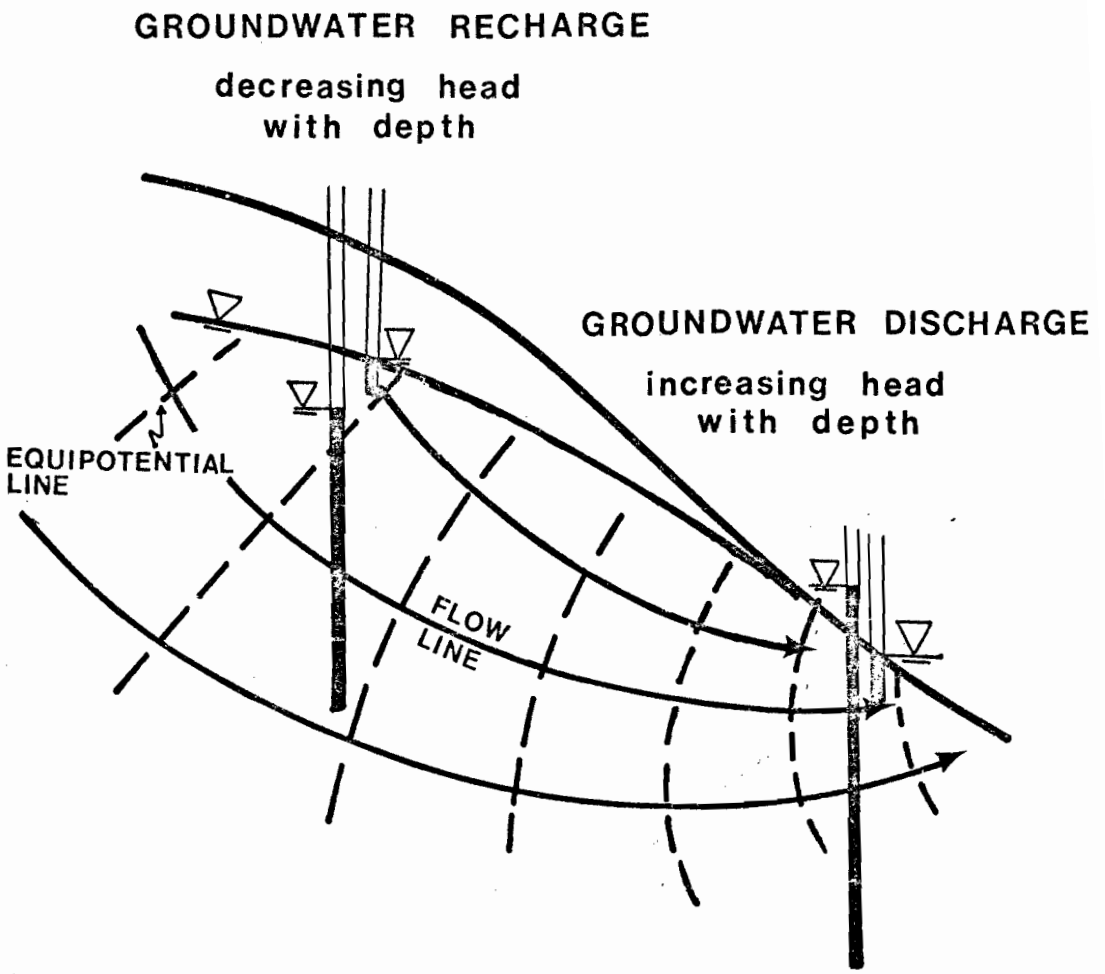

FIG 1.3 NEOCLASSICAL GROUNDWATER FLOW

(after Patton, 1973)

1.3c Slope Stability and Mechanical Properties

There is a considerable wealth of data on the stability of slopes and the mechanical behaviour of sensitive clays in the Ottawa Valley. Several approaches to the problem have been reported upon in the literature, each with varying degrees of success. Wong (1975) completed a field survey type of investigation. Apart from the limitations of this method, which were discussed previously, it should also be noted that this approach to the mapping of slope stability suffers from a lack of accurate data. Since landslides usually obliterate the slope in which they developed, it is often impossible to determine the pre-slide geometry of the slope. Hence, the positioning of the point on the inclination-slope height diagram is speculative at best.

A regional slope stability study has been carried out by Klugman and Chung (1976) for the Ottawa-Carleton region. Virtually every slope was analysed and maps were produced to show the change in the factor of safety along a given water course. However, many of the factors of safety are less than one for apparently stable slopes. This would indicate that the underlying assumptions used in the strength data and/or the pore pressure parameter are not valid.

Detailed stability analyses have been carried out by several investigators (eg. Sangrey and Paul, 1971; Crawford and Eden, 1967; Lo and Lee, 1974; Eden et al., 1971). Generally speaking, the approach to the detailed calculation is different for each author. The variables open to discussion are: the strength parameters, the position of the water table and the flow regime; it is expected that different points of view would develop concerning the mechanisms of natural slope failure.

Since well-documented case histories of slope failures in sensitive clays are rare (Lo and Lee, 1974), there is a tendency for a single failure to be described by several authors, each one manipulating the data in a certain manner. The slide at Breckenridge, Quebec, has been described by Crawford and Eden (1967), Lo and Lee (1974) and Sangrey and Paul (1967), and likely others. The same is true for other slides such as the Rockcliffe and South Nation Slide. It is difficult to determine who, if any, of the investigators has taken the correct approach. Therefore, the state of the art concerning the stability of sensitive clay slopes in the Ottawa Valley remains one of confusion. Lo and Lee (1974) show "conclusively" that the post peak or residual strengths govern the mechanical behaviour of the clay, while Mitchell (1970) makes a strong case for using the peak strengths, but on samples tested at low confining pressures. Mitchell and Markell (1974), also, used the undrained shear strength to try to relate a stability number to the potential for retrogressive failure. In almost all cases that are described in the literature, some assumption was made concerning the pore pressures that were in effect at the time of failure. The general approach was to perform several analyses with different pore pressure conditions and then choose the value which corresponded to a factor of safety equal to one (Crawford and Eden, 1967; Lo and Lee, 1974).

A probabilistic approach to slope stability in the Ottawa Valley has been formulated by Alonso (1976) and Yong et al. (1977). The basis of the method is to give a measure of the error inherent in the calculated factor of safety. Although the approach is still in the development

stages, it does yield an estimate of the probability of failure rather than just a factor of safety. Mapping of slopes from a probability viewpoint should eventually lead to a more rational approach to land management.

2 - GEOLOGY AND STRATIGRAPHY OF SENSITIVE CLAYS

2.1 Introduction

Landslides that are not artificially induced by man's physical activity are a natural geologic process. It then stands to reason that an understanding of the process entails an adequate knowledge of the regional and local geology. Modern slope failures are presently occurring along the banks of streams and rivers, but the location of the slope failure and the extent to which it will retrogress are difficult to predict. Why does a failure develop in a certain section of a river bank and not a few hundred meters in either direction? La Rochelle (1975) has stated that certain "geological features can result in the conditioning of a clay deposit to flow slides on a long term geological time scale basis". It is therefore essential that the geology, geomorphology and geologic history be evaluated if an appreciation of the geological conditioning of the clay deposits is to be developed.

In this chapter, the surficial geology, stratigraphy and geological history of the Ottawa Valley are given. The surficial geology includes the distribution of the surficial deposits and the landslides associated with the sensitive clay deposits. Surficial maps are essential to a regional study of landslides since the maps delineate those areas where sensitive clays exist, where landslides have occurred in the past and where the potential exists for slides to develop in the future. The stratigraphy is presented here since it forms an integral part of both the investigation into the mechanical behaviour and the groundwater regime. It has been shown by Fransham and Gadd (1977)

and Gadd (1977) that the sensitive clays are made up of four distinct stratigraphic units. The question then arises as to whether the mechanical behaviour of the clay is a function of the stratigraphic unit. Also, Hodge and Freeze (1977) have shown that the permeability contrasts between soil or rock units control the pore pressure distribution in slopes. Hence, the stratigraphy of the sensitive clay deposits is essential to an evaluation of the pore pressure distribution in sensitive clay slopes.

A geological history of a region is an interpretation of the surficial expression and stratigraphy of the component soils. For this study, the geological history is important in that "geologic conditioning" of the clay deposits needs to be assessed if geotechnical engineers are to evaluate the significance of irregularities in the soil profile.

2.2 Distribution of Sensitive Clays

Seventeen maps at a scale of 1:50,000 showing the distribution of sensitive clay deposits and the associated landslides have been compiled by Fransham et al. (1976). It was not possible to include these maps here so a reduced and simplified version is shown in figure 2.1. It is evident from figure 2.1 that the sensitive clays (gold colour) are not continuous, nor are they always found at the surface. Either lack of deposition or erosion has resulted in the clay being discontinuous over the valley. Also shown on figure 2.1 are some of the larger landslides (red) that have occurred in the region. An air photograph of part of the slide directly south of the first letter "a" in "Ottawa River" is shown in figure 2.2. The dissected upland plain is covered with a layer of sand that overlies sensitive clay.

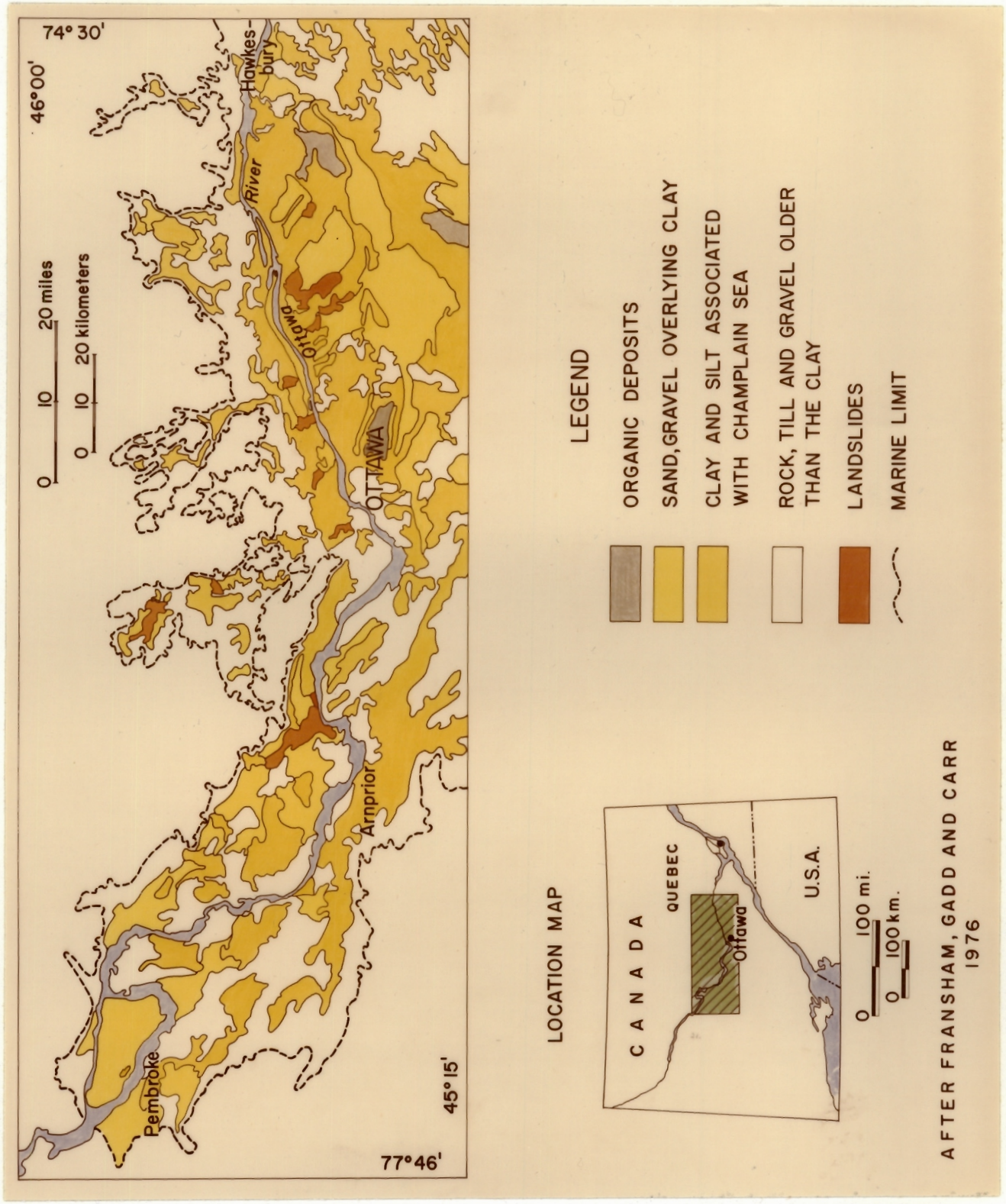

FIG. 2.1 DISTRIBUTION OF SENSITIVE CLAYS AND ASSOCIATED LANDSLIDES

FIG. 2.2 AIR PHOTOGRAPH OF LANDSLIDE SCARS IN THE BANKS OF AN ABANDONED RIVER CHANNEL

The landslide areas are recognized by the rippled pattern which probably represents the remains of the retrogressive slips. The slide is likely ancient and occurred approximately 10,000 years ago. The rivers that flowed through this channel have been dated at 10,200 years before present by Gadd (1975) and, since some of the debris aprons have been removed by river erosion, the river must have occupied the channel at the time of failure. Radiocarbon dates on bog deposits in the bottom of the channels are in the order of 7600 years before present (GSC 681 and GSC 2477). Therefore, the major period of slide activity must have taken place between 7600 and 10,200 years before present.

From a study of the original maps, it can be seen that few slides of any significance have developed north of Arnprior. Gadd (in preparation) is analysing the results of stratigraphic drilling in the area to the north of Arnprior and may shed some light on any stratigraphic differences that may be limiting the development of slope failures.

2.3 Stratigraphy of Sensitive Clays

The stratigraphy of the sensitive clay deposits of the Ottawa Valley has been investigated primarily by Gadd (1963, 1975, 1977). The two clay theory, which was the preliminary interpretation has already been discussed in the literature review. Through the analysis of cores from stratigraphic borings made in the Ottawa Valley, Fransham and Gadd (1977) and Gadd (1977) have proposed that the sensitive clays be subdivided into four distinct stratigraphic units: varved clay; deep water marine clay; prodelta or prograding delta marine clay; and shoaling prograding delta marine clay. A generalized stratigraphic column is shown

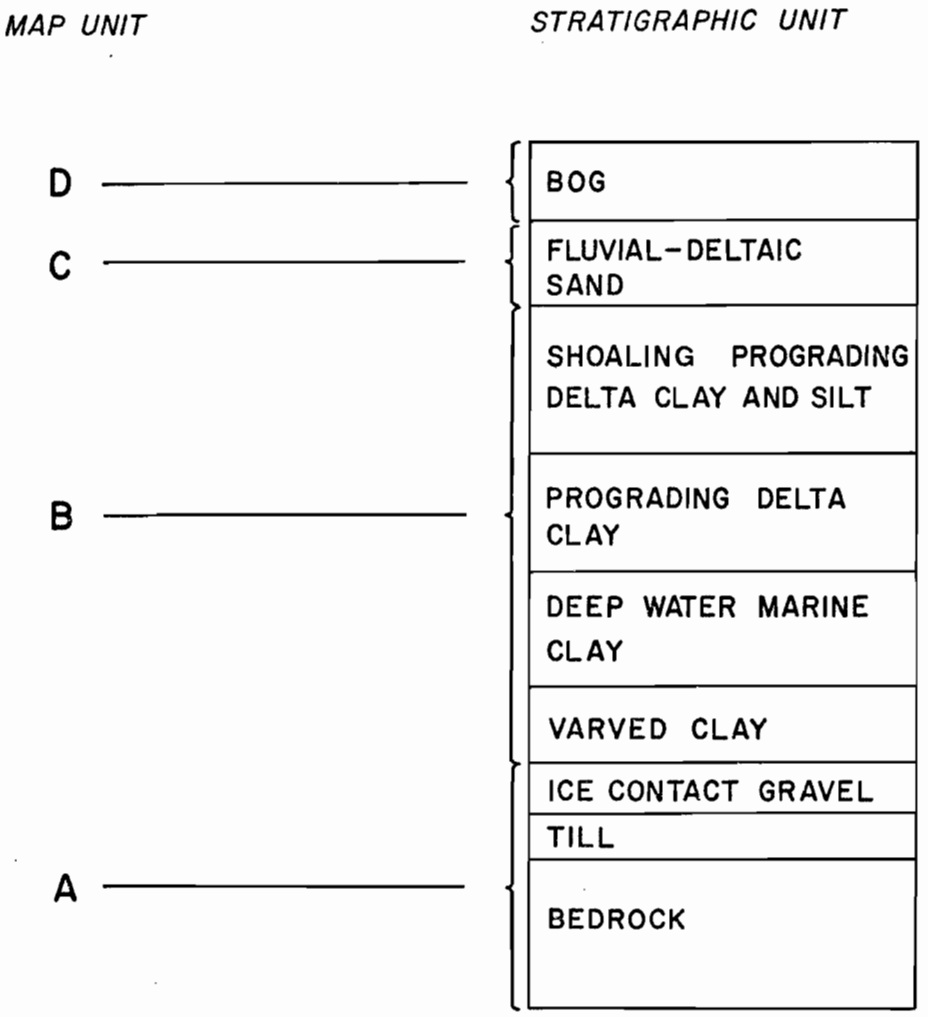

FIG 2.3
STRATIGRAPHIC COLUMN

in figure 2.3 and gives not only the sensitive clay units but also the other surficial materials, and their position in the column. Under the heading of map units in figure 2.3 are the letters A to D representing the map units shown in figure 2.1.

A description of each of the four sensitive clay units will follow here. Included in the description are: the criteria used to identify a particular unit; colour plates of the clay units; and an interpretation of the original depositional environments. Samples of cores from the Geological Survey of Canada's drilling program in the Ottawa Valley were used to determine index properties for each of the clay layers. The location of the borings and the data from the index property tests are given in Appendix A. A summary of the mean properties for each facies follows the visual description of the units.

2.3a Varved Clay

Varved clay has been identified in the Ottawa Valley by several investigators (Johnston, 1916; Antevs, 1925; Gadd, 1963; Bozozuk, 1972). Varved clay is generally the first clay layer overlying the glacial till. Plates 2.1 and 2.2 show the banded nature of the clay. According to Twenhofel (1950) varved clay is deposited in a glacial lake which is near to the end moraine of a glacier. The alternating bands are due to the cyclic climatic changes occurring during the course of the year. The summer part is lighter in colour and is composed of a mixture of sand, silt, and clay. The darker winter portion is composed of fine clay. In addition to the summer layers being lighter than the winter bands, the summer bands are usually thicker.

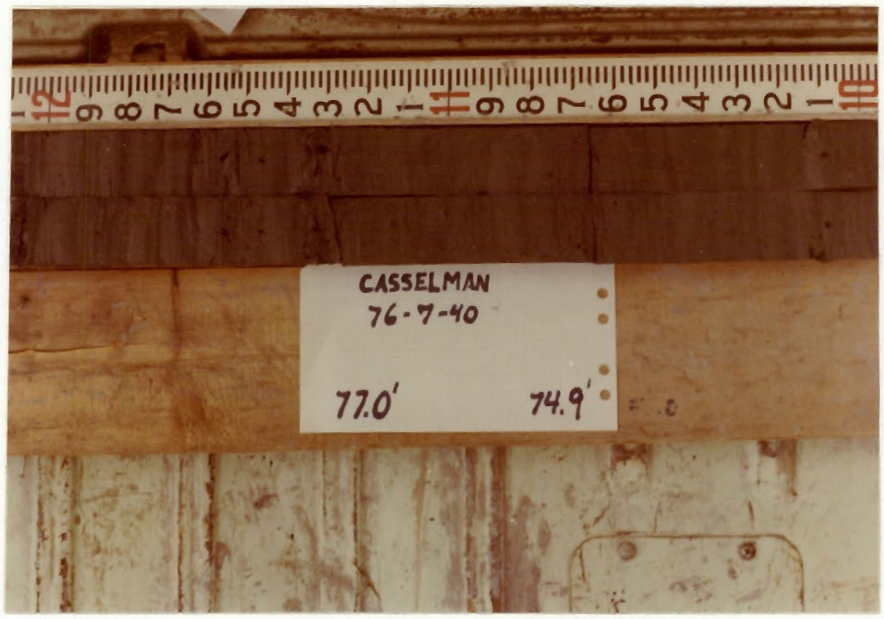

PLATE 2.1 VARVED CLAY

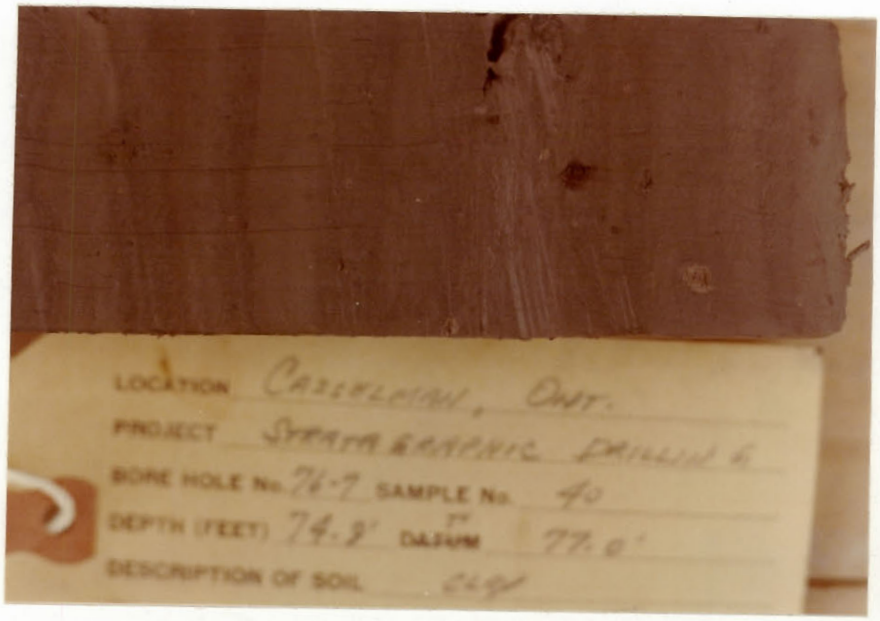

PLATE 2.2 CLOSEUP OF VARVED CLAY

In the summer, the volume of melt water is considerably higher than in the winter, and, as a consequence, there is an increase in the size of material transported in the basin. As the freeze-up progresses, the volume of flow and the energy are diminished, and the fine clay size particles settle out. In the Ottawa Valley, the varved clay appears to be the only fresh water clay associated with the post glacial inundation.

2.3b Deepwater Marine Facies

Overlying the varved clay is a layer of more massive sediment which appears to have relatively little texture or colour banding. Marine fossils were found at the base of the layer, indicating that the depositional environment had changed from freshwater glacial lake to marine. Plates 2.3 and 2.4 show typical sections of what is being called deepwater marine clay. The deepwater term reflects the period when the depth of water was likely at a maximum and there was a minimum amount of sediment already deposited in the basin. The depth of the water has resulted in relatively little structure with the exception of the black mottling that can be seen in the two plates.

The origin of the black mottling for the sensitive clays of the Ottawa Valley is not fully understood. However, Berner (1974) in a study of the Black Sea, concluded that the colour was due to the presence of black iron monosulphides. These compounds are relatively unstable and, if there is a sufficient supply of elemental sulphur, would form pyrite and pyrrhotite during the compaction. It is hypothesized that the supply of sulphur was likely limited, therefore the transformation could not take place and the colour remained even in sediments 10,000 years old. Since the black colouring is chemically unstable, it disappears

PLATE 2.3 DEEPWATER MARINE CLAY

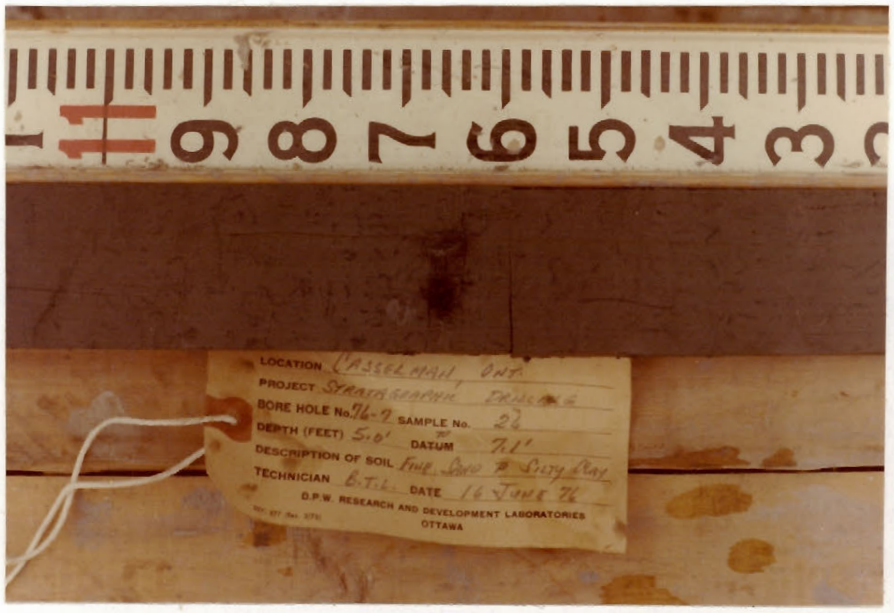

PLATE 2.4 CLOSEUP OF THE ABOVE PLATE SHOWING AN ICE RAFTED PEBBLE AND THE CHARACTERISTIC BLACK MOTTLING (note, label does not correspond to this sample)

within a matter of hours upon exposure to air. Any future study into the cause of the black mottling will have to take steps to preserve the colour until a series of identifying tests can be made.

2.3c Prograding Delta Facies

The transition from the deepwater marine conditions to what is being called the prograding delta facies is not abrupt and on a visual basis does not appear to have represented a major change in the depositional environment. The prograding delta facies is perhaps the most significant of the four clay units in that much of the material involved in landslides is made up of this unit. The depositional environment was not constant and changed through time from the deepwater marine conditions to the fluctuating conditions representing the seasonal variations in current and volume of material available for deposition. This process has resulted in a facies which exhibits both colour and textural banding. The clays are either red and grey banded or light and dark grey banded. Band widths vary in thickness, but on the average, are about 2 to 3 cm. Silt seams or partings are not uncommon and can be up to 0.6 cm thick. Black mottling, present in most of the cores, can be found in either the red or grey bands and is usually in layers which diffuse outward from a darker central band. Berner (1974) suggests that, where black material is present in a discrete layer rather than disseminated, the origin of the black colour could be due to changes in rates of sedimentation, rather than changes in salinity. Since the black mottling was observed in both the red and the grey bands, it seems likely that differential rates of sedimentation caused by factors other than the annual climatic changes could have produced the black bands. Plates 2.5 and 2.6 are typical

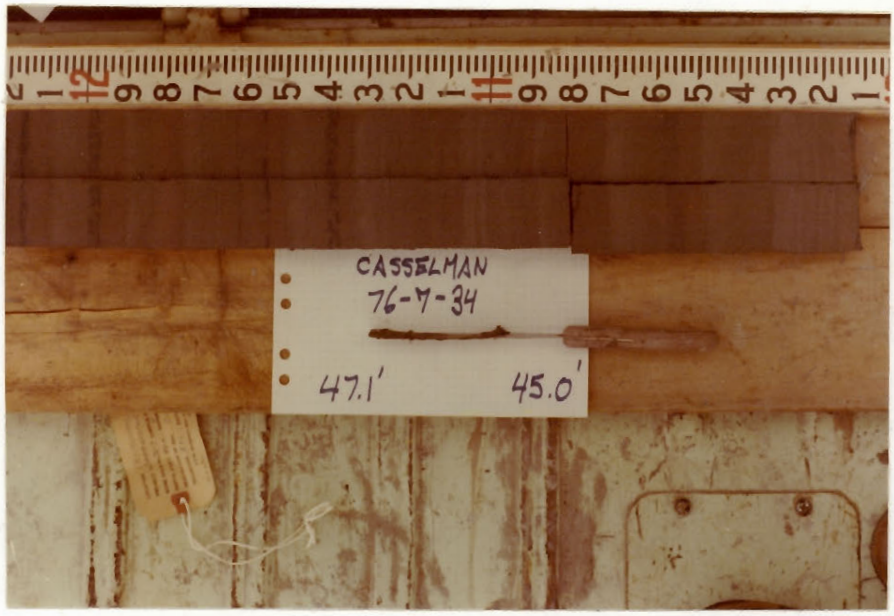

PLATE 2.5 PRODELTA CLAY

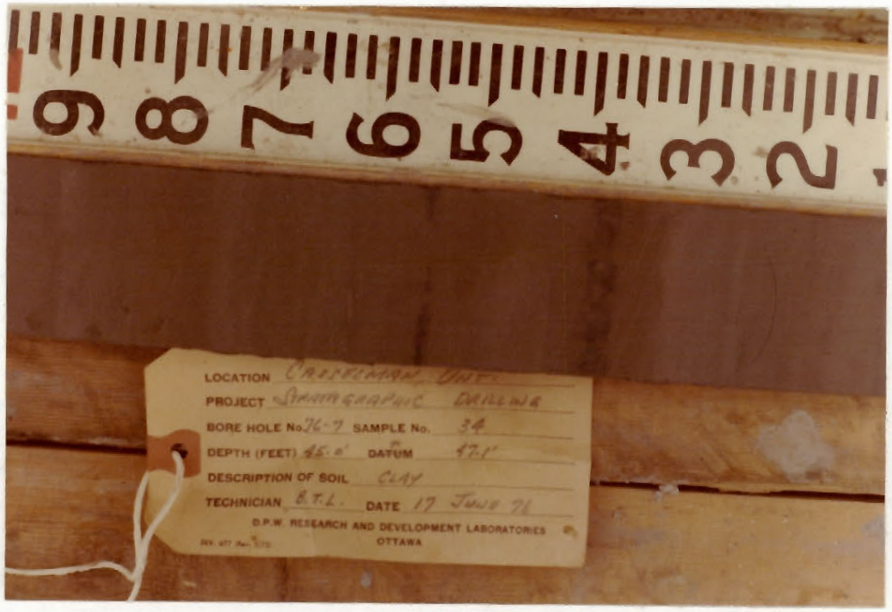

PLATE 2.6 CLOSEUP OF PRODELTA CLAY SHOWING BLACK MOTTLING AND THE RED-GREY BANDING

of the material likely to be found in this unit. The true red colour did not reproduce well on the photos and is generally redder when viewed in natural sunlight. The contacts between the individual layers are not sharp. This would indicate that the change in the depositional environment responsible for the banding was gradational.

The origin of the red bands is also not understood. Grain size analysis on carefully selected red and grey bands indicated that the red bands were on the average 6-7% finer in grain size. The colour could be due to a dominance of red feldspars since the gneissic rocks surrounding the Ottawa Valley are generally quite pink in colour. However, Haynes and Quigley (1976) indicated that there were no detectable differences in mineralogy between the red and grey bands. Discussion of the use of X-ray diffraction techniques for quantitative mineralogy (Yong, 1975) suggests that, due to a number of factors, the height of the peaks for each of the minerals may not be directly correlative to a known standard. It may be entirely possible that the subtle differences between the composition of the red and grey bands are beyond the present means of analysis.

2.3d Shoaling Prograding Delta Facies

This unit is the uppermost of the clay sequence. The main difference between this unit and the prograding delta facies is that there are more and larger discrete silt partings, reflecting the general lowering of the sea. A comparison of plates 2.5 and 2.6 showing the prograding delta facies and plates 2.7 and 2.8 indicate that there is a strong resemblance between the two units. The shoaling facies maintains the red-grey or light-dark grey banding which was characteristic of the previous unit. The thin

PLATE 2.7 SHOALING PROGRADING DELTA CLAY

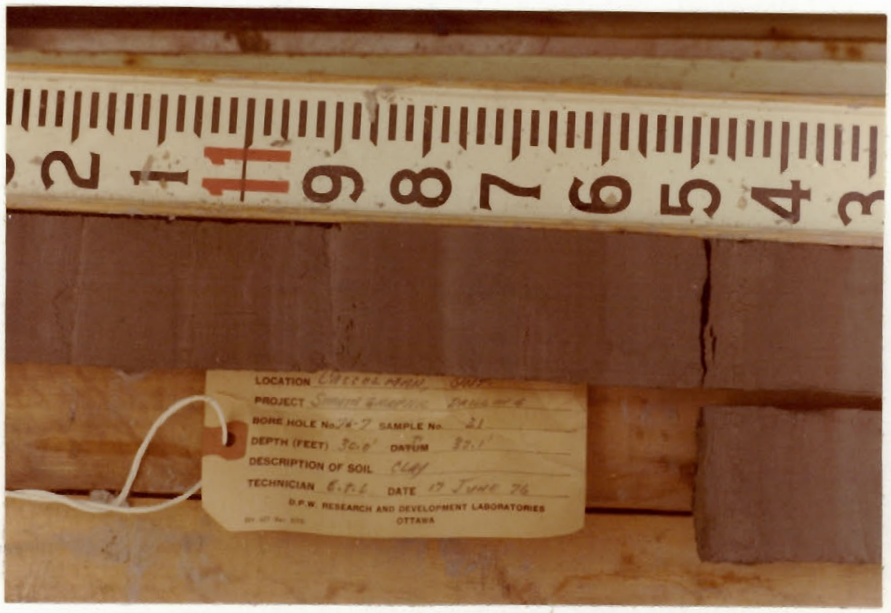

PLATE 2.8 CLOSEUP OF SECTION OF CORE SHOWN IN PLATE 2.7
(note, silt bands at 10.9 and 11.2)

silt partings, which are commonly found, can be seen at locations 10.05, 10.45, 10.9 and 11.2 on plate 2.7. Also evident is the slumping and distortion of the beds (11.35-11.6 on the scale).

The silt layers do not appear to occupy any regular place in the banding of this unit. It is therefore suggested that the silt bands were deposited during periods of exceptionally high flow, likely during floods or during low tides. The slumping which is also found indicates that the depositional environment was somewhat turbulent. The lack of black banding could reflect more oxidizing conditions or a greater supply of elemental sulphur.

2.3e Fluvial Sand

Although this unit is not part of the sensitive clay sequence, it is important in that it acts as a groundwater storage basin and, likely has influence on the pore pressure distribution found in the underlying clay. No index property tests were performed on the sand, so that only a visual description can be given here. Plate 2.9 shows that the sand appears to be fairly uniform and medium fine. Some banding is evident and, in a few cases, there are thin clay or silt bands. The continuity of these silt or clay bands is now known. The sand unit is about 2-3 meters thick and covers a large portion of the clay found to the east of Ottawa (yellow on figure 2.1). Minor amounts of lag gravel have been identified by Gadd (1975). However, these deposits are small and relatively insignificant in terms of the regional hydrogeology.

2.4 Summary of Index Property Tests

Mean values of index property tests performed on clay samples are listed in table 2.1. Although there is considerable scatter about the mean, there does appear to

PLATE 2.9 FLUVIAL SAND

SOIL UNIT	SPECIFIC GRAVITY	BULK DENSITY	NATURAL WATER CONTENT	LIQUID LIMIT	PLASTIC LIMIT	CLAY SIZE	SILT SIZE	SAND SIZE
		$x10^3 N/m^3$	%	%	%	%	%	%
VARVED CLAY	2.79	18.9	36.6	33.2	18.6	32	45	23
DEEPWATER	2.79	17.0	50.2	47.4	24.6	62	37	1
PRODELTA	2.79	16.8	55.5	53.3	23.7	70	30	0
SHOALING PRODELTA SILT	2.79	17.2				14	82	4
SHOALING PRODELTA CLAY	2.80	17.9	48.5	43.6	25.4	50	50	0

TABLE 2.1 SUMMARY OF MEAN INDEX PROPERTY TESTS FOR ALL FOUR SOIL UNITS

be some change in properties between the soil units. The specific gravity was the most constant of all the index properties. The mean of 2.79 for all but the shoaling prograding delta clay which is 2.80 indicates a common source for the sediments. Bulk densities vary from a minimum average of 16.8 kN/m^3 for the prodelta clay to a high of 18.9 kN/m^3 for the varved clay. Since the specific gravity is essentially the same for all the units, the variation in the bulk density must be due primarily to the differences in void ratio. Natural water contents averaged about 2-5% greater than the mean liquid limit. The lowest water content was for the varved clay at 37%, while the prograding delta clay averaged 56%. It should be noted that the water content for the prograding delta clay ranged from a low of 43% to a maximum of 83% (see Appendix A for data) indicating that the mean value is not truly representative of the actual field water contents that may be expected. The same can be said for the liquid limit, where variation is not represented by the mean. The plastic limit was a minimum of 19% for the varved clay and a maximum of 25% for the shoaling prograding delta clay. The variation in the plastic limit was not usually more than $\pm$ 5% from the mean.

Mean values of the sand, silt, and clay percentages represent an interesting statistic. The varved clay had the coarsest overall grain size distribution with an average of 32% clay, 45% silt and 23% sand. The coarseness of the sediment indicates that the ice margin was close enough to cause the deposition of large amounts of silt and sand size particles. The deepwater clay shows a definite fining of the sediments and averages 62% clay, 37% silt, and only 1% sand. Variation of the grain size about the mean values is in the order of 14%. The prograding delta facies exhibited a considerable scatter about the mean. Clay size ranged

from 47% to 93% with an average of 70%. The wide variation is due to the banded nature of the sediments which reflect a depositional environment that was likely affected by the annual fluctuations in current velocity and volume of material available for sedimentation. However, on the average, the prodelta clay has the finest grain size distribution (clay 70%, silt 30%) of the four stratigraphic units. The shoaling prograding delta facies consisted of banded clay layers and silt seams. Due to anisotropy, it is meaningless to quote mean values of grain size for the entire unit. Therefore, mean values are given for the predominantly silty material and a second set for the more clay size rich sediment. The clay bands averaged an equal amount of silt and clay (50% - 50%). The silt showed very uniform grain size, and in certain samples, as much as 92% was silt size with the remaining 8% composed of sand and clay size materials.

The significance of the grain size data is that the trend is towards coarser sediments at the base and top of the sequence with the finest sediments found in the middle. This would tend to indicate that there is a complex relationship between the depth of the water in the basin, the influx of sediment for deposition, the position of the ice front, and the prevailing climate. The overall anisotropy is a minimum in the deepwater clays and increases both downwards and upwards through the section.

2.5 Geological History of the Ottawa Valley

A geological history of a region is based on the interpretation of the stratigraphic column in terms of the origin of the sediments, their depositional environments and the geological process that have affected the sediments

during the time interval following their deposition. The geological conditioning to flowsliding mentioned in the introduction to this chapter is the end result of the geological process that has occurred during and after the formation of the sensitive clay deposits.

Only one till layer has been identified in the Valley which would suggest a single advance and retreat of the ice through the region (Gadd, pers. comm.). There is no evidence pointing towards a readvance of the ice front across the sensitive clays, hence any over-consolidation of the clay cannot be linked to a surcharge by ice. The till varies in thickness and where present is generally less than 2 meters thick. Charron (1975) has shown till thickness up to 30 meters in the Russell area.

Overlying the till is a layer of varved clay that was deposited in a post glacial freshwater lake. The origin of the lake was due to an ice dam near Quebec City that restricted the influx of sea water (Gadd, 1964). The varved clay is relatively continuous over the Valley and is generally in the order of 2 to 8 meters in thickness.

The change in depositional environment to marine appears to have been rapid. The transition from freshwater varved to deepwater marine clay has been observed to occur in a matter of a meter or so of sediment. In the description of the deepwater clays, it was shown that the clay has an irregular black mottling indicative of either a reducing environment or a lack of elemental sulphur which did not allow for the transformation of the unstable iron monosulphides into more stable sulphides. The clay being essentially structureless would lead to the conclusion that the depositional environment was likely static and there was little

variation that would lead to the formation of textural or colour banding.

As the ice migrated further to the north, a channel linking the Great Lakes with the Champlain Sea opened up through North Bay (Prest, 1970). A large delta formed at Petawawa, Ontario, resulting in the deposition of sand and gravel. As the land rebounded in response to the removal of the ice mass, the deltas that had been forming near the shores of the Champlain Sea migrated eastward towards the Gulf of St. Lawrence. The result of the migration of the deltas was the deposition of the banded clays and a sand capping. The delta clays were likely deposited in a constantly changing environment. Variation in current velocity and volume of sediment have resulted in an anisotropic stratigraphic unit. It would appear that, during the prodelta clay deposition, the rate of sedimentation was irregular enough to result in the formation of black sulphide banding.

As the sea regressed, a drainage system developed on the exposed sediments. A larger Proto-Ottawa River meandered and eroded channels into the sediment package. River trimmed scarps to the north of Ottawa indicate that the Proto-Ottawa River was at least 5 km wide compared to about 1.6 km today. The location of the Proto-Ottawa channels appear to coincide with the regional bedrock faulting pattern (Gadd, 1975). With the continued regression of the sea, the ancient Ottawa River channels were abandoned in favor of its present day course. An indication of the erosion that has occurred since the withdrawal of the sea can be seen in figure 2.1. In this figure, the yellow colour representing the sand symbolizes the remnants of the original deltaic plain. The gold colour (clay) between the sand indicates

the ancient channels that have since been abandoned. It was shown in the description of figure 2.2 that the banks of these abandoned channels were unstable during the period when the river occupied the channel and that a major period of landslide activity likely occurred early in the history of the region. These slopes are likely now in equilibrium with the slope geometry and groundwater conditions and probably do not represent a serious threat to engineering structures.

Tributaries of the Ottawa River (eg. Green Creek, South Nation River) are now eroding channels and it is along the banks of these rivers that modern landslides are occurring.

With the regression of the sea, the groundwater regime changed from what was practically a no flow condition to the recharge-discharge system that is in effect today.

2.6 Summary

In the introduction to this thesis, it was shown that knowledge of the regional and local geology is of fundamental importance in slope stability studies. Furthermore, if the geological controls of slope stability are to be evaluated, then the distribution, stratigraphy and geologic history of the sensitive clay deposits are essential.

The distribution of the sensitive clays and some of the larger landslides in the Ottawa Valley have been presented in figure 2.1. This figure shows that a considerable part of the terrain at elevations lower than the marine limit is covered with a layer of sensitive marine clays. Due to the extent of the clay deposits, some river banks may become unstable with time and threaten engineering structures.

The description of the sensitive clays varies depending on the person who happens to be logging drill core or mapping an excavation or embankment. In an effort to standardize the soil descriptions, photographs of the four stratigraphic units that make up the sensitive clay deposits have been included in the thesis and show that each of the units has relatively well defined visual characteristics. Index property tests were performed and show more quantitatively the similarities and differences between the units. Since there are obvious differences in the visual characteristics of the sensitive clay units, a normal progression in the research philosophy is to determine whether the various units control either the mechanical behaviour of the clay or the groundwater regime and, in the end result, the stability of natural sensitive clay slopes.

The geological conditioning to flowsliding is in fact an integral part of the geological history of the region. In most respects, the history of the Ottawa Valley is relatively simple. At different times, a freshwater lake and then a marine sea occupied the Ottawa Valley. Following the retreat of the sea, a drainage system developed, which eroded channels through the sediments. It is the banks of these rivers that are prone to slope instability. The main objective of presenting the geological history is for it to serve as a base for interpreting the geotechnical, geochemical and groundwater data given in the following chapters and, ultimately, to help in determining the geological controls of slope stability.

3 - MECHANICAL AND CHEMICAL PROPERTIES

3.1 Introduction

It was shown in Chapter 2 that the sensitive clay deposits of the Ottawa Valley are in fact made up of four distinct stratigraphic units. Since it was postulated that the depositional environments for each of the units was likely different and that the units themselves had different visual characteristics, it remained to be investigated if the mechanical behavior varied between the units. If there was indeed a difference in the behavior of the units, then it could be postulated that the landslide phenomenon could in part be controlled by the stratigraphic column at a given site. The objective of this section is not to determine the actual strength parameters that should be used in stability analyses, but rather to investigate and relate the mechanical behavior to the stratigraphic unit.

To evaluate the mechanical behavior of the four stratigraphic units, a site near Casselman, Ontario, was chosen. The criteria for selecting this site were based on the following: 1) the four stratigraphic units must be present; 2) the site must be easily accessible; and 3) the geologic setting should be similar to those in which landslides are occurring, thus enabling the results of the field investigation to be translated into the stability of nearby slopes.

A boring near Bourget, Ontario (boring 74-1 in figure A1, Appendix A) indicated that a complete suite of units could be anticipated in the same general vicinity.

After a field reconnaissance survey, a site along the CNR right of way, 5.5 km west of Casselman, appeared to satisfy the selection criteria. Access was available along the railway line and the site is about 0.5 km south of the South Nation River, which is noted for a particularly large slope failure in 1971 (Eden et al., 1971). A location map and detailed site profile are shown in figures 3.1 and 3.2.

The site investigation consisted of: 1) the drilling of two boreholes (76-1-1 and 76-1-2) for stratigraphic interpretation and in situ vane tests; 2) the installation of ten piezometers (five at each boring); and 3) two supplementary borings at each site for the recovery of good quality Osterberg tube samples. The two boreholes were placed at 30 meters from the crest of a ravine (76-1-2) and 130 meters from the crest (76-1-1). Vane shear tests and shelby tube samples were obtained on an interval of 1.5 meters. The shelby samples were extruded on the site and used to determine the stratigraphy as the drilling progressed. Upon completion of the hole, elevations for the Osterberg samples were determined. In choosing the sampling elevations, every effort was made to obtain samples from each of the units as well as from obvious breaks in vane shear versus depth record. In all, ten Osterberg samples were obtained, five from each site. In addition to the above mentioned testing program, a portion of the clay from boring 76-1-2 was used to determine the pore water chemistry.

Both boreholes were cased to bedrock, thereby allowing for limited bedrock coring. The objective of the coring was to identify the rock type and to install a piezometer. In both holes, open fractures were encountered in the bedrock and the drill string dropped about 2.5 cm.

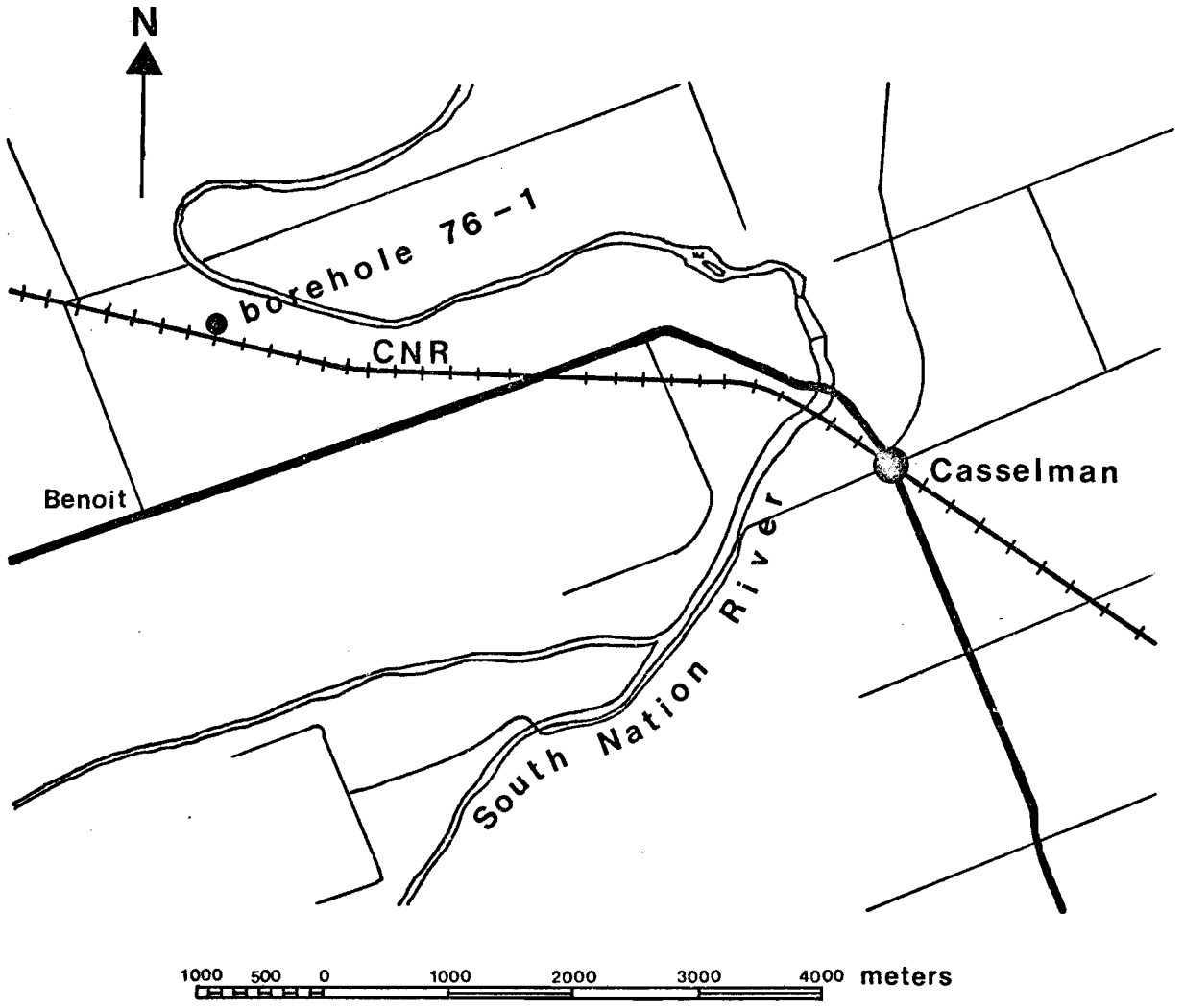

FIG 3.1 LOCATION OF BOREHOLE 76-1

West ←

→ Casselman

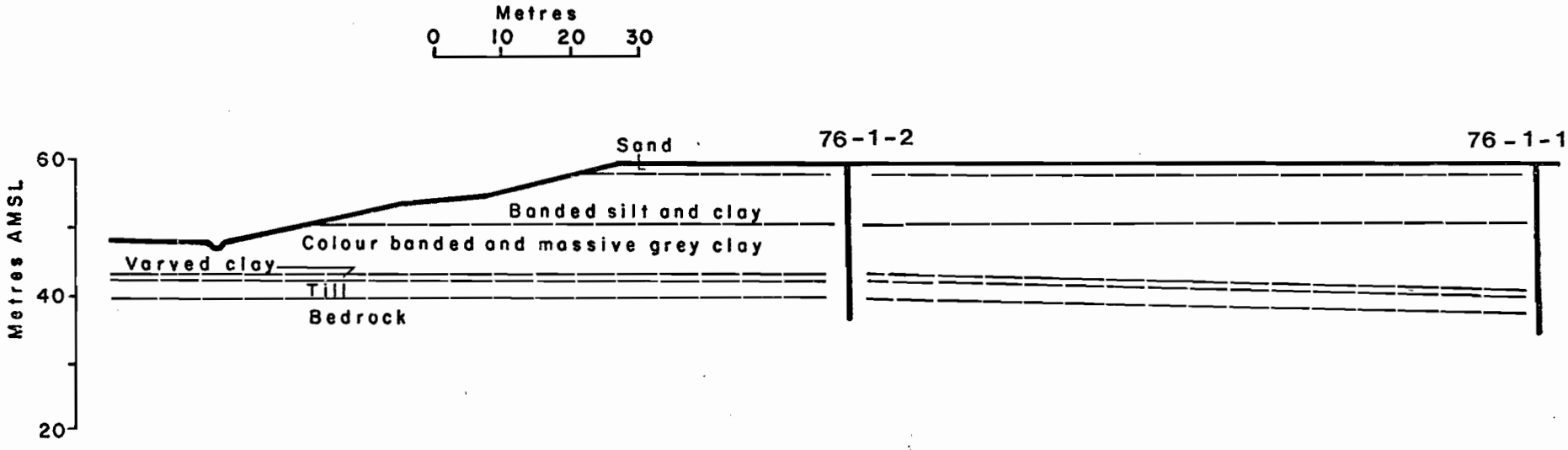

FIG 3.2 SITE PROFILE AND BOREHOLE LOCATIONS

All the drilling water was lost into the fractures, indicating a well developed system of joints or solution channels. No local outcrops of the same limestone recovered by coring were available and it is not known if the rock permeability is due to jointing or solution features.

Geotechnical profiles for boreholes 76-1-1 and 76-1-2 are given in figures 3.3 and 3.4 respectively and show: the stratigraphic log; the elevations of the Osterberg samples and the piezometers; the undrained shear strength versus depth; and the variation of the preconsolidation pressure versus depth. It should be noted that all of the four stratigraphic units were identified at the site thereby allowing for the sampling and testing of each unit.

3.2 Undrained Strength Tests

Field vane shear tests were performed on 1.5 m intervals over the entire profile. Strength data for boring 76-1-2 was supplemented by laboratory fall cone tests. The results for both sites show similar trends in undrained shear strength with depth. The lowest strength of 20 kPa is found at a depth of 2-5 meters. There is a linear increase in strength to 40 kPa at about 15 m whereupon there is a relatively sharp increase in the strength to 60 kPa followed by a linear increase to between 80 and 100 kPa at a depth of about 22.5 m. The break in the strength versus depth curve at 15 meters does not appear to be associated with the stratigraphic interpretation indicating that the undrained shear strength is independent of the stratigraphy.

Remolded strengths with depth were obtained at both sites and the results of the remolded strength and the sensitivity are summarized in table A1 in Appendix A. For

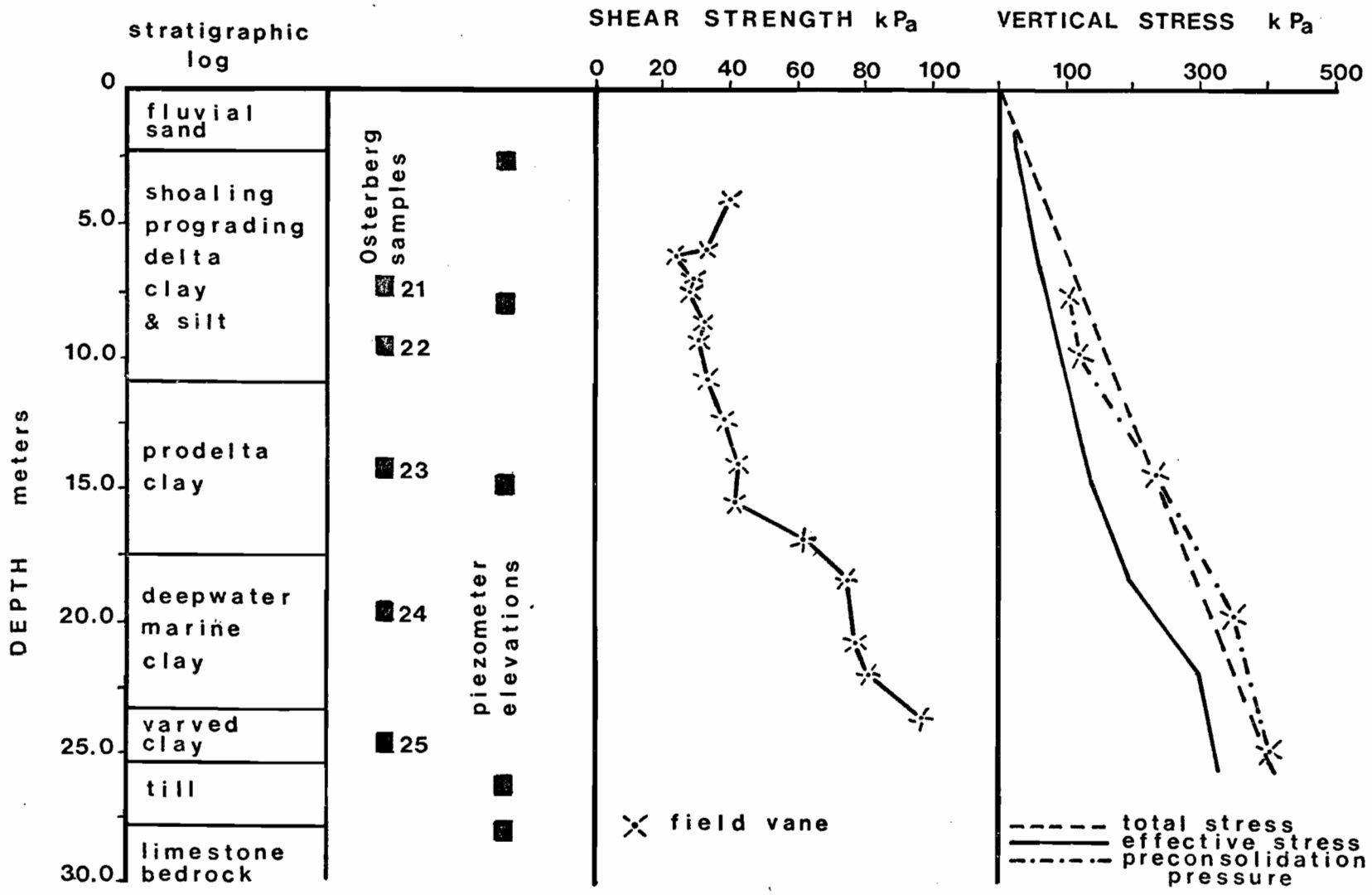

FIG 3.3 GEOTECHNICAL PROFILE - borehole 76-1-1

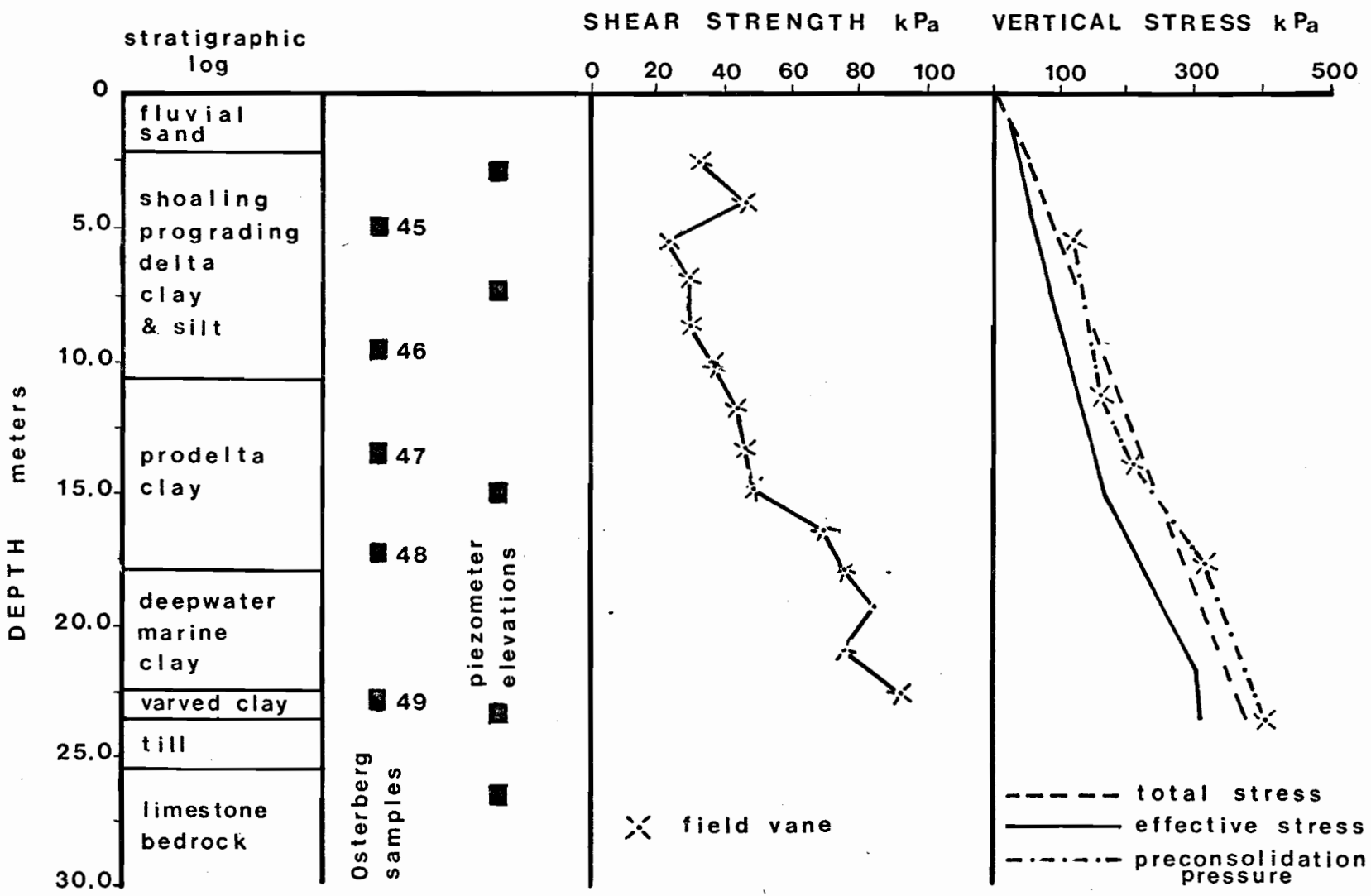

FIG 3.4 GEOTECHNICAL PROFILE - borehole 76-1-2

borehole 76-1-1, there did not appear to be any significant trends in the variation of either the remolded strength or the sensitivity with depth. Remolded strengths varied from 1.3 kPa to 6.5 kPa while the sensitivity varied from 6 to 32. For borehole 76-1-2, there is a definite increase in the sensitivity with depth. The sensitivity from the field vane showed that there was a minimum sensitivity of 5 near the surface increasing to a maximum of 71 at 22.3 m. Although there is considerably more scatter for the sensitivities calculated using the fall cone, there does appear to be an increase in sensitivity with depth.

Effective overburden pressures were obtained using pore pressures determined through monitoring of the piezometers. The results of the pore pressure measurements will be covered in detail in the next part and are discussed here only as they relate to the variation in the undrained strength with depth and the preconsolidation pressure. It can be seen from figures 3.3 and 3.4 that there is a similar trend in the effective overburden stress with depth as in the undrained strength with depth. A ratio of shear strength to effective overburden stress was calculated using a regression analysis. The ratio was 0.27 with a correlation coefficient of .89 which indicates a good correlation between the two variables, and furthering the conclusion that the vane strength is not related to the stratigraphy but is a function only of the overburden stress.

3.3 Consolidation Behaviour

Consolidation tests were performed on each of the ten Osterberg tube samples. The purpose of this testing was threefold. Firstly, to establish confining pressures for the triaxial tests. Secondly, to investigate if there

was any difference in the consolidation behaviour between the four stratigraphic units, and thirdly to determine the variation in the preconsolidation pressure with depth.

Void ratios are seldom constant for soils; therefore, to facilitate comparison of the ten consolidation tests, the results have been plotted as strain versus log pressure. Figures 3.5 and 3.6 show the consolidation curves, the apparent preconsolidation pressure, the sample number and the facies for borings 76-1-1 and 76-1-2 respectively. The sample numbers correspond to the numbers beside the Osterberg sample locations shown in figures 3.3 and 3.4. The variation in the preconsolidation pressure with depth is also shown in figures 3.3 and 3.4.

Four samples were obtained from the shoaling prograding delta facies: 21, 22, 45, and 46. The apparent preconsolidation pressure is well defined in all samples by a sharp break in the strain versus log pressure curves. The preconsolidation pressures are 108.0 kPa and 125.0 kPa for samples 21 and 22 respectively and 120.0 kPa and 159.0 kPa for samples 45 and 46 respectively. A comparison of the preconsolidation pressures with the mean effective overburden pressures (figures 3.3 and 3.4) shows that the clay is overconsolidated by about 20 to 50 kPa.

The two samples from the prodelta facies (23 and 47) exhibited similar strain-log pressure curves as the shoaling facies. The preconsolidation pressures are 239.0 kPa and 206 kPa for samples 23 and 47 respectively. Mean effective overburden pressures are 135.0 kPa and 150 kPa respectively resulting in an overconsolidation of between 50 to 100.0 kPa.

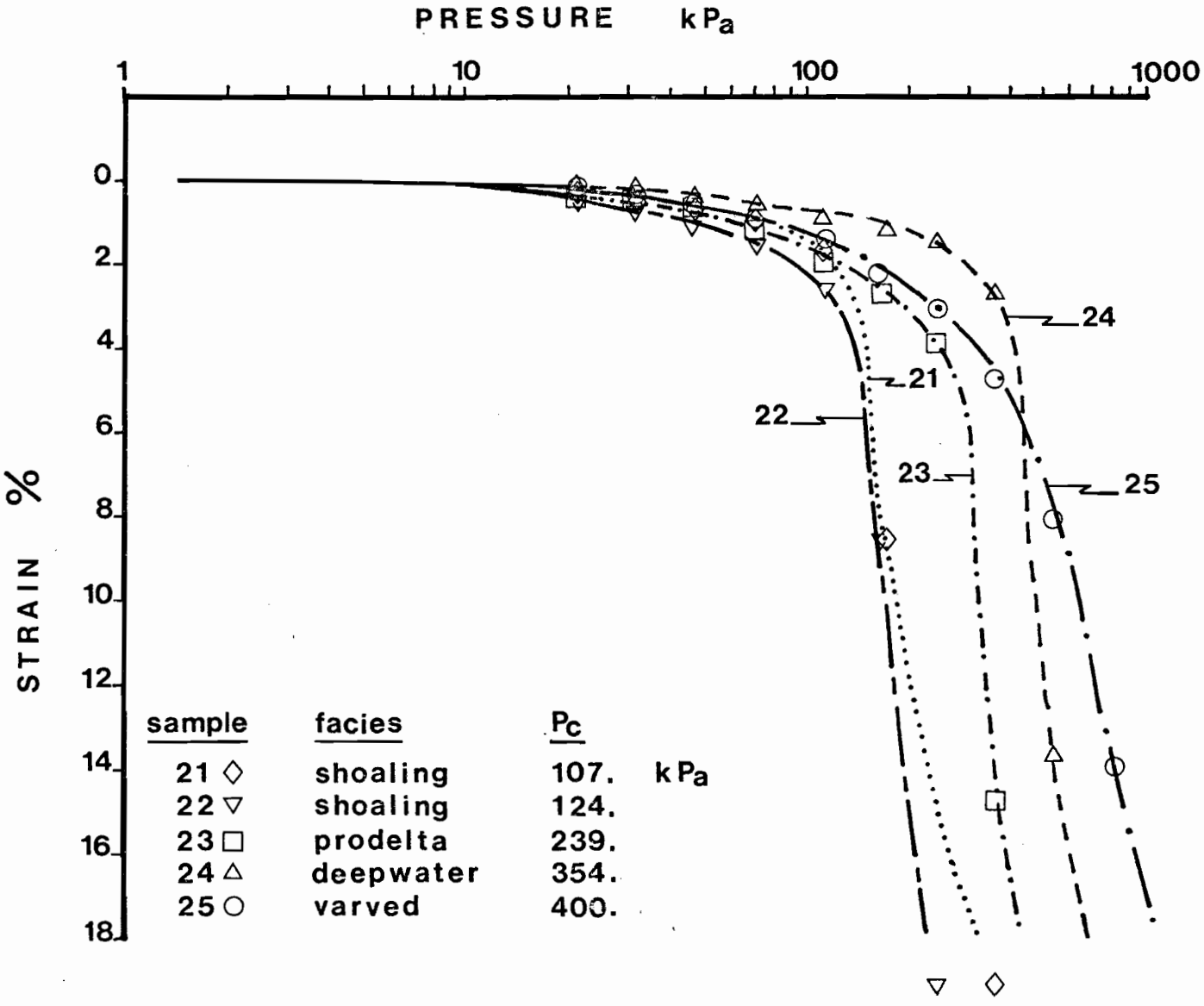

FIG. 3.5 CONSOLIDATION RESULTS - borehole 76-1-1

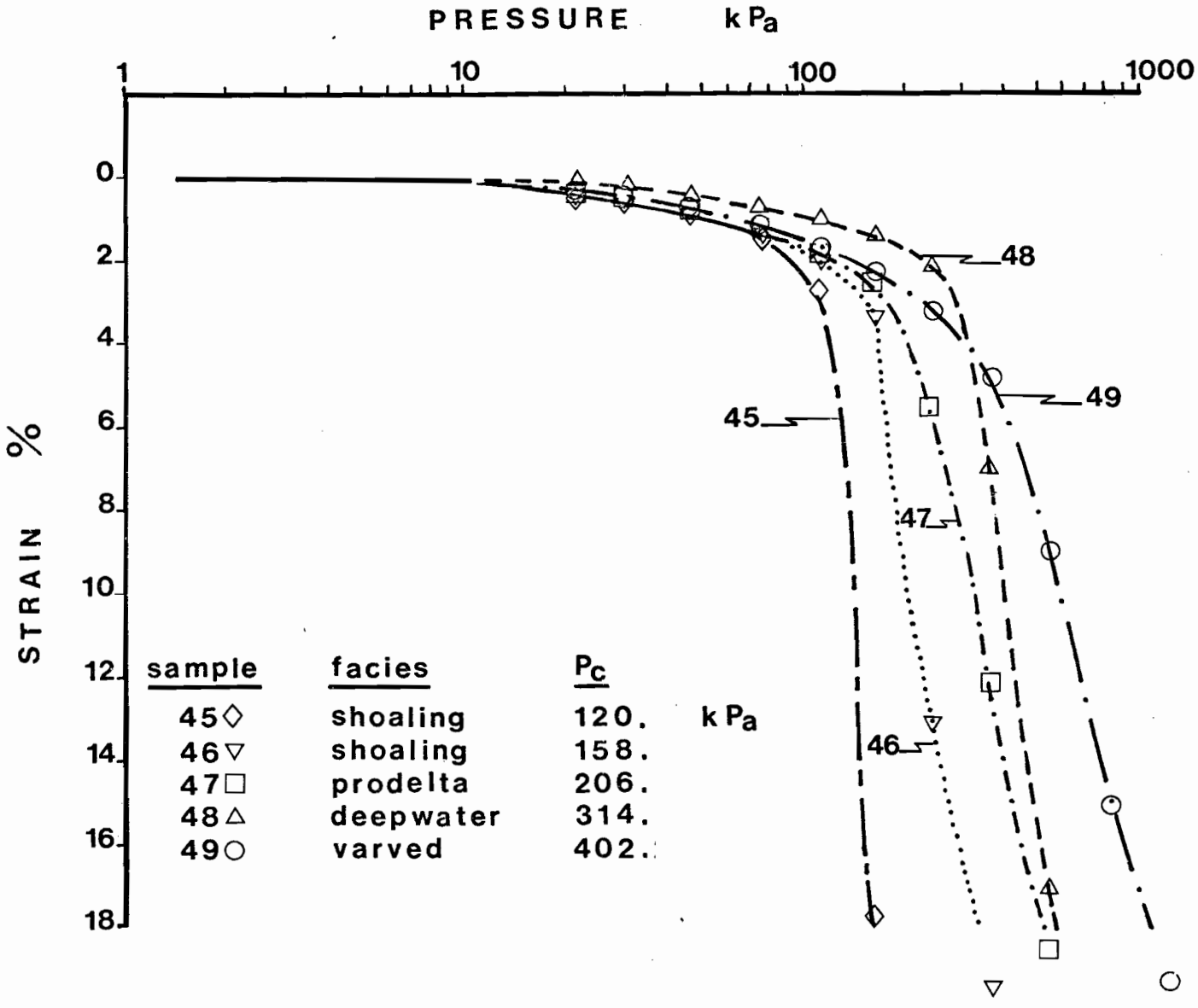

FIG 2.6 CONSOLIDATION RESULTS - borehole 76-1-2

One sample was obtained from the deepwater marine facies (24) and one from the boundary between the deepwater and the overlying prodelta clay (48). The consolidation curves for these two samples (figures 3.5 and 3.6) show that the clay is apparently stiffer than the overlying sediments. For the shoaling and the prodelta facies, the preconsolidation pressure occurred at about 2% strain, as compared to the deepwater facies where the preconsolidation pressure is at about 1% strain. An influencing factor could be that the clay is overconsolidated by 120.0 kPa to 160.0 kPa. The preconsolidation pressures are 354.0 and 314.0 kPa for samples 24 and 48 respectively. Both the higher preconsolidation pressure and the greater degree of overconsolidation may contribute to the general stiffening of the clay.

Samples 25 and 49 were obtained from the varved clay facies and show the difference between the consolidation behaviour of a freshwater clay as compared to the overlying marine clays. The break at the apparent preconsolidation pressure (see figures 3.5 and 3.6) is not nearly as pronounced as for the marine clays and the preconsolidation pressure is not exceeded before 3 to 4% strain or approximately double the marine clays. The preconsolidation pressures are 401.0 and 402.0 kPa for samples 25 and 49 respectively and are overconsolidated by 75.0 to 95.0 kPa.

All of the marine clays showed a definite break in the strain-log pressure curve at the preconsolidation pressure while the freshwater clay did not exhibit the same sharp break. The sharp break in the curve may be attributed to the flocculated structure of the marine clays as compared to the relatively non-flocculated fabric of the freshwater

clays. The deepwater marine clay was the most overconsolidated. No erosional break in the stratigraphic column was identified, which leads to the conclusion that the overconsolidation is due either to an increase in effective overburden stress or may be due to some aspect of the soil chemistry. To check the preconsolidation pressure for controls by the effective overburden stress, a regression analysis was performed on pairs of preconsolidation pressure and mean effective overburden stress. The slope of the curve was 0.79 with an intercept of -0.43 and a correlation coefficient of -0.95. The proximity of the correlation coefficient to 1.0 indicates an excellent correlation between the two variables and that the preconsolidation pressure is a function of the overburden stress. A similar regression analysis was performed on pairs of undrained strength (Su) and the preconsolidation pressure (Pc). The regression analysis resulted in a Su/Pc ratio of 0.24 and a correlation coefficient of 0.96. The Su/Pc is comparable to values reported by Haynes and Quigley (1976) and the correlation coefficient again indicates an excellent correlation between the two variables.

The overconsolidation ratio (OCR) for each of the soil units varied according to the depth from which the sample was obtained and the effective overburden stresses. The varved clay and deepwater facies had OCRs of 1.3 and 1.7 respectively, while the prodelta and shoaling facies had 1.5 and 1.4 respectively. The ratios indicate that the clay is lightly overconsolidated with respect to the effective overburden stress.

Apart from differences in the shape of the strain-log pressure curves, there does not seem to be any significant control of the preconsolidation pressures by

the stratigraphy. However, if one presumes that the permeability contrasts do in fact govern the pore pressure distribution (Hodge and Freeze, 1977), then the preconsolidation pressures are indirectly controlled by the stratigraphy.

3.4 Triaxial Testing

The primary objective of this section is to investigate the variation in the stress-strain characteristics, in the stress paths and the resulting Mohr envelopes between the four stratigraphic units. In this manner, it should be possible to determine if a particular stratigraphic unit is more susceptible to instability. Since Osterberg tubes were used to collect the samples, causing some disturbance, the Mohr envelopes were not used for the stability analyses. c' and $\emptyset$' can be obtained from either consolidated drained triaxial tests, consolidated undrained triaxial tests with pore pressure measurements, or drained direct shear tests (Duncan and Buchignani, 1975). A single drained test can take up to one week to complete depending on the permeability of the clay. Undrained tests with pore pressure measurements are considerably faster and a single test can generally be completed in one day. From each Osterberg tube sample, it is possible to perform four triaxial tests. Since there are ten tubes, hence forty tests, it was felt that undrained triaxial tests were the only feasible method to obtain the required strength parameters in the time available. Cell pressures used for defining a Mohr envelope should cover the range of anticipated in situ stresses. Effective overburden pressures can be obtained by measuring pore pressures in the field and horizontal stresses can be related to the vertical stress by the coefficient of earth pressure at rest (Ko). However, uncertainty exists

as to the value of Ko that should be used for sensitive clays of the Ottawa Valley (McEniry, 1978). Bozozuk (1977) suggests that Ko vary from 0.5 to 0.75. Work by Brooker and Ireland (1965) indicates that Ko may exceed 1.0 for heavily overconsolidated soils. From figures 3.4 and 3.5, it can be seen that the effective overburden stress ranges from 0.0 to about 300 kPa at 25 meters depth. Considering that the clays are only slightly overconsolidated, it was assumed that Ko would not exceed 1.0. Therefore, cell pressures for the triaxial testing program were chosen to span the entire range of effective overburden pressures. Equipment limitations would not accommodate cell pressures less than 34.0 kPa, hence the smallest confining pressure was set at this value. Other cell pressures were 68.0, 137.0 and 275.0 kPa. A back pressure of 206.0 kPa was used to ensure saturation. The tests were carried out at a constant loading press speed of 1.25×10^{-5} m/min. Pore pressures, deformations, and loads were measured using pressure gauges, dial gauges, and a proving ring respectively. Lo and Morin (1972) have shown that the energy stored in a proving ring during loading to failure will affect the post failure behaviour of the clay. It is acknowledged that a proving ring is not the best method for measuring loads, however no alternate means were available. Stress versus strain curves, pore pressure versus strain curves, stress paths, and failure envelopes are given in Appendix A for each tube sample (figures A2 to A21). Failure in all samples was defined as the maximum shearing stress.

Sampling disturbance and its effects on the stress-strain behaviour of sensitive clays has been discussed by Raymond et al. (1971). It is acknowledged that Osterberg tubes are not of the same quality as block samples, however the sampling method is often dictated by: the equipment

available; time; and cost. Osterberg samples were chosen for this study because they provided an optimum combination of cost and quality.

It is also acknowledged that simple consolidated undrained triaxial testing may not be the most sophisticated method for obtaining c' and Ø'. Here again, the testing program was designed to suit the equipment available. Also, due to the number of tests (38) that were to be performed, it was felt that standardized sampling and testing procedures would allow for a relative comparison between the triaxial tests.

Stress-strain and pore pressure-strain curves for the tube samples obtained from the shoaling prograding delta facies are shown in figures A2, A3, A7 and A8 for samples 21, 22, 45 and 46 respectively. Four triaxial tests were performed on all of the tube samples with the exception of sample 46 where only three were possible. Two of the triaxial samples for each tube were tested at confining pressure less than the preconsolidation pressure (Pc) and two greater than Pc. The change in the stress-strain behaviour above and below Pc can be seen on the above mentioned figures. Below Pc, the deviator stress increases rapidly with strain up to failure at about 1% strain, whereupon there is a substantial decrease in the deviator stress to a residual stress that is approximately 75% of the peak stress. For those samples tested at confining pressures greater than the preconsolidation pressures, the deviator stress reached a maximum at 3% strain and then remained constant up to 5% strain. Pore pressures show an increase with strain up to failure, whereupon they remain essentially the same, for those samples tested below Pc. Above Pc the pore pressures continue to increase even up to strains of 5 and 6%.

Stress paths are also an indication of the confining pressure in relation to Pc (Lambe and Whitman, 1969). Stress paths and mohr envelopes have been plotted for samples 21, 22, 45 and 46 on figures A12, A13, A17 and A18 respectively. The stress paths for samples tested at confining pressures less than Pc show a general increase in p ($(\sigma_1^1 + \sigma_3^1)/2$) up to failure after which both p and q ($(\sigma_1 - \sigma_3)/2$) decrease. Above the preconsolidation pressure, p decreases to failure while q decreases only by about 5 to 10.0 kPa following failure. With the exception of sample 21, the failure envelope can be approximated by two straight lines, the first connecting mohr circles for samples below Pc and the second being a straight line through the origin and tangent to the circles representing samples tested above Pc.

Samples 23 and 47 represent the prodelta facies. Stress-strain diagrams and failure envelopes are given in Appendix A (figures A4, A9, A14 and A19). For convenience, reference to a specific stress-strain, pore pressure-strain, stress path or mohr circle will be by a two number code. For example, the code for the stress-strain curve for sample 23, tested at a confining pressure of 34.0 kPa, is 23-34.0. Of the six samples tested at confining pressures less than Pc, all failed at strains of 1.5 to 2.0% with the exception of 47-137.0 which had a peak stress of 1.0%. After failure, all samples exhibited a 10 to 25% reduction in the deviator stress. Samples 25-275.0 and 47-275.0 were tested at confining pressures greater than Pc. However, contrary to the tests on the shoaling facies, where the deviator stress reached a maximum and remained constant, the prodelta facies experienced a decrease in the deviator stress by about 10-25%.

Stress paths for samples 23 and 47 show the same trends as the shoaling facies except for the samples tested above Pc where there was a decrease in q following failure. The failure envelopes for both samples were relatively linear and yielded cohesion values of 29.0 kPa and 30.0 kPa for samples 23 and 47 respectively and friction angles of 14.4^{o} and 17.8^{o} for the same two samples.

Sample 24 was obtained from the deepwater clay and sample 48 from the boundary between the deepwater and the prodelta clay. One triaxial test was spoiled for sample 24, hence only three tests could be made on the remainder of the Osterberg tube. Stress-strain and mohr envelopes for both samples are given in figures A5, A10, A15 and A20 in Appendix A. There appears to be a change in the stress-strain relationships for samples 24-34.0, 24-68.0, and 48-34.0 from that of the prodelta and shoaling facies. The deviator stress reaches its maximum at 1.0 to 1.5% strain whereupon there may be only a slight decrease or increase in the deviator stress up to 6% strain. Pore pressures also reached a maximum at about 1% strain and then remained constant. For samples tested at confining pressures other than the three above-mentioned samples, all show a sharp peak stress followed by strain softening. Pore pressures for the samples having strain softening remain: constant (sample 24-137.0); decrease after failure (sample 48-68.0); or increase (samples 48-137.0 and 48-275.0). It can be seen from figures A15 and A20 that the mohr circles result in a relatively linear failure envelope. The envelope was located by performing a regression analysis of the p and q values at failure and then back calculating c' and $\emptyset$' (see Attewell and Farmer, 1976, for method). c' is calculated to be 15.0 and 17.4 kPa for samples 24 and 48 respectively while $\emptyset$' is 29.0^{o} and 24.7^{o} respectively.

The fourth clay unit is the varved clay and samples 25 and 49 were obtained from this unit. Stress-strain and failure envelopes are given in figures A6, A11, A16 and A21 in Appendix A. Triaxial tests 25-34.0, 25-68.0, 49-34.0 and 49-68.0 have stress-strain curves with no sharp peak deviator stress. The deviator stress reaches a maximum at 1-2% and then remains constant up to 6% strain. Pore pressures for the same samples decrease after 1% strain and in the case of sample 25-34.0 is zero after 3.5% strain. The remaining samples tested at higher confining pressures have a peak deviator stress at about 1.5% strain followed by a reduction in the deviator stress of between 25 and 50%. Apart from sample 25-137.0 where the pore pressures decreased after 1.5% strain, the pore pressures reached a maximum at 1.5% strain and remained constant up to strains of 5%.

The stress paths and failure envelopes are shown in figures A16 and A21. The stress paths at low confining pressures are curved with p increasing by 20 to 40 kPa up to failure. At higher confining pressures, the stress paths are straighter and p decreases by about 20 kPa up to failure. The failure envelope for sample 25 has a pronounced curve while sample 47 has an envelope that is essentially linear. c' and $\emptyset$' were calculated from a linear regression and are 22.0 and 4.0 kPa for the cohesion and 29.0^{o} and 37.0^{o} for the friction angle.

From the preceding results, it is evident that there are essentially three types of stress-strain curves. Those for samples tested at low confining pressures where the deviator stress increases to a maximum at about 1.5% strain and then remains constant up to strains of 5% (see curve 25-34.0, figure A5). The second type of curve is the

rapid increase in the deviator stress up to failure (about 1.5% strain) followed by a 10 to 40% reduction in the deviator stress by strains of 5% (eg. sample 48-137.0, figure A10). The last type of curve is for those samples tested at confining pressures above the preconsolidation pressures. For those samples, the stress-strain curves exhibit a non-linear increase in the deviator stress to a maximum at 2.5% strain and then show a decrease in the deviator stress by no more than 5%. The pore pressures can also be classified into three types of curves depending on the preconsolidation pressure of the sample and the confining pressure. For samples tested with low confining pressures, but that have preconsolidation pressures of more than 400 kPa (samples 25 and 49), the pore pressures decrease after failure. For samples tested having the second type of stress-strain curve, the pore pressures increase to failure and then remain more or less constant or may show a slight decrease in pore pressures. Samples tested well in excess of the preconsolidation pressure (eg. 21-275.0) show an increase in the pore pressures even up to six percent strain.

A first impression of the triaxial results is that they tend to conform with the microfissuring model for sensitive clay developed by Mitchell (1970). Mitchell (1970) identified the three zones of sensitive clay behaviour as: the low stress zone where the strength is governed by microfissuring in the clay and the behaviour is similar to that of a granular material. Upon shearing, there is dilatancy and either a volume increase or a decrease in the pore pressures occurs. In the intermediate zone, the strength is controlled by the bonding and it is largely independent of the mean normal stress. In the third zone, where the mean normal stress is in excess of the preconsolidation pressure, the

clay behaves in an elastic-plastic manner. The boundaries between the zones can be expected to shift depending on the preconsolidation pressure of the clay. The sensitive clays of the Ottawa Valley have been divided into two groups: the fissured clays as described above and intact clays (Scott et al., 1976). Both clay groups are highly sensitive and landslides are evident in slopes composed of both fissured and intact clay. Generally speaking, the intact clay is found to the north of Ottawa while the fissured clay is located to the south of Ottawa (ibid.). It would appear that the intact clay is stronger than the fissured clay since unfailed slopes in the intact clay are generally higher and steeper than slopes in the fissured clay. Although the soil from the Casselman site was not analysed specifically for fissures, clay exposures within a kilometer of the site were fissured.

The contribution of the microfissure to the dilation of the clay during shearing is questionable. Yong and Warkingtin (1966) have shown that dilatancy is an integral component of the shearing resistance in overconsolidated clays. Moreover, Scott et al. (1976) have shown that dilatant behaviour occurs in intact clay tested at low confining pressures. Consolidation tests presented in the previous section indicate that the overconsolidation ratios vary between 1.3 for the varved clay facies and 1.7 for the deepwater facies. The clay therefore is only slightly overconsolidated with respect to the effective overburden pressure. However, since all of the triaxials tests were performed using the same set of confining pressures, the tests performed on the shoaling and prodelta facies are either close to or above the apparent preconsolidation pressure. The confining pressures for the deepwater and

the varved clay facies are below the preconsolidation pressure. The apparent preconsolidation pressure for the deepwater facies is between 314 and 354 kPa. Hence, at a confining pressure of 34.0 kPa, the behaviour of the clay approximates that of a heavily overconsolidated clay.

It should be apparent from the foregoing discussion and the stress-strain curves in Appendix A that the behaviour of the sensitive clay is a function of the preconsolidation pressure and the cell pressure at which the sample was tested. There does not appear to be any dependence of the effective stress parameters on the stratigraphic unit. This conclusion is similar to a study by McEniry (1978) on the undrained shear strength of the different clay facies for the Ottawa Region.

The question still to be answered is: what parameters govern the stability of natural slopes? Since the triaxial tests for each Osterberg tube sample span the full range of possible in situ stresses, it is apparent that a mohr envelope for each individual tube sample may not be representative of the c' and Ø' operative on a potential failure plane. The uncertainty in the choice of strength parameters is further justification for using a probabilistic approach to slope stability.

3.5 Chemistry and Mineralogy of Sensitive Clay Deposits

The relationships between the behaviour of sensitive clays and the chemistry of the pore fluid has been studied for some time (Rosenqvist, 1946; Bjerrum, 1954; Torrance, 1975; Yong, 1975; Haynes and Quigley, 1976). The interpretation of the pore water chemistry has generally been towards proving that the sensitivity of Eastern Canada

and Scandinavia clays is in part due to the leaching out of the salts from the pore fluid. A study of the pore water chemistry requires essentially two prerequisites. The first is a suitable method for determining the species and concentration of the various ions. The second requirement is a knowledge of the original depositional environment so as to determine the amount of leaching that has taken place since the formation of the clays. Unfortunately, there are upwards of ten methods for determining the pore fluid chemistry of a soil (Yong, pers. comm.) each of which results in different ionic concentrations. Ideally, the salt concentration and species should be determined in situ without any fabric disturbance. However, the tools for such an evaluation are not as yet available (Yong, 1975). The lack of test method standardization amongst researchers in the field of pore fluid chemistry makes the interpretation of results from different sources difficult.

There has been little research into the original environments in the Ottawa Valley. A possible approach would be a study of the micro fauna in the sediments. Many species have a very low tolerance to changes in salinity and are therefore good indicators of the paleosalinity (Gadd, pers. comm.). On the basis of a micro fauna study of one borehole east of Ottawa by the Atlantic Geoscience Centre, it would appear that there is a general reduction in the salinity towards the surface, however sufficient analysis was not made to determine the limits of the paleosalinity (Gadd, unpublished data). The geological history presented in the previous part must therefore be used as a preliminary basis for the interpretation of chemistry data.

Torrance (1975) reviewed the existing literature for chemical data on the sensitive clays of the Ottawa area. Five geochemical profiles are presented. The pore fluid chemistry has been related "to leaching and weathering processes and to the two-deposit origin of Leda clay in the Ottawa area". The two-clay theory was advanced by Gadd (1962) but has since been revised to include the four stratigraphic units described previously. Torrance has concluded that leaching of the sediments has been intense with the exception of the data for the South Nation Slide. The observations also indicate that the fissuring of the clay is the result of chemical weathering. Since the interpretation was based on the preliminary geological history of the region, it would appear that the conclusions presented by Torrance need to be reinterpreted.

Yong (1975) used a different method for determining the geochemistry of the soil and as a result sodium is no longer the dominant cation, which is usually the case for pore water chemistry determined on the fluid squeezed out of the soil (Haynes and Quigley, 1976). Although the results are not directly correlative with those presented by Torrance (1975) and Haynes and Quigley (1976), they do show a trend towards an increase in salt concentration with depth, which is consistent with the other investigators' findings.

Haynes and Quigley (1976) made an extensive study of the soil obtained from a number of borings near Hawkesbury, Ontario. Unfortunately, all of the samples were obtained from borings made in the bottom of an old abandoned channel and do not represent the complete stratigraphic column. Approximately thirty meters of sensitive clay has been eroded from the location of the borings. It is also

possible that there is a layer of fluvial clay overlying the sensitive marine clays at this site (Gadd, pers. comm.). The fact that the salinities are lowest just below the crust may indicate a surficial layer of freshwater clay.

A contract arrangement was made with Carleton University to analyze the samples obtained from boring 76-1-2 for pore water chemistry. The testing was carried out under the supervision of Torrance by Ault. Four major cations, Na^{+}, Mg^{+2}, K^{+}, and Ca^{+2}, were determined on the pore fluid squeezed out of the samples by high pressure consolidation. The resulting geochemical profile, pH and Eh are shown in figure 3.7. Na^{+}, the dominant cation, shows a marked decrease in concentration from ± 900 ppm to 105 ppm, at a depth of 8 meters, a linear increase to 500 ppm at 17.5 m followed by a sharp increase in concentration to 1350 ppm. The remaining three cations are found in about equal concentration. There is a decrease in the Ca^{+2} and Mg^{+2} cations from 100 ppm and 75 ppm respectively at a depth of 2.5 m to 12 and 22 ppm respectively at 17.5 meters, and then an increase to 52 and 60 ppm respectively. K^{+} showed a general increase in concentration with depth, 15 ppm at 4 meters to 33.5 ppm at 17.5 meters, followed by a sharp increase to ± 65 ppm. The data point of 180 ppm at 2.5 m is likely spurious and may be in error by one order of magnitude.

In situ porewater chemistry is a function of the original sea water composition plus the processes (eg. erosion, leaching, weathering) that have affected the chemistry through time. Comparison of the geochemical profile shown in figure 3.7 with those found in the literature must take the above-mentioned factors into consideration.

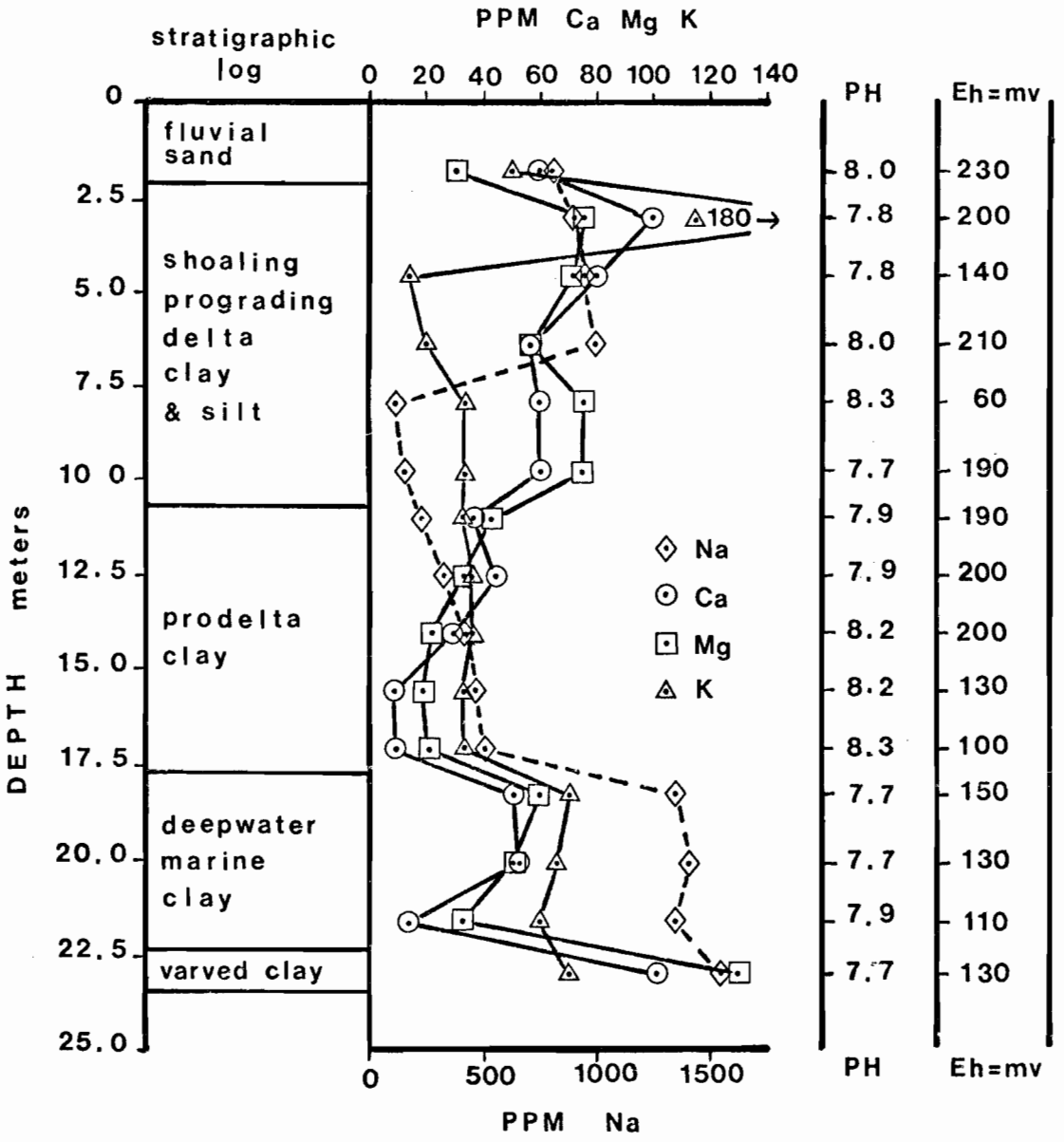

FIG 3.7 GEOCHEMICAL DATA

borehole 76 - 1 - 2

Data from Torrance (1975) and Haynes and Quigley (1976) show that Na^+ varies from a minimum of 20 ppm up to a maximum of 9600 ppm. The maximum concentration was recorded for a sample obtained from a boring in the bottom of an abandoned Proto-Ottawa River channel. Leaching has probably not been dominant in the development of the geochemical profile, since the area is relatively flat and hydraulic gradients are low. Hence, the pore water chemistry may reflect the original depositional environment. The soil at the Casselman site has likely been leached, as is evident by the Na^+ concentrations of less than 1500 ppm. The other three cation concentrations are similar to those reported upon in the literature.

Figure 3.7 shows that there is a sharp increase in the cation concentration at the boundary between the deepwater-prodelta clay. There is a distinct possibility that the depositional environment underwent a dramatic change from deepwater conditions to prodelta conditions. The change, however, was not abrupt from a visual standpoint as the clay seemed to show a gradation between the two units. Prest (1970) has shown that the Great Lakes drained for a time through the Ottawa Valley. This influx of freshwater may have been substantial enough to change the depositional environment. The increase in the salt concentration towards the surface may be due to a general increase in the salinity of the sea due to a reduction in the volume of meltwater originating from the glacial ice. With less mixing of fresh and salt water, the entire depositional environment may have been more saline during the deposition of the shoaling prograding delta clay. The lower ionic concentrations at the interface between the fluvial sand and the shoaling prograding delta clay could signify either leaching or the onset of the freshwater environment of the fluvial systems.

No quantitative mineralogy was made on the samples obtained from the boreholes. Haynes and Quigley (1976) concluded that the grain size distribution affects the mineralogy. The coarser the material, the higher the percentage of non-clay minerals. Based on the grain size data presented in table 2.1, one could expect that the prodelta facies would have the highest percentage of clay minerals, with the varved clay and the shoaling prograding delta having the least percentage of clay minerals.

3.6 Summary

Detailed slope stability studies required an estimate of the shear strength along a potential failure surface. The problem of determining the variability of strength parameters on a regional scale is beyond the scope of this thesis. However, it was considered practical to investigate the mechanical behaviour of the sensitive clay on a local scale in an effort to evaluate if there was a significant geological control of the strength characteristics.

It was shown in Chapter 2 that the sensitive clay deposits of the Ottawa Valley can be divided up into four distinct stratigraphic units. To determine if the mechanical behaviour of the clay was influenced by the stratigraphy, a field and laboratory testing program was initiated. Two borings were made near Casselman, Ontario, where shelby and Osterberg tube samples were taken and field vane shear tests performed. The shelby tube samples were used for stratigraphic analysis and porewater chemistry, while triaxial and consolidation tests were performed on the clay recovered by Osterberg sampling.

The results of the field vane shear tests are shown in figures 3.3 and 3.4. The testing interval was 1.5 meters and undrained strength measurements were made in each of the stratigraphic units. It is evident from figures 3.3 and 3.4 that the changes in undrained shear strength do not appear to coincide with the changes in the stratigraphic column. A regression analysis was made comparing the undrained shear strength and the effective overburden stress. The correlation coefficient between the two variables is 0.89, which indicates that for the most part the undrained shear strength is a function of the effective overburden stress.

The consolidation tests also show that there is little correlation between: the preconsolidation pressure (figures 3.3 and 3.4); the shape of the strain-log pressure curve (figures 3.5 and 3.6); and the stratigraphic unit. A regression analysis of the preconsolidation pressure versus the effective overburden stress yielded a correlation coefficient of 0.95, thus indicating an excellent correlation between the two variables.

The stress-strain curves and mohr envelopes from the triaxial tests did not yield any evidence that the mechanical behaviour is a function of the stratigraphic unit, but that it is instead dependent on the confining stress in relationship to the preconsolidation pressure.

The implication of the above-mentioned test results is that the behaviour of the sensitive clay is independent of the stratigraphic unit. It does appear though that the behaviour is dependent on the effective overburden stresses and the apparent preconsolidation pressure. From

a slope stability standpoint, it means that the effective stresses need to be accurately determined, so that triaxial tests can be performed at the anticipated in situ stresses. Moreover, soil samples for testing should be obtained from depths corresponding to the position of the failure plane and not specifically from the different stratigraphic units.

The results of the pore water chemistry analysis (figure 3.7) show an irregular cation profile with depth. The relatively low Na^+ concentration (105-1500 ppm) indicates that the clay has been leached. A comparison of the chemistry profile (figure 3.7), the geotechnical profile (figures 3.4 and 3.5), and the sensitivities (table A5) does not suggest that there is a significant correlation between the chemistry and the mechanical behaviour. This finding confirms an earlier study by Seekings (1974) for the sensitive clay involved in the South Nation River landslide, which is in a similar geologic setting as the Casselman site and is located some 5 km to the north.

4 - GROUNDWATER INVESTIGATIONS

4.1 General

Under rapid loading of cohesive soils, it is possible to determine the stability of a slope or embankment on the basis of a total stress analysis. In such a case, the angle of friction is taken to be zero, hence it is not necessary to evaluate the effective stresses acting on the failure plane. However, for natural slopes which have established some sort of equilibrium with the groundwater conditions, the slope should be analysed using effective stress procedures (Duncan and Buchignani (1975)). Since the effective stress is equal to the total stress minus the pore pressure, it follows that an estimate of the pore pressure distribution along the failure plane is required for the analysis. The understanding of the pore pressures "... must be based on a knowledge of the groundwater flow systems, which is in turn dependent on the regional geologic environment and the configuration of hydraulic conductivity contrasts... Where extensive funding is available and a slope failure or potential failure has been identified, piezometers can be installed and pore pressures can be measured directly. However, even with such measurements, extrapolations must often be made over large distances to approximate the pore pressure distribution between known points. These approximations can be improved with the use of mathematical models of the groundwater flow system. Such models can provide an independent check on the measured pore pressures and when anomalies arise, they may point to unanticipated field conditions that can lead to modification of field investigations." (Hodge and Freeze, 1977).

The above quote sums up well the problems involved with a field only investigation of the groundwater regime. Firstly, a field study is usually costly and can only be justified when a potential failure is identified, and, secondly, the data may not always be of sufficient quality and quantity to allow for a reasonable interpolation between piezometers. It is also evident that mathematical models can play a significant role in the understanding of the groundwater flow system, but it should be kept in mind that the use of a mathematical model alone does not afford the user any assurances that the calculated pore pressures are in fact close to the field values.

It is evident that field and numerical analysis complement each other; therefore, the research into the groundwater regime consists of both these components. Field data was obtained from three sites that were monitored from early May to late August. A finite element model developed by Neuman et al. (1974) was used to simulate the groundwater flow through sensitive clay slopes. Before any prediction was made on the role that geology plays in the pore pressure distribution in sensitive clay slopes, the model was checked against one of the field sites. After adjustments in the hydraulic conductivity and introduction of a bedrock sink term (to be described in a later section), a reasonable approximation of the pore pressure distribution at the field site was obtained mathematically.

With the hydraulic conductivities obtained from the simulation of the field sites, an investigation of the pore pressure distribution in slopes of different geologies was made. Since it appears that the hydraulic conductivity contrasts are the controlling factor in the pore pressure

distributions (Hodge and Freeze, 1977), it was decided that a concentration of effort would be made towards modelling those geological factors that would result in the largest contrasts in a given slope. Geological factors that are considered important are: depth to bedrock; nature of the surficial layer; number of soil layers; strength of a bedrock sink; and the depth of submergence.

In all, forty-six different geologic settings were simulated mathematically. For this thesis, only one slope angle and height were used. If one considers all the permutations and combinations including the forty-six different models that were analysed and a variable slope and height, the number of models required jumps to about 350. This was considered excessive and it was necessary to limit the geological factors investigated to the above-mentioned five.

To aid in the understanding of this part, a flow diagram of the organization is given in figure 4.1. The groundwater investigation is divided into two sections, one dealing with the field component and the other with the numerical analysis. The two sections overlap during the discussion of the verification of the finite element method using field data and also in the summary and conclusions dealing with the geological controls of pore pressure distribution in sensitive clay slopes.

4.2 Field Investigation

4.2a Site Locations

In an attempt to maximize the field input into the groundwater investigation, a classification of slopes

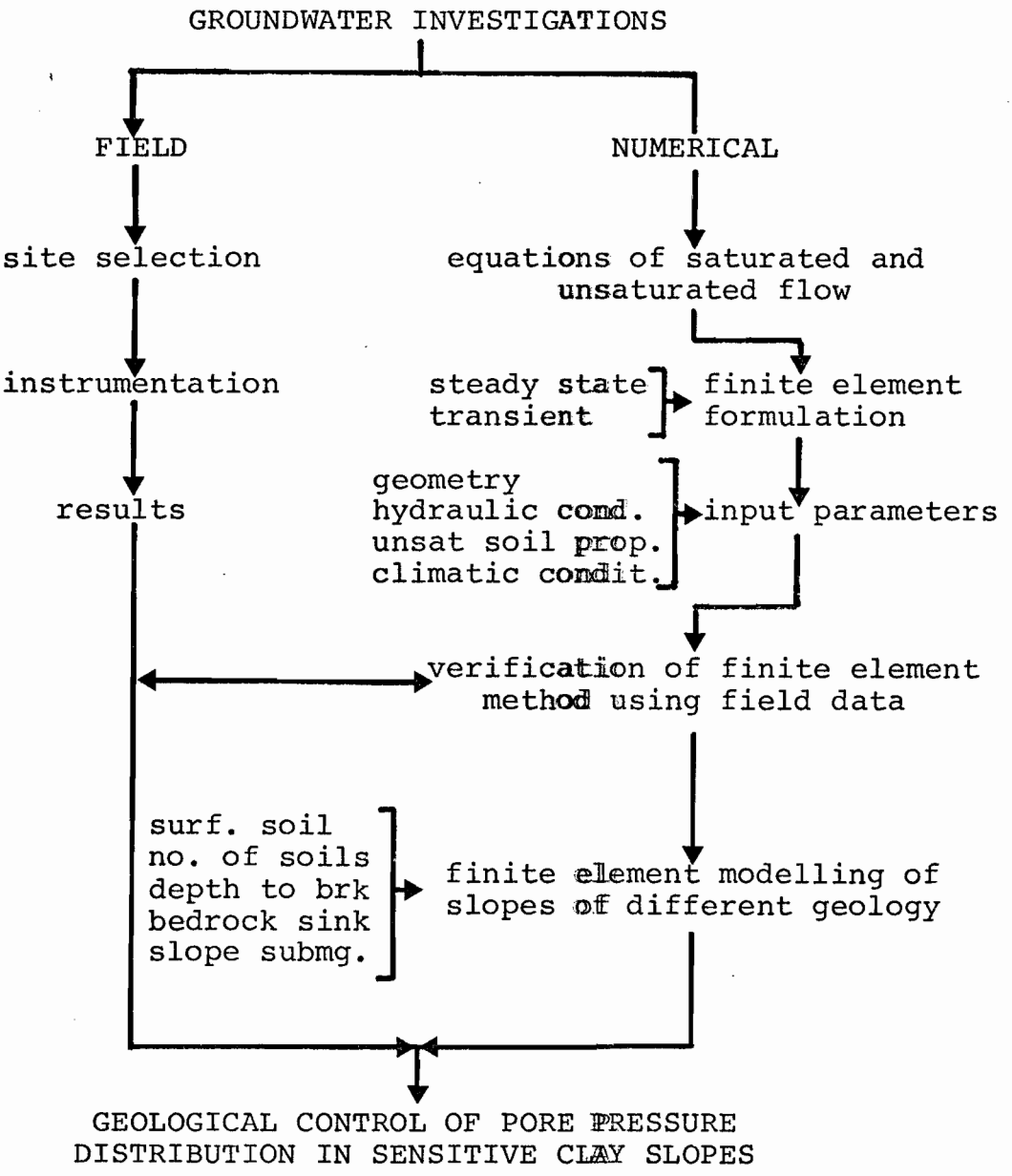

FIG. 4.1 FLOW DIAGRAM FOR CHAPTER 4

in the Ottawa Valley was made according to their stratigraphy. There are essentially two groups of slopes, those with a surficial layer of sand and those with clay at the surface. Charron (1974) has shown that, in a study area to the east of Ottawa, the sand on the surface represents a fast groundwater recharge zone relative to the recharge where clay is found at the surface. Since the rate of recharge will govern the response of the groundwater regime to climatic factors, it was felt that the broad slope classification would serve as a starting point for the field investigation. Profiles of the two settings are shown in figure 4.2.

Three sites were instrumented with piezometers, so that field data could be obtained on the type of pore pressure distribution which could be anticipated in geologic settings type A & B. The location of the field sites is shown in figure 4.3. Sites P1 and P2 are of setting A, while site P3 is of setting type B. The location of sites P1, P2, and P3 correspond to boring sites 74-1, 76-1 and 74-5 respectively, as shown in figure A1 (Appendix A).

Nine piezometers were installed at site P1, four at the crest, three at the mid-slope and two at the toe. In addition perforated pipes were installed at each of the piezometer nests and were used to measure the surface water table elevation. At site P2, ten piezometers were installed in two groups of five. One group or nest was installed near the crest of the slope, while the other group was installed about 130 meters back from the crest. Slope profiles, the elevation of the piezometer tips, and the mean measured pressure head for each of the piezometers are shown in figures 4.4a and 4.4b.

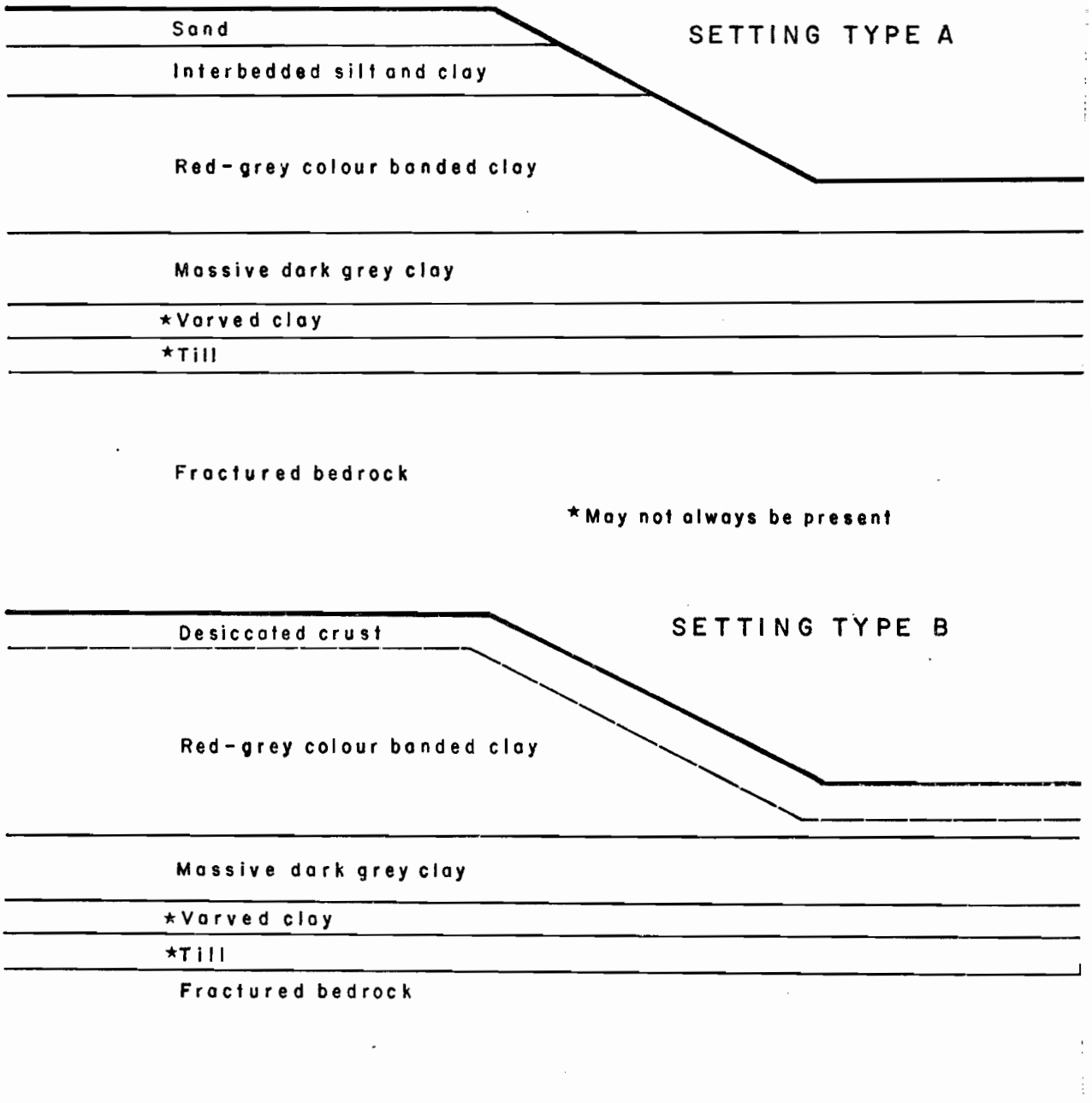

FIG 4.2 TWO TYPICAL SLOPE SECTIONS

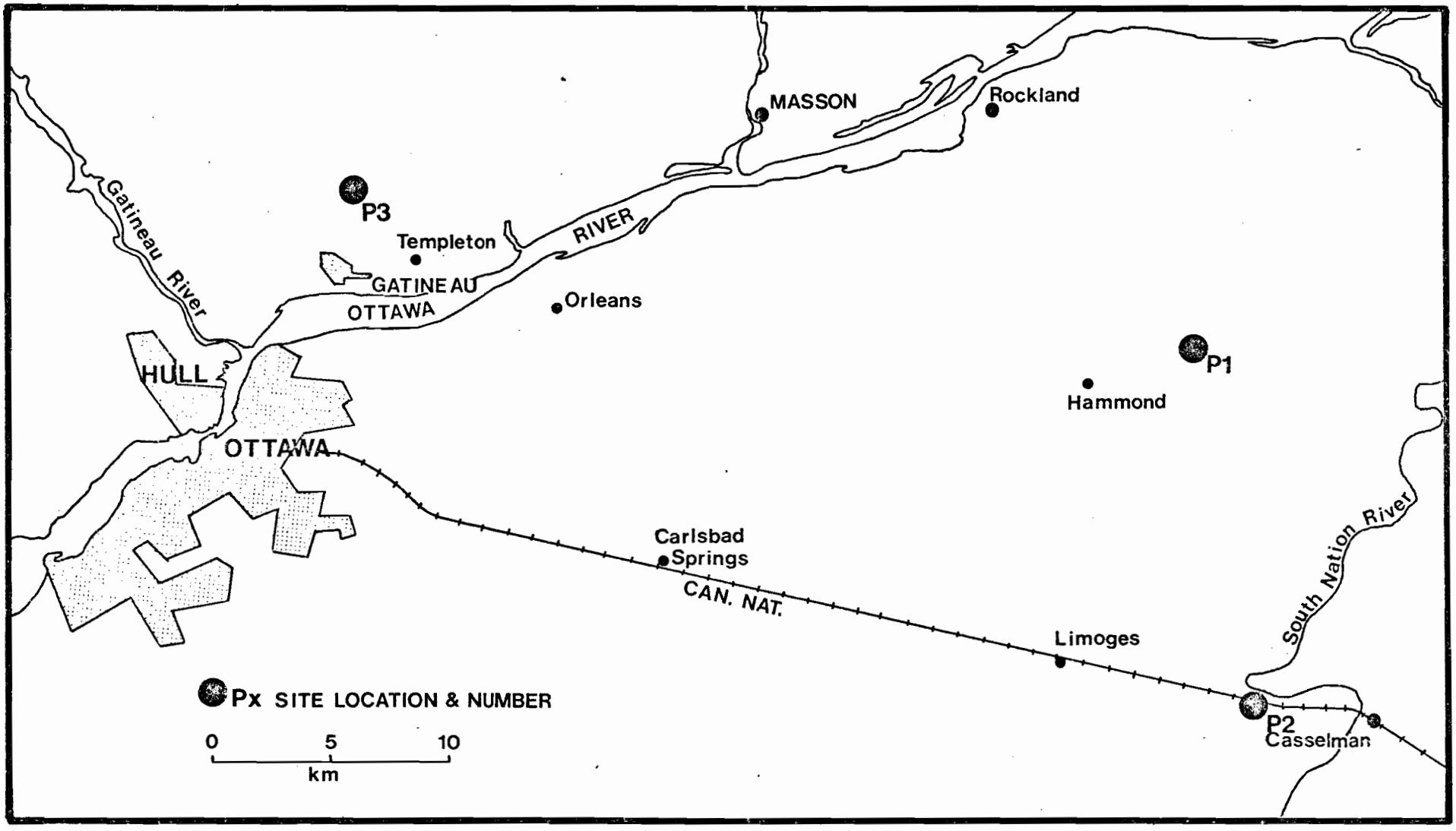

FIG 4.3 LOCATION OF INSTRUMENTED SLOPES

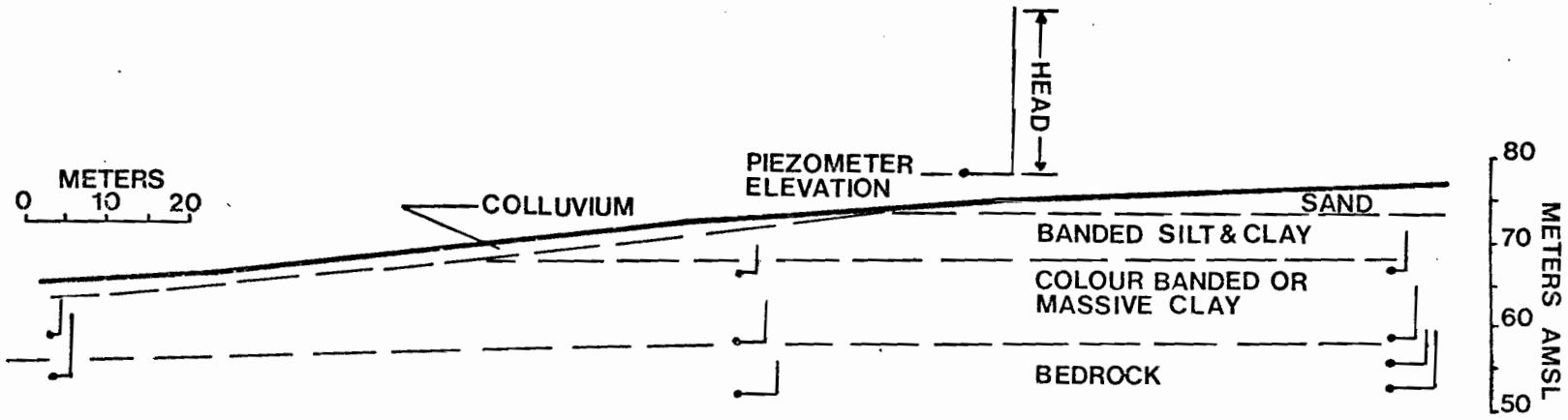

FIG 4.4a
SITE P1 PROFILE & MEAN HEADS

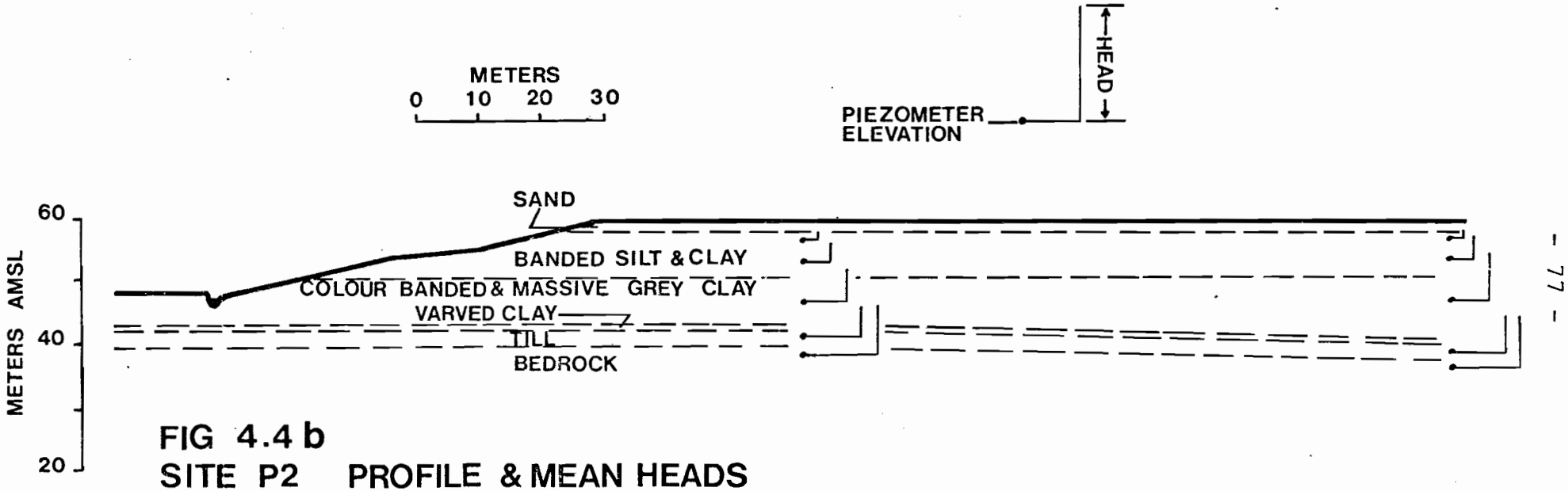

FIG 4.4 b
SITE P2 PROFILE & MEAN HEADS

At site P3, nine piezometers were installed, three at the crest, three at the mid-slope and three at the toe. The site profile, pressure head, etc., are shown in figure 4.4c. The data is not as complete for this site as the other two because of a number of factors. The piezometers had been installed in 1974 and those near the mid-slope had become obscured with soil and grass. Several attempts were made to establish the location of the piezometers, but with little success. It was not until late in the field season that the piezometers were located with the aid of a magnetometer; as a consequence, only one set of readings was obtained for this nest. One of the piezometers at the crest also caused problems. The packer used to measure the pore pressure became stuck down the hole. In order that the packer could be recovered, it was necessary that the entire piezometer be pulled out and the packer removed. Other commitments by the drill crew and the drill rig did not allow for the time required to reinstall the piezometer. The piezometers at the toe of the slope also caused some problems in that they were difficult to reach. The equipment which was used to take the pressure readings had to be carted down the slope with the aid of an all-terrain vehicle. Therefore, due to the logistics involved in taking the readings, more time was required, hence fewer measurements.

4.2b Instrumentation

Considerable research has been made on the design of piezometers and the relative merits of each design. A review of the subject of piezometer design is given by Lindberg (1965). Much of the foundation work related to piezometer characteristics was made by Hvorslev (1951).

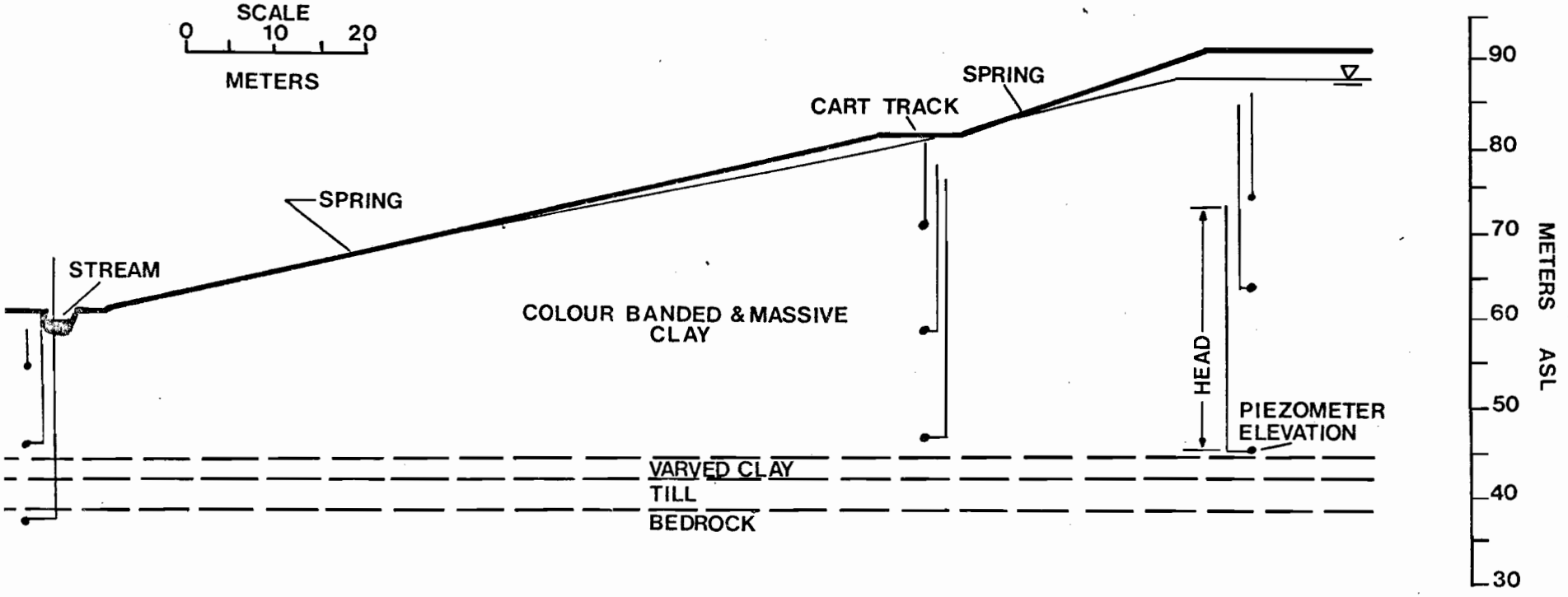

FIG 4.4c
SITE P3 PROFILE & MEAN HEADS

In a paper, he (Hvorslev) stated that "the total volume of flow required for equalization of differences in hydrostatic pressure in the soil and in the measuring device depends primarily on the permeability of the soil, the type and dimensions of the device, and the hydrostatic pressure difference". For a rapid response to changes in pressure, the volume of water required for the equalization of pressure should be kept to an absolute minimum. Also, the intake screen should be large so that the volume of water involved can be drawn from the greatest possible volume of soil. Further consideration for the piezometer design is that there is no seepage along the interface between the piezometer and the soil. Otherwise, the recorded pressure will be influenced by strata other than the one which is of interest.

The piezometers used for this study are essentially the same as described by Brooker et al. (1968). In essence, the device consists of a well point and screen which are installed in a pre-drilled borehole (see figure 4.5a). Pore pressure measurements were made using an inflatable packer and transducer (figure 4.5b). A detailed description of the installation procedures and equipment schematic is given in Appendix C.

4.3 Results of Field Monitoring of Pore Pressures

4.3a Site P1

The most complete set of results was obtained from this site. Readings were made on a weekly basis from early May to late August 1976. It is felt that the time period covered by the readings should have registered the maximum springtime pore pressures and the summer minimum

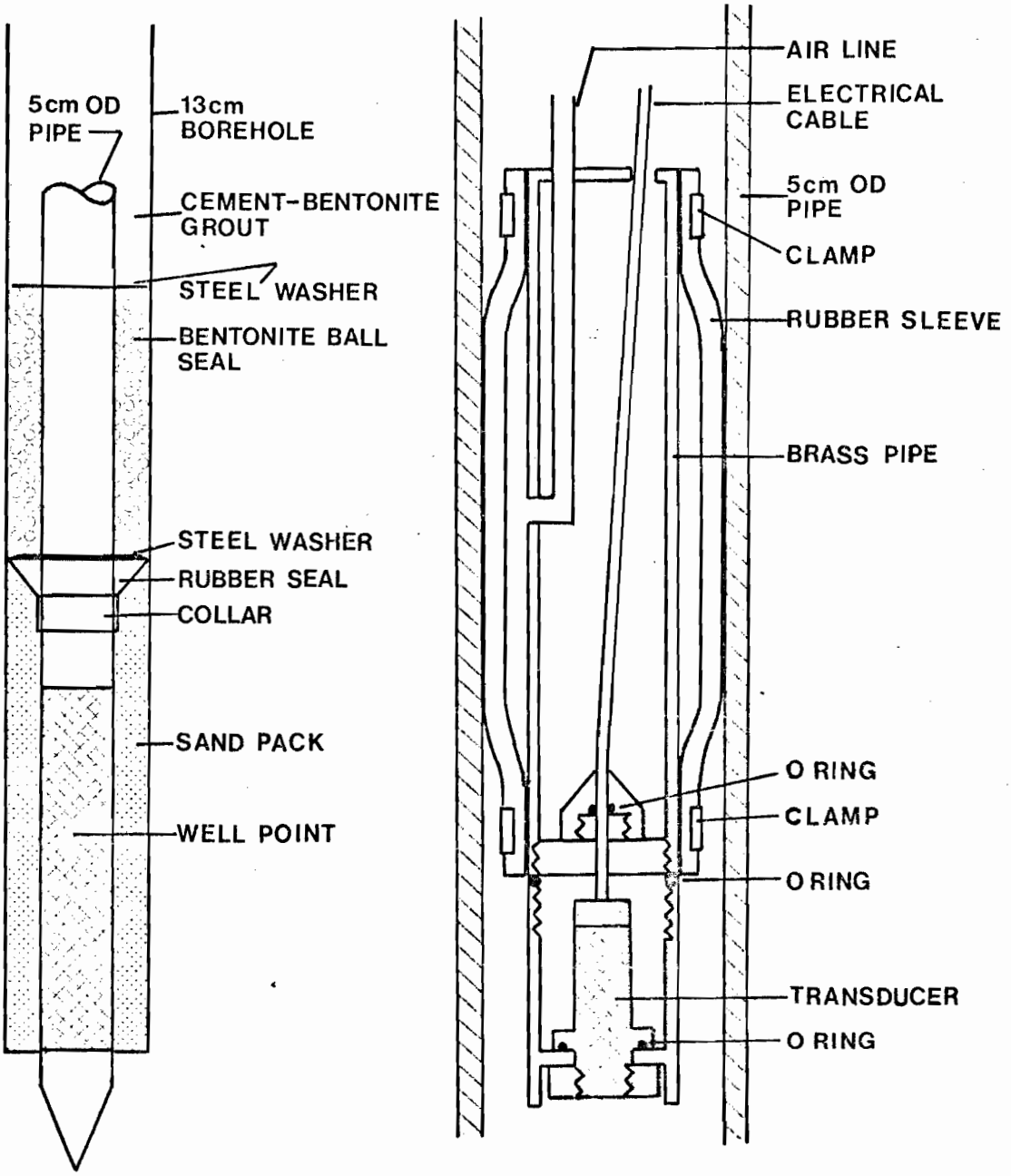

a- WELLPOINT & SEALS b- PACKER ASSEMBLY

FIG 4.5 PIEZOMETER DESIGN

pore pressures. The results have been tabulated and are shown in table 4.1. Mean values of the pressure head have been plotted in figure 4.4a. A graphical representation of the mean, maximum and minimum pore pressure is shown in figure 4.6. These results show that the major component of the groundwater flow is in the vertical direction. Three piezometers are at about the same elevation: one at a depth of 18.5 meters at the crest, one at 15 meters at the mid-slope, and one at 6 meters at the toe. The mean pressure head measured at each of the three piezometers is 3.57 m, 3.37 m and 4.48 m respectively. The distance between the toe piezometer nest and the mid-slope piezometer nest is about 85 meters, which therefore yields a horizontal gradient of 0.012. Vertical gradients at the mid-slope are in the order of 1.40 or better than two orders of magnitude greater than the horizontal gradients.

Variation in pore pressures is not the same throughout the entire slope. Table 4.1 shows the standard deviation and variance of the measured pore pressures. Standard deviations range from a minimum of 1.0 kPa to 9.9 kPa at the piezometers located in the mid-slope nest. All other deviations were within this range. Trends are difficult to establish as there does not appear to be any pattern to the variation. Perhaps what is significant is that the variation in pore pressure cannot be assumed to be a constant throughout the entire slope. Risk analysis of slope stability which incorporates a single variance to represent the entire pore pressure variation (Yong et al., 1977) does not adequately represent the pore pressure behaviour. It can be speculated that the lag in pressure response to precipitation is different throughout the slope, thereby complicating probability estimates of the pore pressure. In other words,

PIEZOMETER NEST AT THE CREST OF THE SLOPE

DEPTH METERS	PORE PRESSURE X 10^2 kPa MEAN	MAXIMUM	MINIMUM	STANDARD DEVIATION	VARIANCE X 10^4 kPa^2
28	.700	.750	.670	.030	.0009
18.5	.350	.431	.220	.062	.0400
15	.585	.750	.501	.079	.0063
9	.502	.631	.460	.059	.0035
PIEZOMETER NEST AT THE MID-SLOPE					
15	.330	.340	.317	.010	.0001
10.5	.512	.714	.388	.099	.0098
5.8	.298	.326	.278	.019	.0003
PIEZOMETER NEST AT THE TOE OF THE SLOPE					
10	.714	.870	.631	.078	.0061
6	.439	.501	.371	.042	.0017

TABLE 4.1 SUMMARY OF PIEZOMETER MONITORING, HAMMOND, SITE P1

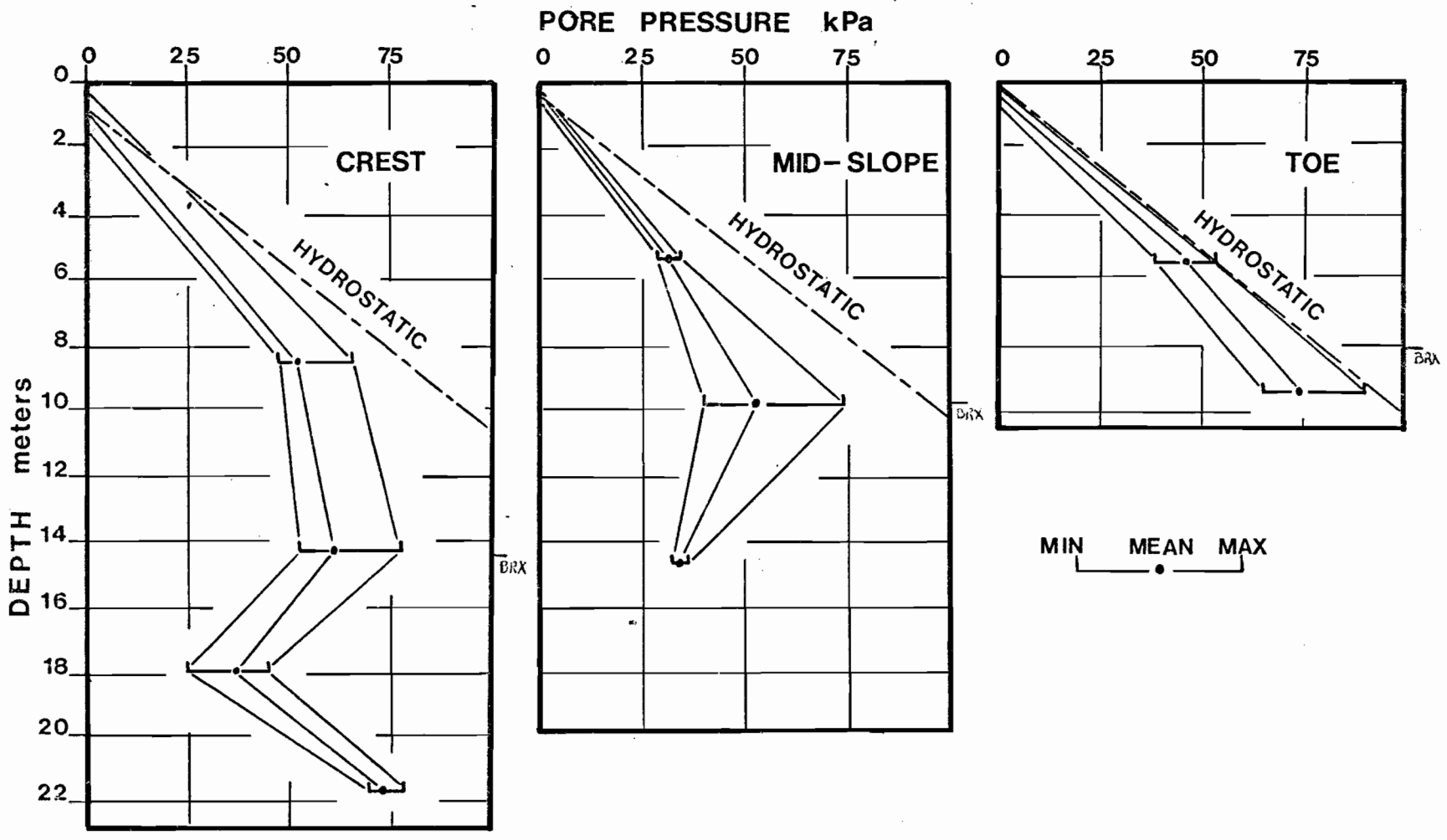

FIG 4.6 PORE PRESSURE VS DEPTH SITE P1

the pore pressures measured in certain portions of the slope may not have had time to adjust to recent precipitation-evaporation, hence there may not be an instantaneous increase in pressure at depth corresponding to fluctuations in the water table surface.

4.3b Site P2

Site P2 has essentially the same geologic setting as site P1. The major differences are that site P2 has a small stream at the toe and the thickness of the surficial material is about 6 meters greater at site P2. Despite these differences, there are certain similarities in the pore pressure distribution. The hydraulic gradients are again larger in the vertical direction as compared to the horizontal. From figure 4.4b, it can be seen that piezometers at the same elevation have close to the same pressure head. Mean, maximum and minimum pore pressures are shown in figure 4.7. The data used to plot the curves shown in figure 4.7 is listed in table 4.2. In general, the standard deviation of the pore pressure measurements at the various piezometers tends to be about the same at the two sites. Of interest at site P2 is the lower piezometric levels in the bedrock. This indicates that the bedrock is not being recharged fast enough to maintain a higher piezometric level. The variation in the pore pressure in the bedrock is smaller than the overlying sediments, which leads to the conclusion that the bedrock aquifer is relatively unaffected by short-term climatic fluctuations. The largest recorded pressure variations are at the mid-depth piezometers near the crest of the slope. These large variations are likely due to the effect of the slope on the recharge of the ground-water during the summer months. In the springtime, during the snow melt, there is sufficient water to maintain high

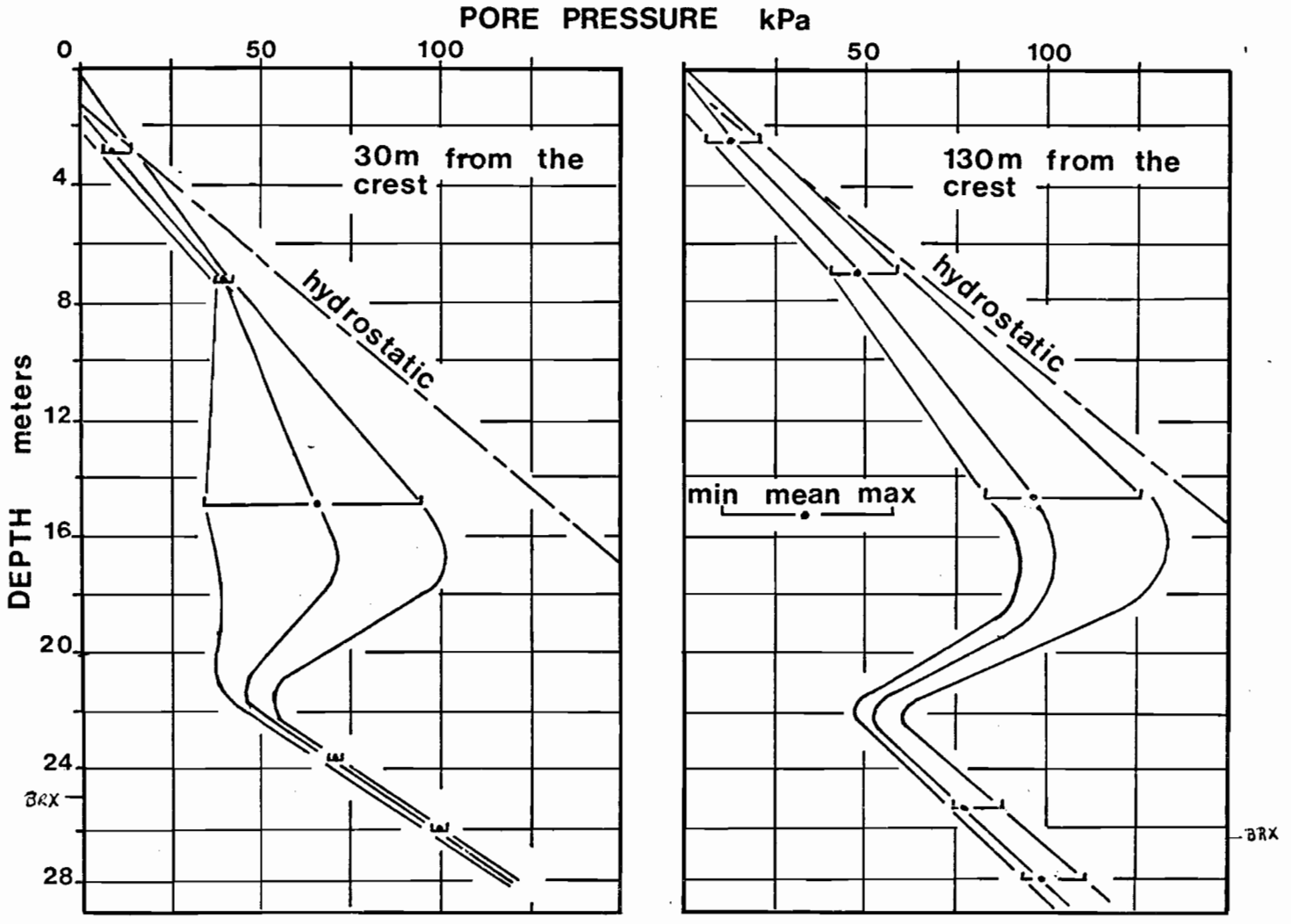

FIG 4.7 PORE PRESSURE VS DEPTH SITE P2

PIEZOMETER NEST 130 METERS FROM CREST OF SLOPE

DEPTH METERS	MEAN	MAXIMUM	MINIMUM	STANDARD DEVIATION	VARIANCE x 10^1 kPa^2
			PORE PRESSURE X 10^2 kPa		
28	.975	1.08	.912	.052	2.72
26	.770	.852	.726	.030	.88
15	.949	1.226	.816	.148	21.93
7.5	.480	.592	.415	.057	3.24
3	.140	.214	.066	.055	3.02

PIEZOMETER NEST 30 METERS FROM CREST OF SLOPE

27	1.000	1.010	.980	.019	.35
24	.678	.693	.661	.015	.22
15.5	.647	.974	.346	.217	46.97
8	.402	.431	.392	.001	..10
3	.118	.156	.092	.026	.70

TABLE 4.2 SUMMARY OF PIEZOMETER MONITORING, CASSELMAN, SITE P2

piezometric levels near the crest; however, as the recharge diminishes during the summer months, the drawdown effect of the slope becomes more influential.

It should also be noted that the upper 14-18 meters of the slope experience near hydrostatic conditions during periods of prolonged recharge. However, the soil below 18 meters experiences below hydrostatic conditions throughout the recording period. In terms of slope stability the portion of the slope having high pore pressures will affect the location of the critical circle as well as the calculated factor of safety. The assumption of complete hydrostatic conditions would definitely underestimate the factor of safety. There appears to be strong climatic control of the pore pressures in at least the upper portion of the slope. This being the case, then the combination of a heavy winter's snowfall, with a minimum amount of melt during the winter and a slow but steady melt in the early spring, would likely produce the highest pore pressure and the minimum factor of safety.

4.3c Site P3

As previously stated, the data from this site are not extensive. The mean pressure heads which are shown in figure 4.4c reflect the general trend of the groundwater flow. As a supplement to this data, a site which was instrumented by the Quebec Department of Natural Resources is included here (Chagnon, 1975). This site is only a couple of kilometers to the east of site P3 and has a similar geological setting. Site P3 had no surficial layer of sand; however, the clay at the surface was fissured and desiccated. Only one piezometer was installed in the bedrock, and that was at the toe of the slope. The bedrock was not cored

and no record could be obtained as to the rock type. Maps of the area indicate that the clay is underlain by Precambrian gneiss (Wilson, 1941).

Curves showing the change in pressure head with depth are presented in figure 4.8. The difference from the two previously described sites appears to be that there is no lower piezometric surface in the bedrock. In fact, the flow regime more or less approximates the neoclassical theory described earlier. There is downdrainage or recharge to the groundwater regime at the crest of the slope, as is shown by the decreasing head with depth. The toe of the slope has artesian pressures indicating a discharge zone. The flow of water from the piezometers at the toe was slow, perhaps 5 litres/min, which would indicate that, even though there is artesian pressures, the permeability is not sufficient to produce large volumes of water. The underlying bedrock must, therefore, be considered to have a significantly lower permeability than the bedrock underlying sites P1 and P2. The bedrock does not maintain a vastly lower piezometric level in the bedrock; it is likely of high enough permeability to cause the break in the pressure-depth curve for the piezometers at the crest (figure 4.8).

The site of the Quebec Department of Natural Resources (DNR) is shown in figure 4.9. Although several piezometer nests were installed and reported upon, only two will be shown here. The same general drawdown or recharge conditions are evident at the crest; however, there are no artesian pressures at the toe. The area is underlain by carbonate rocks, which are much more permeable. The bedrock appears to be able to maintain a piezometric level below that of the elevation of Leamy Creek in the Valley.

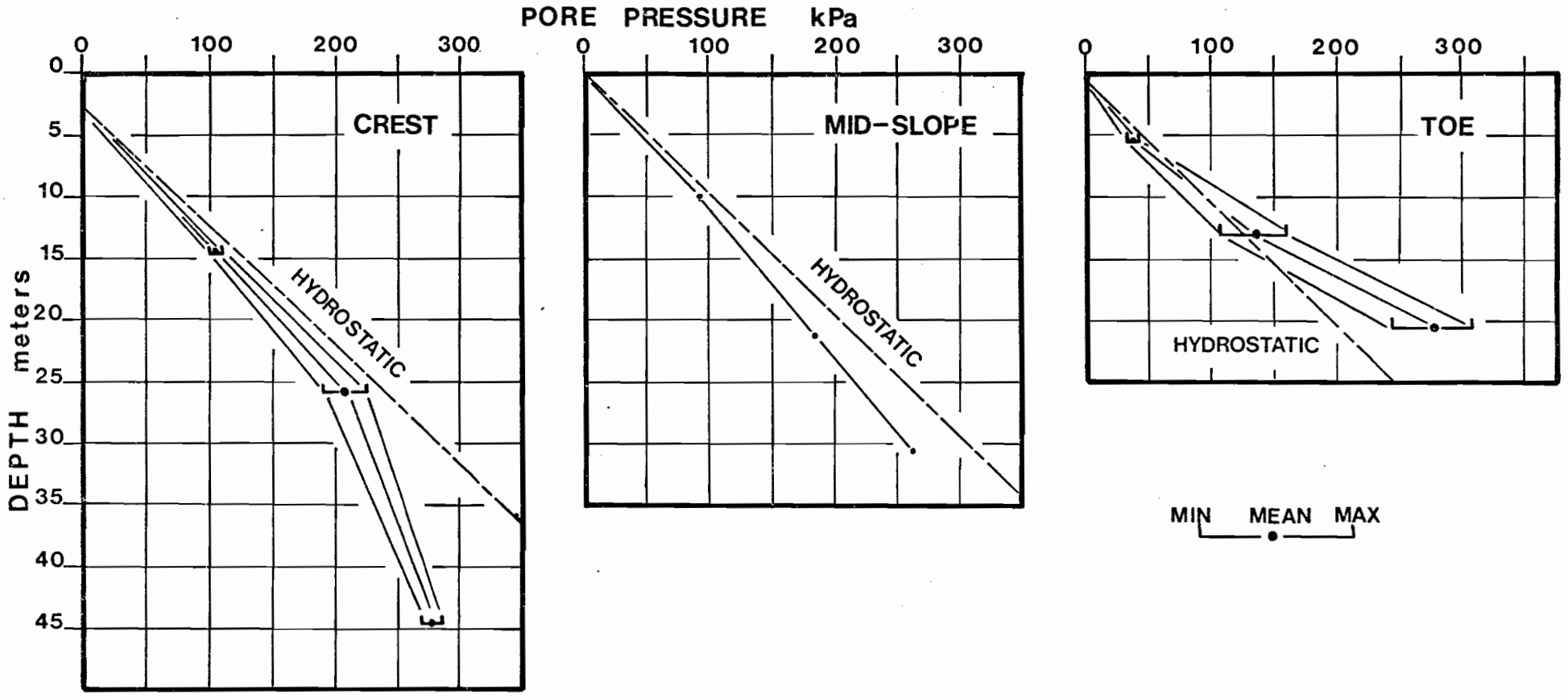

FIG 4.8 PORE PRESSURE VS DEPTH SITE P3

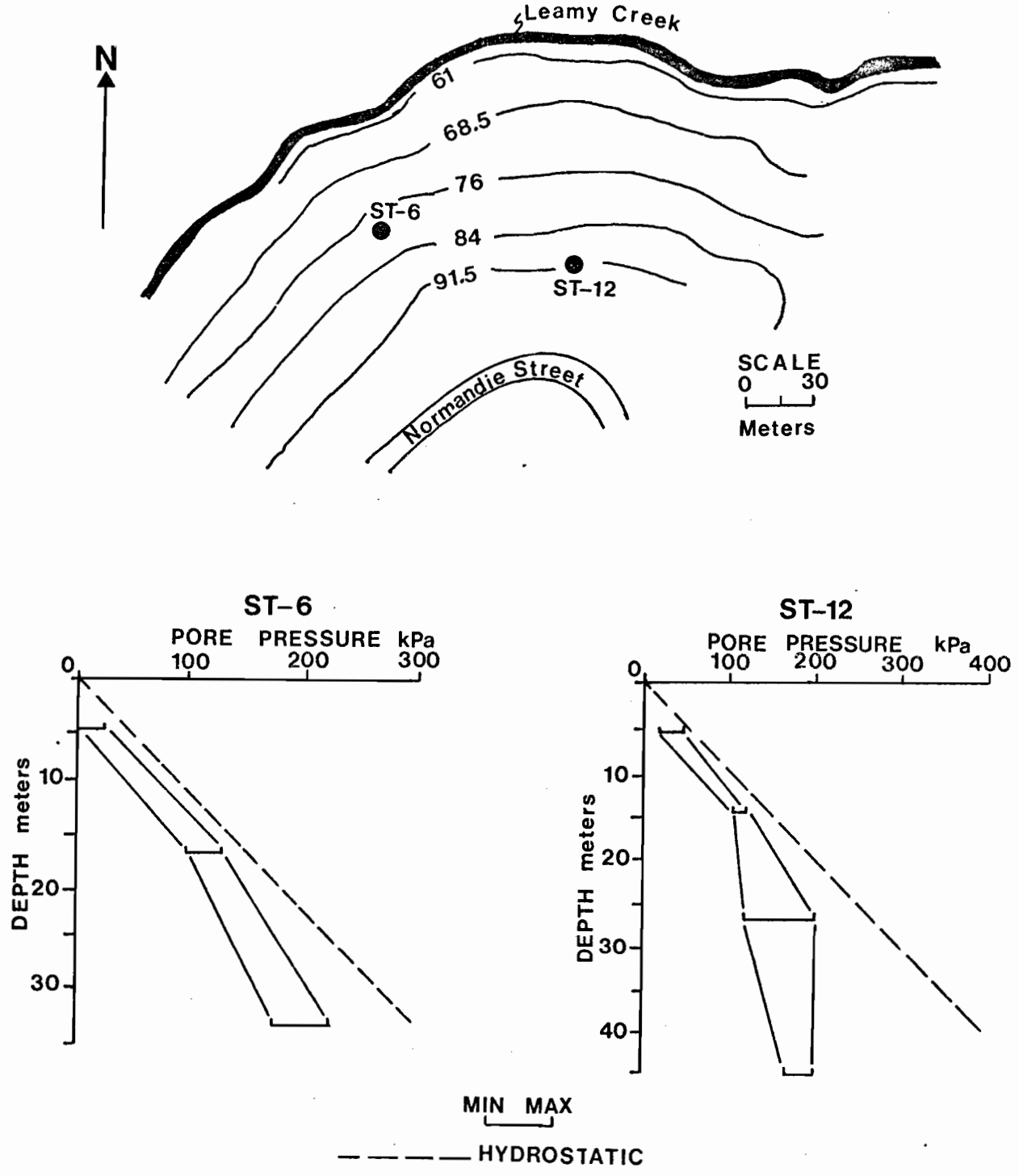

FIG 4.9 LOCATION MAP & PORE PRESSURE VS DEPTH DATA FOR HULL SITE (AFTER CHAGNON 1975)

Even with this lower piezometric level, the pressure-depth curves do not have the same shape as those from sites P1 and P2. This would lead to the conclusion that the surficial layer of sand is important in terms of the flow regime in the underlying clay. The bedrock will govern the amount of drawdown in the crest of the slope and also whether or not artesian pressures will occur at the toe. Common to all four sites is the presence of near hydrostatic pressures near the upper portion of the profile at the crest. Again, the nature of the surficial layer will govern the amount of infiltration at the crest and, ultimately, the recharge to the groundwater system. The higher drainage density in the regions where clay is at the surface than where sand is the surficial layer indicates that there is considerable more runoff in the clay regions. The sand maintains not only a high groundwater table but also keeps the underlying clay saturated.

4.4 Numerical Analysis of Groundwater Flow

4.4a Equations of Saturated and Unsaturated Flow

Saturated flow through porous media has been adequately defined by Darcy's Law. An explanation of the relationship which states that the velocity of flow equals the hydraulic gradient multiplied by a constant can be found in any basic text on groundwater (eg. see Harr, 1962). Darcy's law is presented symbolically in equation 4.1.

$$V_{x_i} = - K_i \frac{\partial h}{\partial x_i} \qquad (4.1)$$

V_{x_i} = velocity
K_i = hydraulic conductivity
h = total head
x_i = length
i = 1, 2, 3 where 1& 2 are horizontal and 3 is vertical

It can be shown (Harr, 1962) that the total head at any point in the flow domain is:

$$h = \frac{p}{\gamma} + x_3 \qquad (4.2)$$

h = total head
p = pressure
γ = unit weight of water
x_3 = height above an arbitrary plane

Where there is a difference in head between two points, water will flow from the point of greater head or potential to that of the lower head or potential. Where the soil is saturated, the pressure is positive. In the unsaturated zone above the water table, there is a soil suction due to the unsaturated nature of the soil and the resulting pressure is negative. The magnitude of the soil suction is dependent on a number of factors, to be described in detail in a later section.

For Darcy's law, K is defined as being a constant. This is the general case for saturated soils; however, in the case of unsaturated soils, K is dependent on the volumetric water content. A more detailed discussion of variation in the hydraulic conductivity as a function of the water content will also follow in a later section.

Consider the water flowing through an element of soil. The components of the flow velocity in the three principal directions can be seen in figure 4.10.

The mass input flux of water is:

$$\frac{\partial M_{in}}{\partial t} = \text{Mass input flux} \qquad (4.3)$$

M = mass
t = time

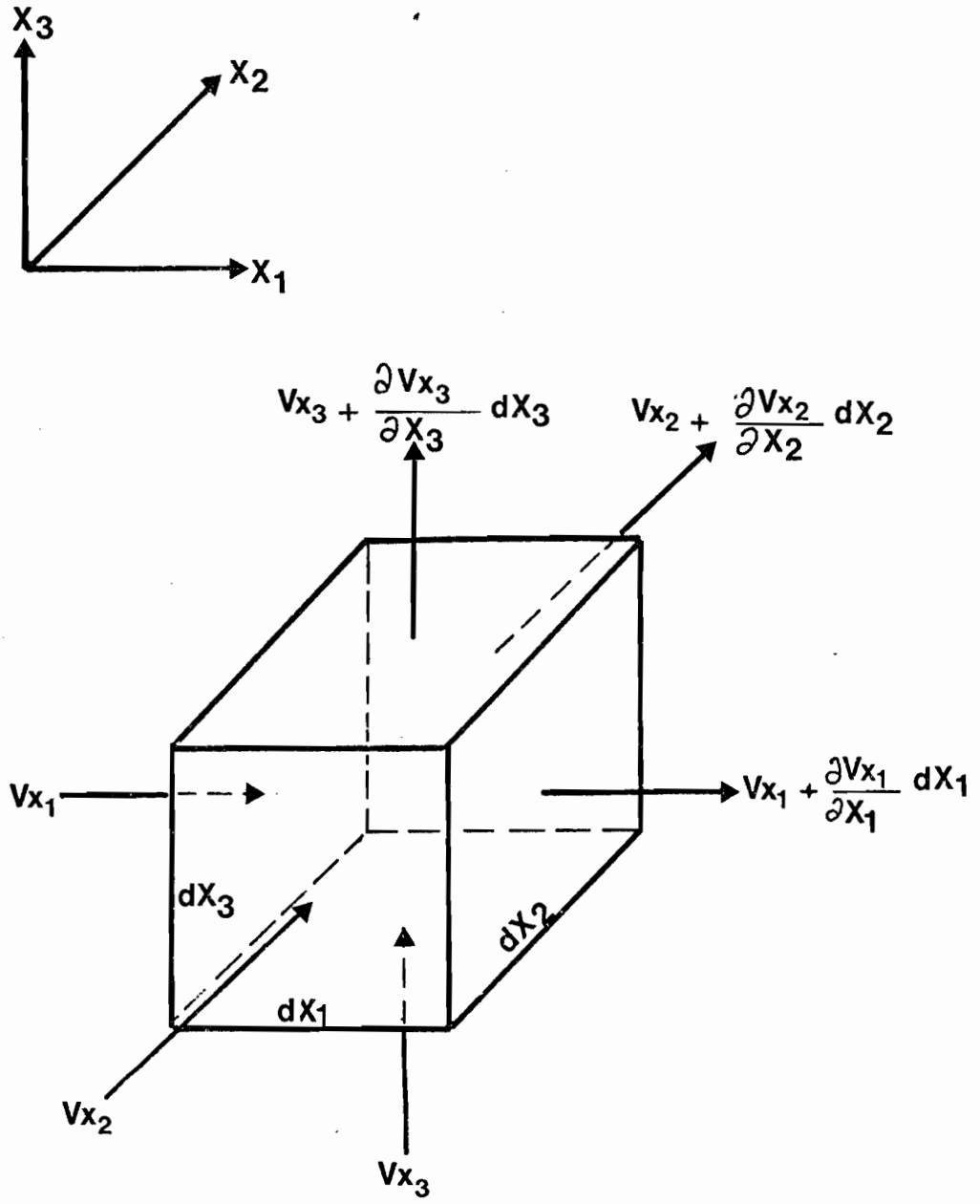

FIG 4.10 FLOW THROUGH A SOIL ELEMENT

and in the principal directions:

$$\frac{\partial M_{in\ x_1}}{\partial t} = \gamma V x_1\ dx_2\ dx_3 \tag{4.4a}$$

$$\frac{\partial M_{in\ x_2}}{\partial t} = \gamma V x_2\ dx_1\ dx_3 \tag{4.4b}$$

$$\frac{\partial M_{in\ x_3}}{\partial t} = \gamma V x_3\ dx_1\ dx_2 \tag{4.4c}$$

Therefore,

$$\frac{\partial M_{in}}{\partial t} = \frac{\partial M_{in\ x_1}}{\partial t} + \frac{\partial M_{in\ x_2}}{\partial t} + \frac{\partial M_{in\ x_3}}{\partial t} \tag{4.5}$$

The mass output flux is:

$$\frac{\partial M_{out\ x_1}}{\partial t} = \gamma\left(V x_1 + \frac{\partial V x_1}{\partial x_1}\ dx_1\right)\ dx_2\ dx_3 \tag{4.6a}$$

$$\frac{\partial M_{out\ x_2}}{\partial t} = \gamma\left(V x_2 + \frac{\partial V x_2}{\partial x_2}\ dx_2\right)\ dx_1\ dx_3 \tag{4.6b}$$

$$\frac{\partial M_{out\ x_3}}{\partial t} = \gamma\left(V x_3 + \frac{\partial V x_3}{\partial x_3}\ dx_3\right)\ dx_1\ dx_2 \tag{4.6c}$$

and:

$$\frac{\partial M_{out}}{\partial t} = \frac{\partial M_{out\ x_1}}{\partial t} + \frac{\partial M_{out\ x_2}}{\partial t} + \frac{\partial M_{out\ x_3}}{\partial t} \tag{4.7}$$

The rate of mass storage in the element equals:

$$\frac{\partial M_{in}}{\partial t} - \frac{\partial M_{out}}{\partial t} = \frac{\partial M}{\partial t} \tag{4.8}$$

Substituting for M_{in} and M_{out} (equations 4.4, 4.5, 4.6 and 4.7) and simplifying, the resultant is:

$$\frac{\partial M}{\partial t} = -\gamma\left(\frac{\partial Vx_1}{\partial x_1} + \frac{\partial Vx_2}{\partial x_2} + \frac{\partial Vx_3}{\partial x_3}\right) dx_1\, dx_2\, dx_3 \qquad (4.9)$$

In many problems, it is possible to assume that there is no component of flow in the x_2 direction and that the flow is essentially two dimensional. In the present case, where the flow in slopes is being considered, it is assumed that the slope is of infinite uniform extent in the x_2 direction. Although no slope is of infinite uniform extent, it is generally possible to assume two dimensional flow in which $dx_2 = 1$.

For two dimensional flow, equation 4.9 simplifies to:

$$\frac{\partial M}{\partial t} = -\gamma\left(\frac{\partial Vx_1}{\partial x_1} + \frac{\partial Vx_3}{\partial x_3}\right) dx_1\, dx_3 \qquad (4.10)$$

For an incompressible fluid and soil skeleton, the change in mass storage is reflected in the change in the volumetric moisture content.

$$\frac{\partial M}{\partial t} = \gamma \eta S_\omega \qquad (4.10a)$$

η = porosity
S_ω = degree of saturation

Hence equation 4.10 becomes:

$$\frac{\partial Vx_1}{\partial x_1} + \frac{\partial Vx_3}{\partial x_3} = \frac{\partial \theta}{\partial t} \qquad (4.11)$$

θ = volumetric moisture

$$\theta = \eta S_{\omega} \tag{4.12}$$

In the general form,

$$\frac{\partial Vx_i}{\partial x_i} = \frac{\partial \theta}{\partial t} \tag{4.13}$$

where i = 1, 3
repeated subscripts imply summation

Substituting equation 4.1 for Vx_i, equation 4.1[3] becomes:

$$\frac{\partial}{\partial x_i} \left(K_i \frac{\partial h}{\partial x_i} \right) = \frac{\partial \theta}{\partial t} \tag{4.14}$$

The hydraulic conductivity may and usually is anisotropic. In two dimensions, the hydraulic conductivity is represented by a tensor K_{ij}. Substituting equation 4.1[4] into 4.2 and letting $p/\gamma_{\omega} = \psi$, where ψ is defined as the pressure head, equation 4.1[4] becomes:

$$\frac{\partial}{\partial x_i} \left(K_{ij} \frac{\partial x_3}{\partial x_i} + K_{ij} \frac{\partial \psi}{\partial x_i} \right) = \frac{\partial \theta}{\partial t} \tag{4.15}$$

It is convenient here to introduce Kronecker's delta for $\frac{\partial x_3}{\partial x_i}$; hence equation 4.15 becomes:

$$\frac{\partial}{\partial x_i} \left(K_{ij} \delta_{i3} + K_{ij} \frac{\partial \psi}{\partial x_i} \right) = \frac{\partial \theta}{\partial t} \tag{4.16}$$

if $i = 3$, $\delta = 1$
if $i \neq 3$, $\delta = 0$

Equation 4.16 can be represented in terms of ψ rather than ψ and θ. Defining c as the slope of the moisture characteristic curve (see figure 4.11a), we have

$$c(\psi) = \frac{\partial \theta}{\partial \psi} \tag{4.17}$$

and

$$\frac{\partial}{\partial x_i} \left(K_{ij} \, \delta_{i3} + K_{ij} \frac{\partial \psi}{\partial x_i} \right) = c(\psi) \frac{\partial \psi}{\partial t} \tag{4.18}$$

To account for the elastic properties of the water and aquifer, the specific storage S_s is introduced into equation 4.18 and is added to the right hand side of the equation.

$$S_s = \frac{\partial \theta}{\partial \psi} = \frac{\partial \psi}{\partial t} \tag{4.19}$$

S_s = specific storage

In the current work by Neuman et al. (1974), the specific storage is taken to be zero in the unsaturated zone, since the compressibility on the storage of water is negligibly small in comparison to the effect in the moisture content.

Moving all terms to the left hand side:

$$\frac{\partial}{\partial x_i} \left(K_{ij} \, \delta_{i3} + K_{ij} \frac{\partial \psi}{\partial x_i} \right) - \left(c(\psi) + \beta S_s \right) \frac{\partial \psi}{\partial t} = 0 \tag{4.20}$$

β = 0 in the unsaturated zone
= 1 in the saturated zone

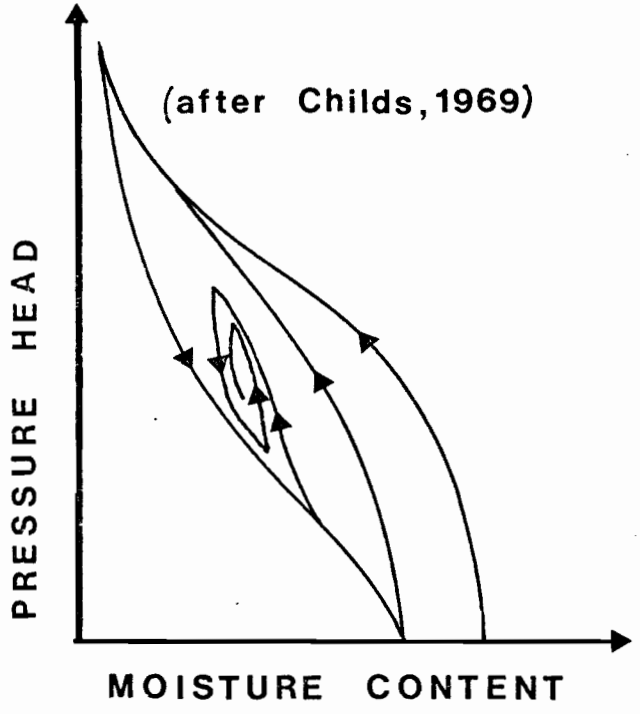

FIG 4.11 (a) PRESSURE HEAD VARIATION WITH MOISTURE CONTENT

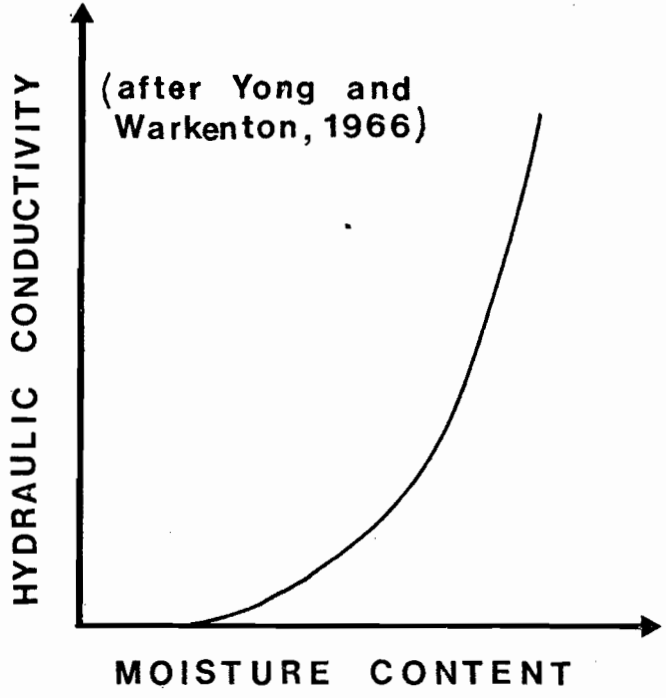

FIG 4.11 (b) HYDRAULIC CONDUCTIVITY VERSUS MOISTURE CONTENT

In the unsaturated zone, K_{ij} is a function of the moisture content as can be seen in figure 4.11b. To account for a varying hydraulic conductivity, it is convenient to multiply K_{ij} by K^r where $0 < K^r < 1$. For fully saturated soils, $K^r = 1$.

Equation 4.21 has been used by Neuman et al. (1974) to solve problems involving saturated-unsaturated flow in porous media.

$$\frac{\partial}{\partial x_i}\left(K^r K_{ij}\,\delta_{i3} + K_{ij}\frac{\partial \psi}{\partial x_i}\right) - \left(c(\psi) + \beta S_s\right)\frac{\partial \psi}{\partial t} + S = 0 = A(\psi) \qquad (4.21)$$

where S is a sink term used to simulate the uptake of water by plants. Since the uptake by plants has been neglected here, the value of S is zero. $A(\psi)$ is a quasilinear operator that is defined in the flow region.

4.4b Finite Element Formulation

Equation 4.21 is the governing equation for the unsaturated-saturated flow in porous media. A solution to the equation has been arrived at using a finite element discretization scheme (Neuman et al., 1974). Since unsaturated flow is a transient phenomena which is most commonly associated with infiltration and evapotranspiration from soils, a number of simplified assumptions were required so that the problem could be easily solved. Although it

is not the intention of this thesis to cover the entire spectrum of finite element applications in hydrogeology, certain concepts of the method are required so that a proper interpretation of the modelling results can be made. A review of the finite element method as applied to engineering problems in general can be found in Zienkiewicz (1971) while flow through porous media solutions have been summed up by Witherspoon and Neuman (1973).

There are two approaches in arriving at a finite element representation to a given problem. The first is to replace the given equations by a functional whose minimization gives a correct solution to the problem. The second approach is a representation directly from the governing equations. The direct approach does not require that a variational principal exist, hence the method can be extended to a large number of problems for which no variational principal has been found. The direct approaches lead to a set of integral equations and are known as the weighted residual methods (Zienkiewicz, 1971, p. 39). The general review of the weighted residual method given here follows that of Zienkiewicz (1971) and Gale (1975).

An approximate solution to a set of differential equations with unknown pressure function $\{p\}$ in a region V is desired. The governing equation can be written as

$$A(\{p\}) = 0 \tag{4.22}$$

where A is some quasilinear differential operator that is defined in the flow region. The boundary condition to be satisfied is

$$C(\{p\}) = 0 \qquad \text{on the boundary S.} \qquad (4.23)$$

A trial function satisfying the boundary conditions can be written in the general form

$$\{p\} = \{\xi\}\ (\psi) \qquad (4.24)$$

$\{\xi\}$ are specified linearly independent coordinate functions and (ψ) is a set of values: eg. the pressure heads at the nodes in the flow region. Substitution of the trial solution in equation 4.22 does not generally yield an exact solution, and a residual (R) remains (equation 4.25).

$$A(\{p\}) = R \neq 0 \qquad (4.25)$$

The reduction of R in the flow region V to some minimum value will then result in the best solution. A minimum residual can be obtained by forcing R to be zero at every point in V. To achieve this, a weighting function W_i is chosen, which is a function of the coordinates, for each point at which a value of (ψ) is desired. It is then possible to write a system of simultaneous equations in the form

$$\int_V W_i\ R\ dV = \int_V W_i\ A(\{\xi\}\ (\psi))\ dV = 0 \qquad (4.26)$$

from which the values of (ψ) can be obtained at the required points in V (eg. the nodal points).

Zienkiewicz (1971) has shown that the choice of the weighting function determines the weighted residual method used. In Neuman et al. (1974), the Galerkin process was chosen in which the weighting function is made equal

to the coordinate function $\{\xi\}$. According to the Galerkin method, an approximate solution to the problem of saturated-unsaturated flow at any instant of time, t, is obtained in the form of a finite sequence

$$\psi^N (x_i, t) = \psi_n (t)\ \xi_n (x_i) \qquad n = 1, 2, 3 \ldots N \qquad (4.27)$$

where $\psi_n(t)$ are time-dependent coefficients and x_i is the vector of the Cartesian coordinates. In order to determine the coefficients of ψ so as to minimize the residual, $A(\{p\})$ in equation 4.22 must be orthogonal to each of the coordinate functions or, in other words, equation 4.26 must equal zero for each of the nodal points (Neuman et al., 1974).

For the finite element discretization scheme, the flow region is divided up into a number of elements - the idea being to solve each of the elements independently and then combine the solutions (Witherspoon and Neuman, 1973). The elements are triangular; however, in drawing a mesh, quadralaterals can be used and subsequently reduced to triangles. A typical triangular element is shown in figure 4.12a in which the verticies are the nodal points. For convenience, the nodal points are given a letter code of i, j, and k, which have space coordinates X_i, Y_i; X_j, Y_j; X_k, Y_k; respectively. Each node is associated with a unique subregion of V (see shaded region of figure 4.12b), containing all the elements in the immediate vicinity of the node. The node is also associated with a global coordinate function, which is defined as being linear within each element and piecewise linear over the flow region V. The coordinate functions ξ_i, ξ_j and ξ_k are chosen to have a value of unity at the nodal point in question and zero at all other nodal

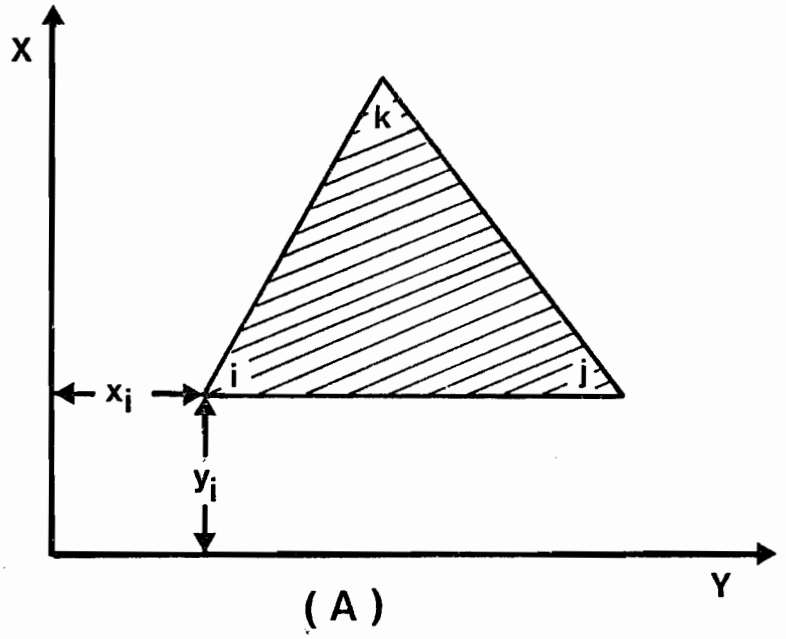

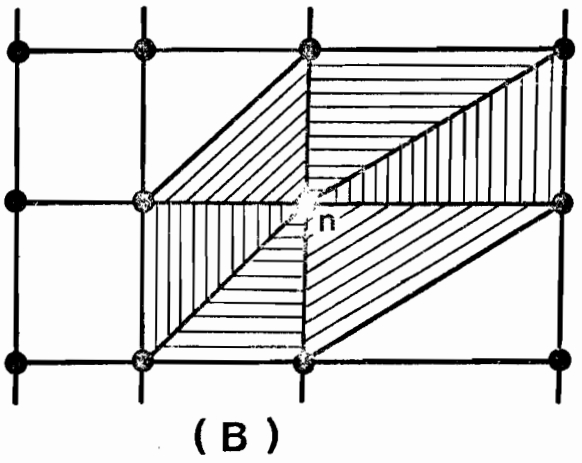

FIG 4.12 A - TRIANGULAR ELEMENT

B - FLOW REGION ASSOCIATED WITH NODE n

points. The coordinate functions are sometimes referred to as "roof", "pyramidal", or "chapeau" functions due to their shape. Substituting the coordinate functions into equation 4.27, it is evident that the value of the pressure head at any point in the flow region is equal to the time dependent coefficient. Up to this point, only the global coordinate functions have been considered; however, in each element, the local coordinate function is the face of a pyramid which represents the global coordinate function.

$$\text{Thus,} \quad \xi_n(x_i) = \bigcup_e \xi_n^e (x_i) \tag{4.28}$$

where U equals union and means that

$$\xi_n(x_i) = \xi_n^e (x_i) \quad \text{where } x_i \in V^e \tag{4.29}$$

The relationship between the local coordinate functions and the Cartesian coordinates is given in Appendix C and will not be explained further here. By virtue of equation 4.29, it is possible to rewrite equation 4.26 in the following manner:

$$V_n (\psi_n \xi_n^e) = \int_{V^e} A(\psi_n \xi_n^e) \xi_n^e \, dV = 0 \tag{4.30}$$

which allows for the summation over all the elements.

The Galerkin process states that

$$\psi^N = \psi_n \xi_n \tag{4.31}$$

Therefore, substituting equation 4.31 and 4.21 into equation 4.30, equation 4.32 results.

$$\int_V \left(\frac{\partial}{\partial x_i} \left(K^r K_{ij} + K^r K_{ij} \frac{\partial \psi}{\partial x_i} \right) \right.$$

$$\left. = \left(\{C(\psi) + S_s\} \frac{\partial \psi}{\partial t} + S \right) \xi_n \, dV = 0 \right. \tag{4.32}$$

Using Green's first identity and equation 4.32, it follows that:

$$\int_V \left(\frac{\partial}{\partial x_i} \left(K^r K_{ij} \frac{\partial \psi}{\partial x_j} \right) + \frac{\partial}{\partial x_i} \left(K^r K_{x_i} \right) \right) \xi_n \, dV$$

$$+ \int_V \left(K^r K_{xy} \frac{\partial}{\partial Y} + K^r K_x \right) \xi_n \, dV$$

$$= \int_{\Delta_1^e} \left(K^r K_{xy} \frac{\partial \psi}{\partial Y} + K^r K_x \right) \xi_n \, dV \tag{4.33}$$

It is evident from equation 4.27 that the time dependent coefficient is valid only at a given instant of time. Therefore, the time derivative appearing in equation 4.21 must be determined independently of the orthogonalization process (Neuman et al., 1974). A stable solution has been arrived at by using a weighted average of the time derivative over the flow region.

Therefore:

$$\frac{\partial \psi}{\partial t} = \frac{\int_V \{C(\psi) + S_s\} \frac{\partial \psi}{\partial t} \xi_n \, dV}{\int_V \{C(\psi) + S_s\} \xi_n \, dV} \tag{4.34}$$

It is also assumed that the relative moisture capacity and the relative conductivity vary linearly over the element according to

$$K^r = K^r_\ell \; \xi^e_\ell \qquad \ell = i,j,k \text{ the corners of the triangle} \tag{4.35a}$$

$$C(\psi) = C_\ell \; \xi^e_\ell \tag{4.35b}$$

Equation 4.36 represents the sum of the contributions of individual elements over the flow region.

$$\sum_e \int_{V^e} \left(K^r_\ell \; K_{ij} \; \xi^e_\ell \; \frac{\partial \xi^e_m}{\partial x_j} \frac{\partial \xi^e_n}{\partial x_i} \psi_m + K^r_\ell \; K_{ij} \; \xi^e_\ell \; \frac{\partial \xi^e_n}{\partial x_i} \right.$$

$$\left. + \; (C^e_\ell \; \xi^e_\ell + S_s) \; \frac{\partial \psi}{\partial t} \; \xi^e_n \right) dV = \sum \int_A K^r_\ell \; K_{ij} \; \xi^e_\ell \; \frac{\partial \xi^e_\ell}{\partial x_j} \psi_m$$

$$+ \; K^r_\ell \; K_{ij} \; \xi^e_\ell \; M_x \; \xi^e_m \; dA - \int_{V^e} S \; \xi^e_m \; dV \tag{4.36}$$

It is possible to simplify equation 4.36 into

$$A_{nm} \; \psi_m + F_{nm} \; \frac{d\psi m}{dt} = Q_n - B_n - D_n \tag{4.37}$$

$$n, m = 1, 2, 3 \ldots N$$

where

$$A_{nm} = \sum_e K^r_\ell \; K_{ij} \int_e \xi^e_\ell \; \frac{\partial \xi^e_n}{\partial x_i} \frac{\partial \xi^e_m}{\partial x_j} \; dV$$

$$A_{nm} = \sum_e \frac{\alpha}{4\Delta} K^{-r} \left(K^s_{11} b_n b_m + K^s_{13} (b_n c_m + b_m c_n) + K^s_{33} c_n c_m \right) \quad (4.38a)$$

$$F_{nm} = \sum_e \int_{V^e} (C_\ell \xi^e \xi^e_n + \beta S_s) \, dV$$

$$= \sum_e \frac{\alpha\Delta}{12} \left((2C_n + C_p + C_q) + 4\beta S_s \right) \quad \text{if } n = m \quad (4.38b)$$

$$F_{nm} = 0 \qquad \text{if} \qquad n \neq m \quad (4.38c)$$

$$Q_n = - \sum_e \int_{\Gamma^e} V \xi^e_n \, d\Gamma = - \sum_e \frac{(LV)_n}{2} \quad (4.38d)$$

$$B_n = \sum_e K^r_\ell K^s_{i3} \int_{V^e} \xi^e_\ell \frac{\partial \xi^e_n}{\partial x_i} \, dV = \sum_e \frac{\alpha}{2} K^{-r} (K^s_{13} b_n + K_{33} c_n) \quad (4.38e)$$

$$D_n = \sum_e \int_{V^e} S \xi^e_n \, dV \quad (4.38f)$$

The subscript ℓ refers to the corners of the triangle as shown in figure 4.12a; Δ is the area of the triangle. $\alpha = 1.0$ for plane flow and 2π for axisymmetric flow. Since the models simulated for this thesis involve only plane flow, the α is equal to one in all cases. The relative conductivity is taken to be the average over the triangle. The terms b and c are geometric coefficients and are defined in Appendix C. Q_n represents the volume of water that is lost or gained at any nodal

point in the system. At all points not acting as sinks or sources, Q_n equals zero. D_n is the volume of water used by the plants. For the present study, the plants were not taken into account and this part of equation 4.37 was set equal to zero. F_{nm} can be considered to be the amount of water that is stored in the entire flow system when the value of ψ at a node changes by one unit. A_{nm} and B_n are the remaining two parameters and are required to define the pressure head distribution over the flow region.

To integrate equation 4.37, the time domain is divided up into finite time intervals and the time derivatives are replaced by finite differences (Neuman et al., 1974). For the work by Neuman et al., two time integration schemes have been used. The application of the schemes depends on the type of flow system that is anticipated during the simulation. The first scheme is time centred, where at the beginning of each time period the new values of ψ are predicted from a linear extrapolation of the previously calculated values. The time centred scheme is valid where the entire system remains unsaturated at all times; however, where the system is likely to be partially saturated, it is necessary to employ a full implicit backward difference scheme in terms of the pressure head. In this scheme, it is not necessary to know the values of ψ at the start of the time step. This eliminates the problems associated with the change in saturation near the water table. Where a value of ψ in the saturated zone becomes unknown due to a change in saturation, then the value of the pressure head is given a value of zero for the iteration. Those nodes above the water table are evaluated for the pressure head according to equation 4.37, while for the nodes below the water table the term F_{nm} is determined according to the

specific storage since the specific moisture capacity in the saturated zone is zero. When all of the nodes remain unsaturated or part of the system is saturated, but the specific storage does not equal zero in any of the nodes, either of the two schemes can be used. However, if the specific storage in the saturated zone is zero, then the backward difference scheme must be used since the term F_{nm} is equal to zero and equation 4.37 cannot be solved by the time centred scheme.

With the finite element method, there are essentially two types of boundary conditions on the boundaries of the problem. The first is a prescribed pressure head where the time coefficients in equation 4.27 are known at the outset of the simulation. The second type of boundary condition is the prescribed flux boundary, which is accounted for by the term Q_n in equation 4.37 (Witherspoon and Neuman, 1973). Seepage faces and atmospheric boundaries have been shown by Neuman et al. (1974) to be special cases of a prescribed flux boundary. Therefore, for the modelling carried out for this thesis, it was necessary to determine in the preliminary stages of the analysis which boundaries would likely be part of a seepage face and which ones would be considered to act as atmospheric boundaries where climatic influences could be accounted for. Furthermore, the fluxes that are part of the climatic variations were required as well as limits on the anticipated relative humidity and temperature along the atmospheric boundary.

4.4c Climatic Conditions

The potential rate of flux across a soil-atmospheric boundary is determined by climatic conditions;

however, the actual rate is dependent on the hydraulic properties of the surficial layer (Neuman et al., 1974). During evaporation, the upper soil layer will dry out and the suction will increase. The limiting suction at the surface has been determined by Childs (1969) and can be determined from equation 4.39. It can be seen that the minimum pressure head is dependent on the relative

$$\psi_s = \frac{RT\gamma}{M} (\ell n\, r) \quad \text{-- See figure 4.13 for symbols.} \qquad (4.39)$$

humidity and the ambient air temperature. In the field, this means that the soil can only become as dry as the air that is in contact with the soil. A graphical solution to equation 4.39 is shown in figure 4.13 and indicates that the temperature has little effect on the suction, but that the relative humidity is the controlling factor. For field investigation of the potential evaporation for a soil, it is essential that the relative humidity be measured several times during the day. For the present study, this control was not available, hence it was necessary to make some assumptions regarding the minimum surface head. During infiltration, the head was taken to be zero. This is based on the assumption that the relative humidity at the surface is equal to 100%. For evaporation conditions, the minimum surface head was arbitrarily set to -100 meters of water. After a few trial runs of the program using this value, it became evident that at no time did the pressure head on the soil side of the atmospheric boundary become less than -30 meters of water. Since the relative humidity in the Ottawa area can be as little as 10% during July (Agriculture Canada Weather Station, Ottawa), which corresponds to a surface potential of -30,000 meters of water, it would seem that for this region the minimum surface head has little bearing on the evaporation from soils.

FIG 4.13 SURFACE PRESSURE HEAD -VS- RELATIVE HUMIDITY

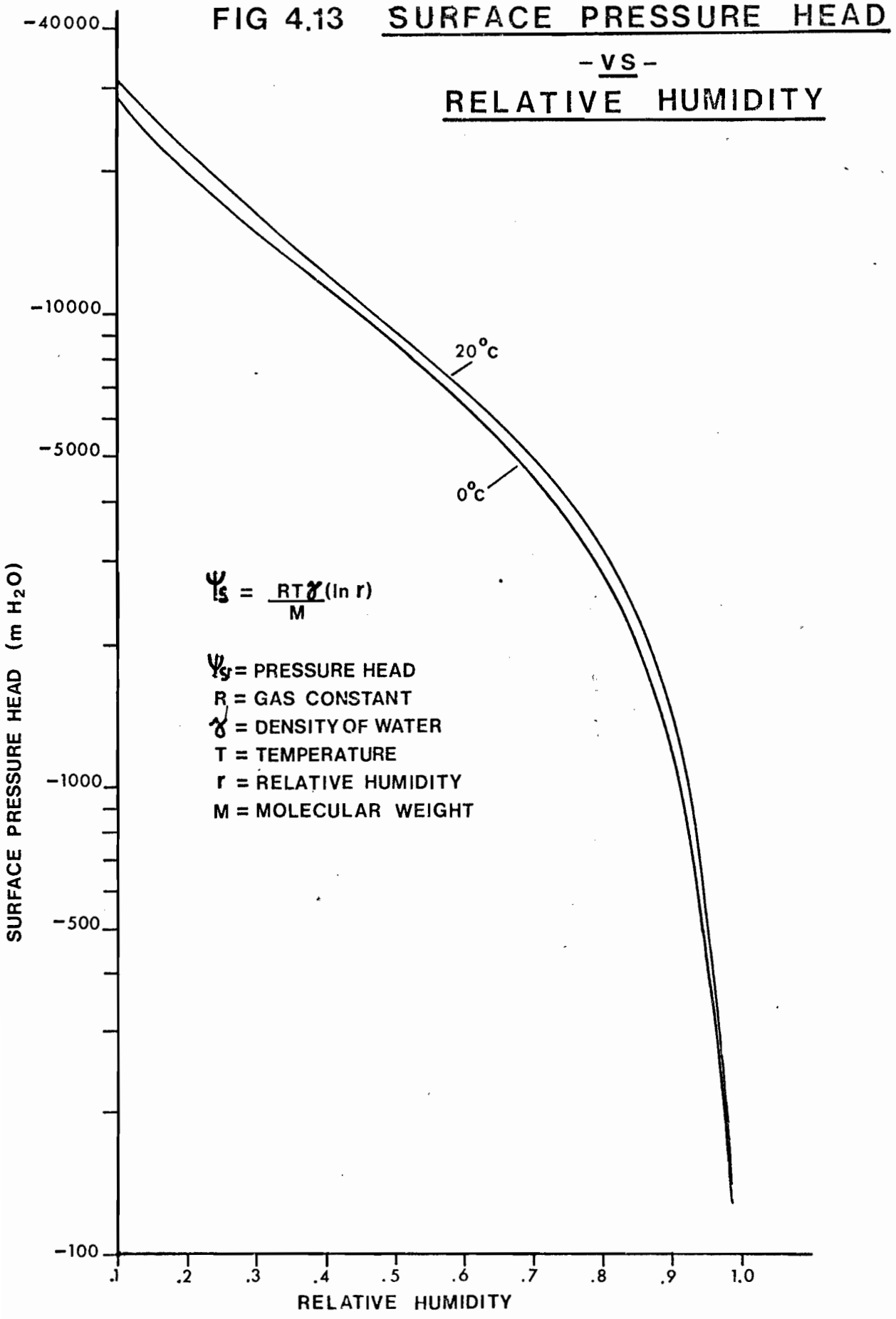

Ultimately, climatic influences are responsible for the potential flux of water across an atmospheric soil boundary. In dealing with a transient problem it is necessary to specify the flux during the time period over which those conditions are valid. In other words, two factors need to be determined: the flux and the time frame. Since precipitation and evaporation are seldom constant over a lengthy period, it was therefore necessary to make some simplifying assumptions so that the climatic conditions could be easily handled.

In the Ottawa area, precipitation falls as snow and as rain. It was assumed that all the precipitation that fell during the months of December through March did so as snow. The entire snowfall remained intact and no water was lost through melting or evaporation. During the month of April, the snow melted at a uniform rate. Normal rainfall for April was added to the snow melt. For the purposes of this study, the ground was considered to be thawed and permeable at the start of the month of April. Precipitation which fell as rain did so on four days during the months of April through November. Each rain period was of equal intensity and started immediately at the beginning of the day and ended instantaneously at the end of the day.

Evapotranspiration potential was calculated using Thornthwaite's method (1948). There are limitations in using this method, i.e. it does not account for factors such as wind velocity, relative humidity, vegetation type. However, in light of the assumptions that were made regarding the form and rate at which the precipitation fell, it was felt that a more rigorous approach was not warranted. Daily potential evapotranspiration was obtained by dividing the

monthly value by the number of rain-free days in the month. A summary of the mean monthly temperature, precipitation, potential evapotranspiration, and moisture balance is shown in table 4.3. In this case, the mean values were used, since maximum monthly values might not occur during the same year.

As previously stated, the time period during which the potential flux is valid must be determined. It was decided that the modelling would start at the beginning of December. Since no infiltration was allowed until April, the time periods were of no consequence. Therefore for the first four months, the time period was doubled with each timestep, i.e. 1 day, 2 days, 4 days, etc. From April through November, the time periods were governed by the precipitation. Since there are four days per month in which precipitation falls, then the remainder of the month is subject to evapotranspiration. Hence, the precipitation days were separated by five to six days of evapotranspiration. Per month, there are approximately eight timesteps, each with a specified finite time interval and a potential flux across an atmospheric boundary. In all of the simulations carried out for this thesis, the groundwater regime was simulated for a period of December through to August. In this manner, it was possible to simulate the spring maximum and the summer minimum pore pressures.

4.4d Saturated-Unsaturated Hydraulic Conductivities

Values for the saturated conductivities for sensitive clays can be found in Bozozuk (1972) and for soils in general in Harr (1962). Using both of these sources,

MONTH	MEAN MONTHLY TEMP °C	MEAN MONTHLY PRECIP CM	POTENTIAL MONTHLY EVAPOTRANS CM	MOISTURE SURPLUS CM	MOISTURE DEFICIT CM
JAN.	-10.9	5.99	0.0	5.99	
FEB.	-9.5	5.69	0.0	5.69	
MAR.	-3.1	6.10	0.0	6.10	
APR.	5.6	6.76	2.90	3.86	
MAY	12.4	7.01	7.62		.61
JUNE	18.2	7.26	11.67		4.41
JULY	20.7	8.13	13.49		5.36
AUG.	19.3	8.15	11.56		3.41
SEPT.	14.6	7.87	7.43	.44	
OCT.	8.7	6.58	3.90	2.68	
NOV.	1.4	7.85	.47	7.38	
DEC.	-7.7	7.70	0.0	7.70	
TOTALS		85.09	59.04	39.84	13.79

Mean monthly temperatures and precipitation from Ottawa Airport Weather Bureau
Potential evapotranspiration calculated using Thornthwaite's method

TABLE 4.3 CLIMATIC DATA AND MOISTURE BALANCE FOR OTTAWA

trial estimates of the hydraulic conductivities were obtained. These values were adjusted during the verification of the finite element method with the field data until a best fit solution was obtained. The saturated hydraulic conductivities used here are given in table 4.4.

The relative conductivity is defined as the unsaturated hydraulic conductivity at a given moisture content divided by the hydraulic conductivity at saturation. Childs and Collis-George (1950), and Marshall (1958) have presented relationships between the pore size distributions that have been calculated from the moisture characteristic and the relative hydraulic conductivity. Yong and Warkentin (1966) and Childs (1969) discuss some laboratory techniques for obtaining the relative conductivity versus the volumetric moisture content. The relative conductivity curves used for this study were obtained from Neuman et al. (1974) and are shown in figure 4.14. It was shown in the section on the development of equation 4.26 that the moisture characteristic exhibits hysterisis. Therefore, if the relative conductivity was to be calculated on the basis of the empirical formula mentioned above, then the relative conductivity also exhibits hysterisis. Since it is not possible at this time to accommodate hysterisis in the finite element formulation, the relative conductivity versus moisture content is a single valued function. It should be noted that the curves shown in figure 4.14 are composed of a series of straight lines. The method of inputting the relative conductivity requires that pairs of K^r and θ be inputted and a linear interpolation is made between the data points. It is therefore necessary to input a sufficient number of points so that the series of straight line portions approximates the actual behaviour.

SOIL LAYER	k_h m/day	k_v m/day	porosity %	specific storage
Fractured Bedrock	8.64×10^{-2}	8.64×10^{-3}	45	0.0
Deep water marine clay	8.64×10^{-6}	8.64×10^{-6}	50	0.0
Prodelta clay	8.64×10^{-3}	8.64×10^{-4}	50	0.0
Shoaling Prodelta	8.64×10^{-2}	8.64×10^{-4}	50	0.0
Fluvial sand	8.64×10^{0}	8.64×10^{-1}	35	0.0

k_h=hydraulic conductivity in the horizontal direction
k_v=hydraulic conductivity in the vertical direction

TABLE 4.4 HYDRAULIC CONDUCTIVITIES FOR THE DIFFERENT SOIL LAYERS

FIG 4.14 UNSATURATED HYDRAULIC CONDUCTIVITY VS MOISTURE CONTENT
(after Neuman 1974)

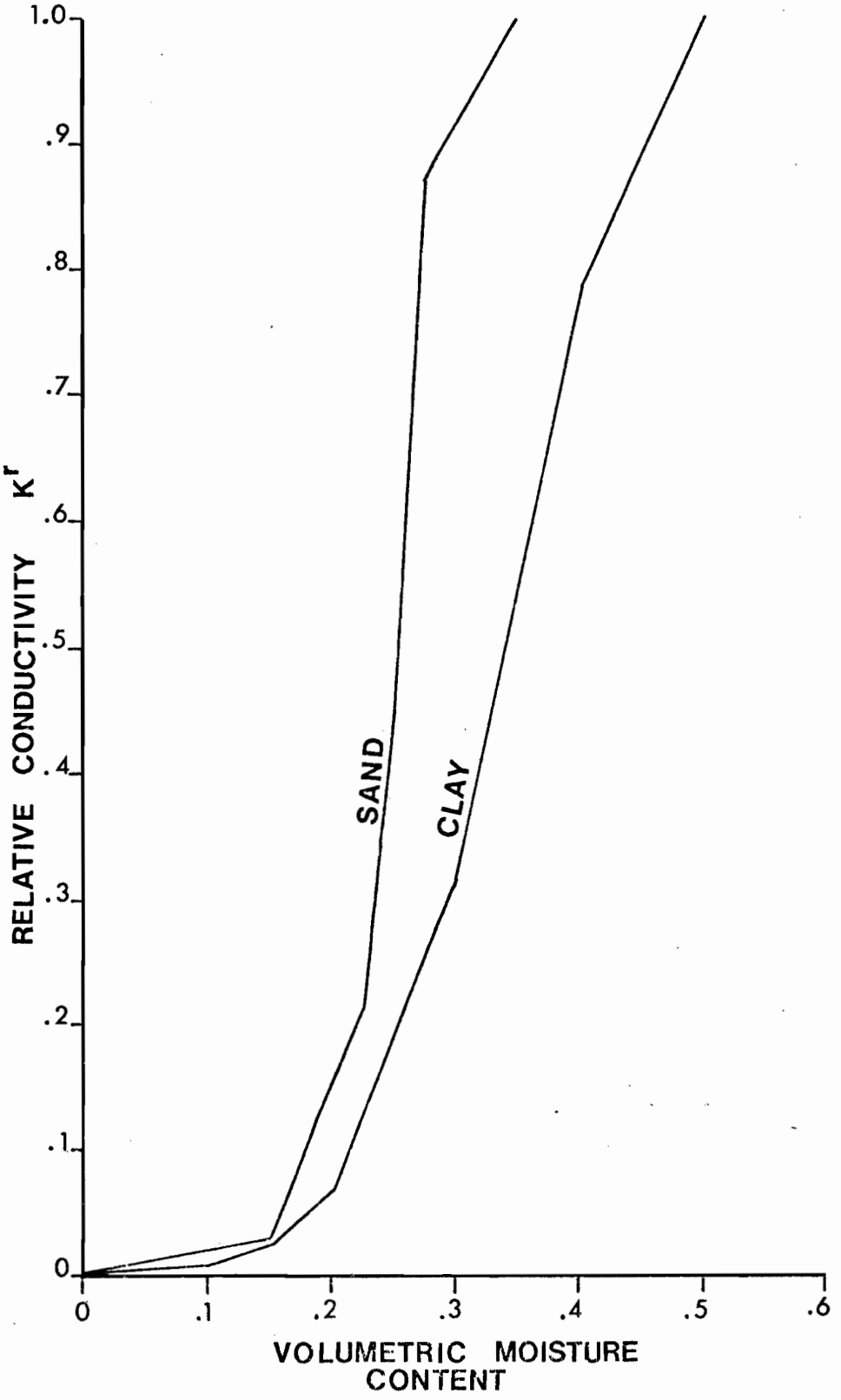

Pressure head versus moisture content curves were also obtained from Neuman et al. (1974) since no data on the sensitive clays was available. Curves for sand and clay are shown in figure 4.15 and demonstrate the differences in the pressure-moisture content relationships for the two broad classes of materials. Sand by virtue of its larger pore size unsaturates to a greater extent under lower suctions than clay.

At this point, it should be apparent that the movement of water through the soil profile is highly dependent on the prevailing moisture conditions. Both the driving potentials and the hydraulic conductivity are governed by the volumetric moisture content. The moisture content is a function not only of the soil type but also of the history of wetting and drying. The fact that hysterisis has been neglected in the solution of the governing equations may introduce considerable error for soils exhibiting large differences in moisture content between the wetting and drying parts of the suction-moisture content curves.

The unsaturated properties which have been presented here are valid for soils only. Since there is fractured bedrock underlying the sensitive clay deposits, it is necessary to make some assumptions concerning the hydrogeologic behaviour of the bedrock. For the geological settings to be investigated for this study, it is not anticipated that the bedrock will be unsaturated. In the eventuality that it does, it is assumed to have the same properties as the sand.

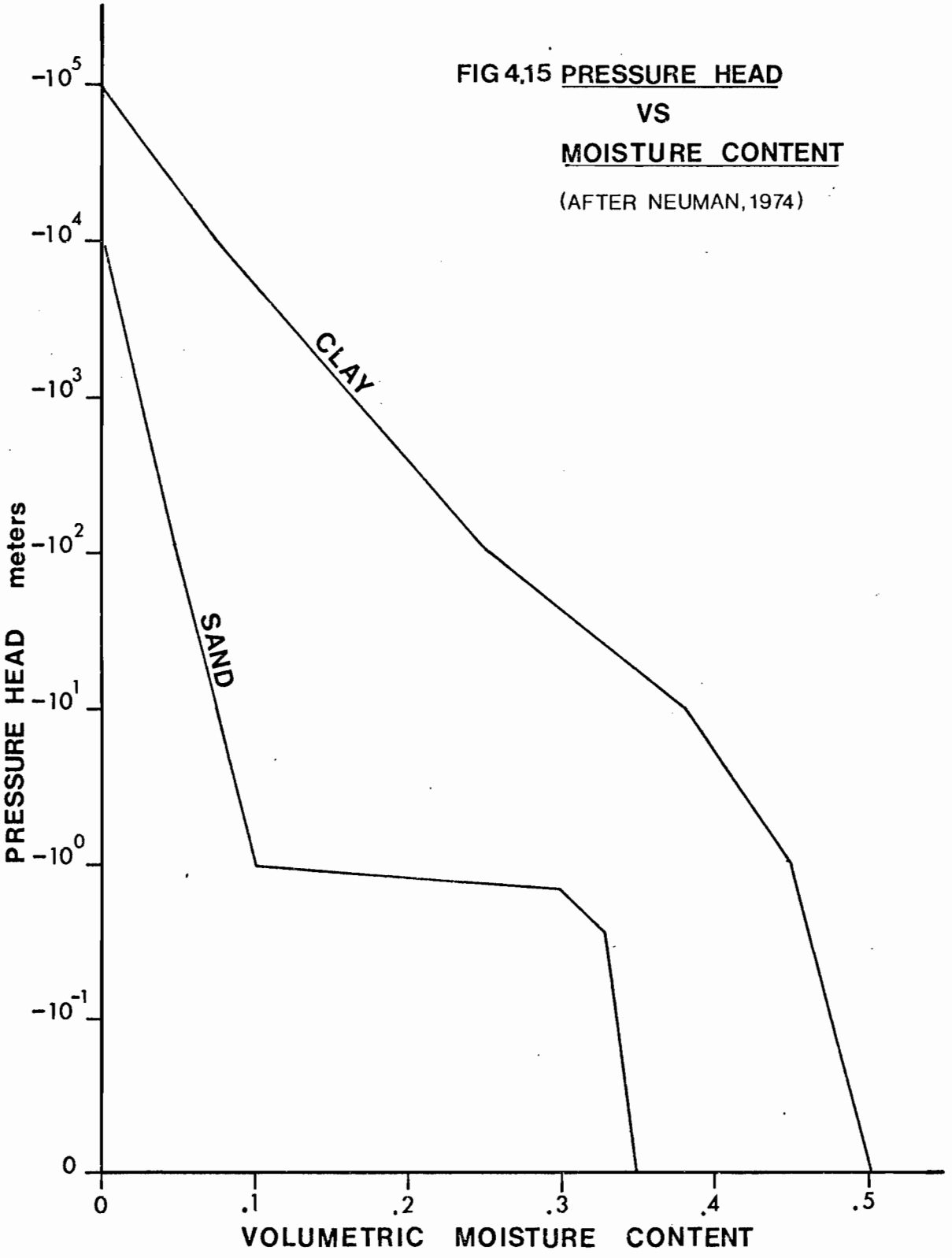

FIG 4.15 PRESSURE HEAD VS MOISTURE CONTENT

(AFTER NEUMAN, 1974)

4.5 Calibration of the Finite Element Method

Neuman et al. (1974) have shown that the finite element solution to the previous equations can be used to solve a wide variety of saturated-unsaturated flow problems. Generally speaking, the model produced results that were compatible with finite difference, analytical solutions and measured values. One of the simulations reported on by Neuman et al. (1974) was that of flow through a layered slope under the influence of infiltration and evapotranspiration. Therefore, if the model is supplied with the proper parameters, it is possible to obtain a reasonably good approximation of the field pressure head distributions.

The objective of this section is to adjust the input data until a satisfactory agreement between the field and the calculated pressure head is obtained. Since actual hydraulic conductivity data was lacking, the results of the modeling could then be used to estimate the hydraulic conductivities of each of the four stratigraphic units.

Site P1 was used for the calibration of the finite element method because the field data from this site was considered to be more complete than the other two sites. Site P2 did not have piezometers in the mid-slope or toe regions, which does not allow for the checking of the measured pore pressures in the critical areas of the slopes with those calculated by the finite element method. Site P3 was rejected for the verification process due to the incomplete data for the piezometers at the mid-slope. A limitation of site P1 is that this site was instrumented before the stratigraphic column for the region had been adequately determined. Hence, it will be noted in the

profile of site P1 (figure 4.4a) that the prodelta and deepwater marine clay have been grouped together into a single unit. Therefore, no hydraulic conductivity for the deepwater marine clay was determined in the verification process.

A finite element mesh consisting of 185 nodes and 173 elements was drawn for site P1. The crest of the slope was considered to be an infiltration-evaporation boundary, while the slope face and the toe area were assumed to be a potential seepage face. Figure 4.16 shows the mesh and the position of the seepage face and the infiltration-evaporation boundary. The length of the seepage face is dependent on the flow of water through the system and the configuration of the soil units. At certain stages in the computation of the pore pressures, it is possible that part of the potential seepage face will remain unsaturated. In the field, the unsaturated part of the seepage face would act as an infiltration-evaporation boundary. However, the program by Neuman et al. (1974) does not allow for the changing of the boundary conditions from a seepage face to a climatic boundary during the course of the simulation. It is therefore likely that the boundary fluxes that were assigned to represent the climatic variations are underestimated since the climatic boundary is probably longer than is shown in figure 4.16.

For each trial solution, different values of the saturated hydraulic conductivities were used. Mean calculated pore pressures were compared to the measured pore pressures by means of a regression analysis and a Pearson correlation coefficient. Each run was checked against the previous run to verify if the new solution was better or worse than the others. This procedure was continued until the best set of hydraulic conductivities was obtained.

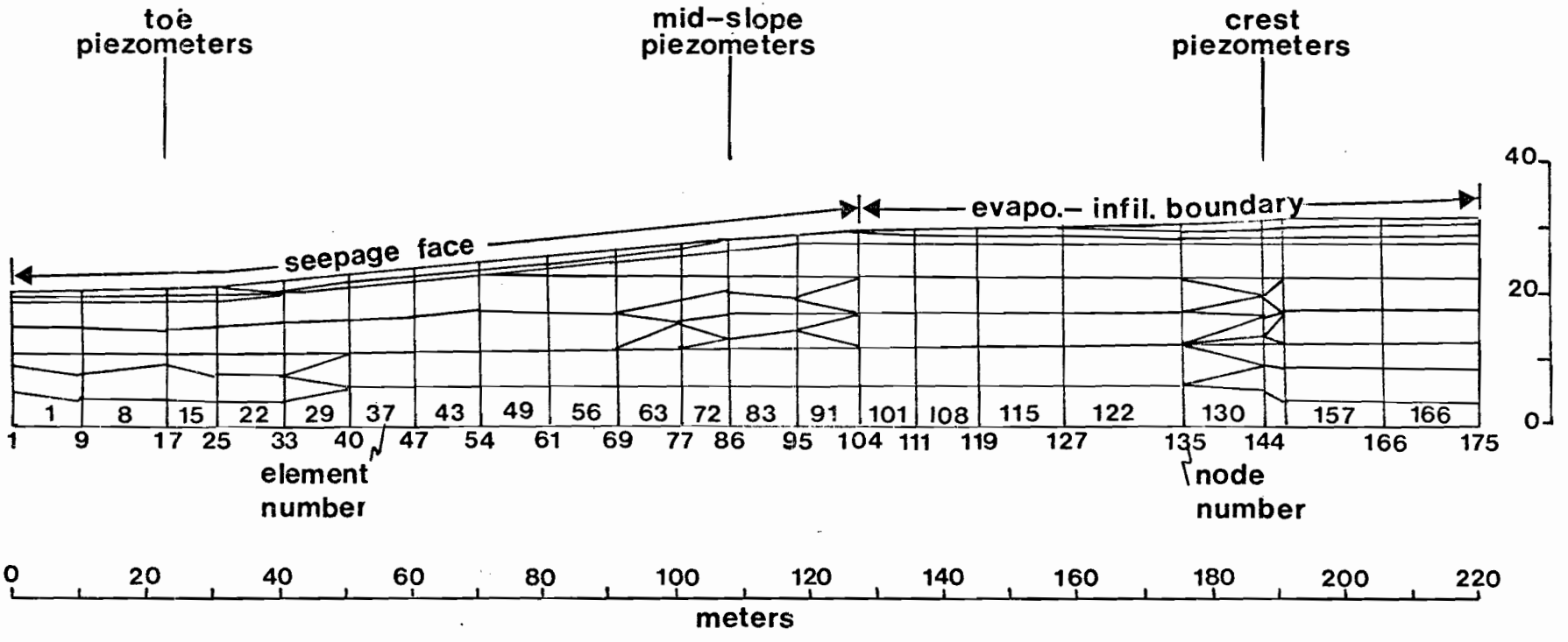

FIG 4.16 MESH AND BOUNDARY CONDITIONS FOR SITE P1

In the course of the trial solutions, it was observed that insufficient drawdown of the piezometric level in the bedrock was occurring. Even by increasing the hydraulic conductivity of the bedrock by several orders of magnitude relative to the overlying clay, the pressure head in the bedrock was being overestimated by about 10 meters of water. It therefore became evident that there was a control on the pressure head at site P1 other than the permeability contrasts between the various stratigraphic units. It was obvious that there was a regional control of the pressure head in the bedrock and that this control was capable of maintaining a lower piezometric level in the more permeable bedrock. Scott et al. (1976) have shown that, as the bedrock outcrops in the river valley bottom, the pressure head in the nearby slopes are changed from artesian to a level that is determined by the surface elevation of the river. Therefore, at site P1, there is likely a situation where a local river has intersected the bedrock surface and is maintaining a lower pressure head in the bedrock. To simulate this phenomenon, it was necessary to artificially extract water from a node in the bedrock. Since the bedrock was considerably more permeable than the overlying clay, the extraction of water at one node resulted in a lowering of the head throughout the entire bedrock. The actual magnitude of the sink term required to produce sufficient lowering of the piezometric level is dependent upon the permeability of the overlying sediments and the configuration of the mesh surrounding the node at which the sink term is applied. It is not possible to use a constant sink term throughout the Ottawa region, hence the actual magnitude of the sink is not a significant factor.

The hydraulic conductivities that gave the best fit solution in conjunction with a sink term are given in table 4.4. It should be noted that, since there was no deepwater marine clay at site P1, the values given in

table 4.4 are an estimate based on the visual characteristics of the clay and the hydraulic conductivities of the other soil units. The hydraulic conductivities for the other soil units appear to be reasonable estimates of the actual hydraulic conductivities that could be obtained in the field. Bozozuk (1972) reported field and laboratory measured hydraulic conductivities that ranged from 3.5×10^{-5} m/day to 2.3×10^{-4} m/day, which is within the range of the hydraulic conductivities listed in table 4.4. Bozozuk (1972) also determined that the ratio of horizontal to vertical permeability was between 1.1 and 1.59 for samples tested in the lab at field stresses. It is likely that these values would be low in comparison to the field since the silt seams that are present in the prodelta and shoaling facies would not be adequately represented by the lab size samples. Therefore, the orders of magnitude difference between the horizontal and vertical conductivities are probably more realistic of the actual field conditions.

At site P1, there were nine piezometers and three surface water table standpipes, thereby allowing for twelve points of comparison between the measured and the computed pressure head. Pressure head vs depth profiles have been plotted for the three piezometer nests (figures 4.17, 4.18 and 4.19). Superimposed on these profiles are the calculated pore pressures. A true correlation between the measured and calculated pressure heads should include an analysis of the variance as well as the mean pressure heads. In working with a transient model, one is trying to accommodate a series of unknown or undefinable climatic and physical conditions. The site geology was defined on the basis of three borings, hence the site as it is represented in figure 4.4a is the best approximation that could be drawn based on the information available. In dealing with the simulation of climatic conditions, certain simplifications were made in order that the number of time steps that were required to cover

FIG 4.17 COMPARISON OF MEASURED AND CALCULATED PRESSURE HEADS
SITE P1 CREST

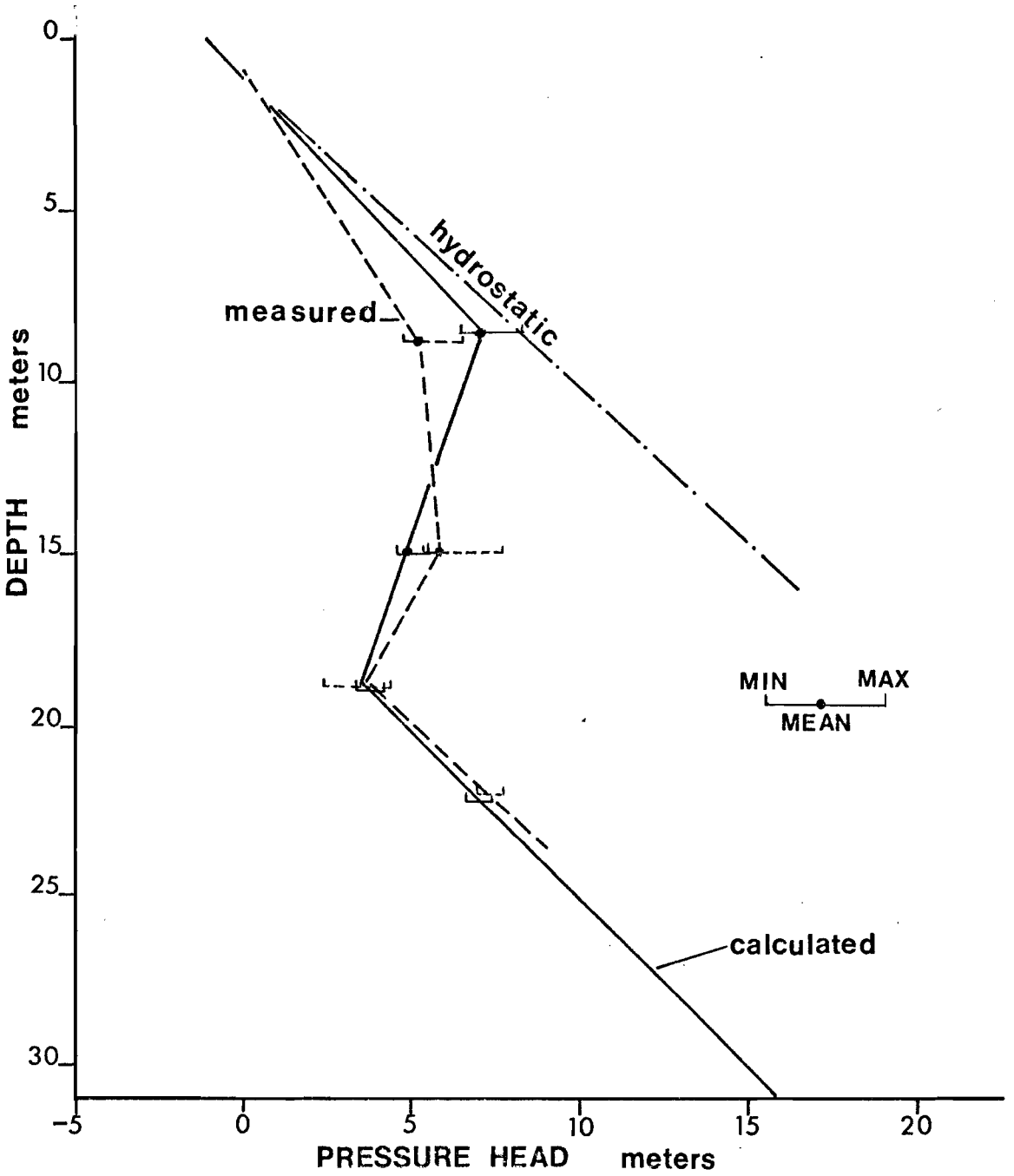

FIG 4.18 COMPARISON OF MEASURED AND CALCULATED PRESSURE HEADS

SITE P1 MID-SLOPE

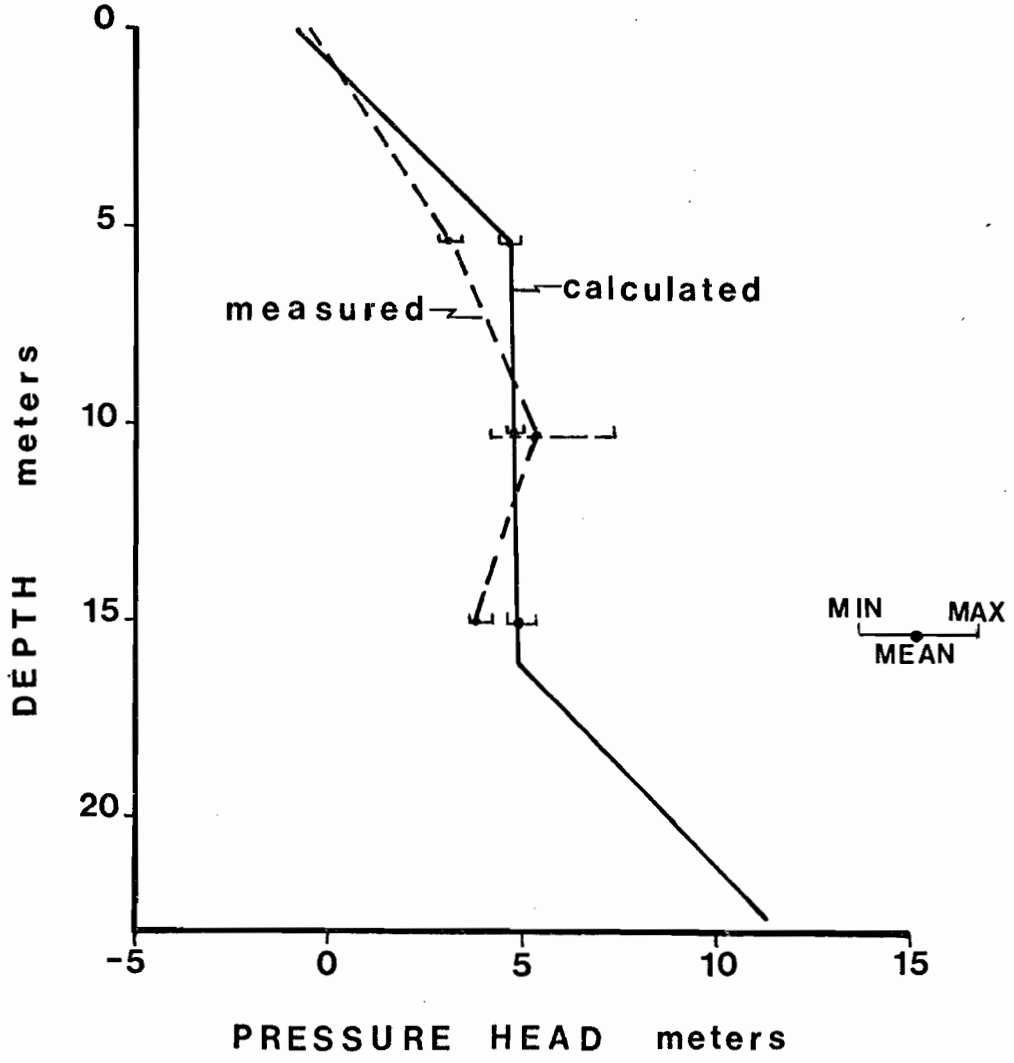

FIG 4.19 COMPARISON OF MEASURED AND CALCULATED PRESSURE HEADS
SITE P1 TOE

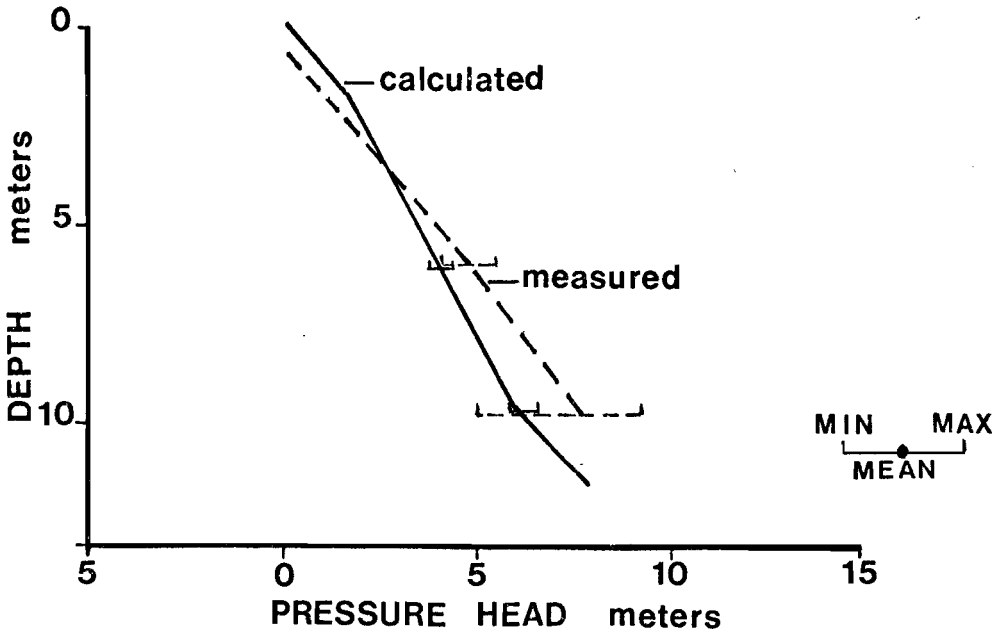

the time period could be kept to a minimum. Flores (pers. comm., 1979) has carried out extensive simulations using the same program and has found that the measured pressure head is very susceptible to the values of evapotranspiration that were used as input. The simulations that are reported upon here have used Thornthwaite's (1945) method for calculating the evapotranspiration and, due to the inherent assumptions in the method, some error was introduced into the calculated pressure heads. In view of the assumptions involved in the set-up of the physical and the climatic models, a perfect correlation between the measured and calculated pressure heads is virtually impossible and requires a field investigation and numerical simulation that is well beyond the scope of this thesis.

At the crest of the slope (figure 4.17), the pressure heads were overestimated in the upper part of the profile, slightly underestimated near the mid-depth part of the profile and were well estimated in the deeper sections. The range of values that were encountered for both the calculated and measured pressure heads appear to be in the same general order of magnitude. However, the variation in the calculated values is generally less than that of the measured ones, which may mean that there are factors influencing the flow patterns that have not been identified in the field or accommodated in the model. This may include more permeable zones that were not identified during drilling or sampling or boundary effects of the model itself.

The same trends that were identified in the crest region were also observed at the mid-slope nest of piezometers; the exception being that the prediction in the lower parts of the profile were overestimated by about 2 meters of water. The variation in the mid-depth

piezometer is an order of magnitude greater than the calculated value, while the range in the other two piezometers is approximately equal. The overestimation of the lower piezometric levels could be attributed to an anisotropic permeability in the bedrock. The permeability in the bedrock is thought to be largely controlled by a system of fractures. Small changes in the opening of the fractures can produce large variations in the effective hydraulic conductivity of the rock mass (Gale, 1975). It is therefore postulated that the assumption of uniform permeability of the bedrock over the simulated flow region may not be entirely valid. However, a testing program, consisting of several boreholes into the bedrock and packer permeability tests in sections of the holes would be required to evaluate the range of hydraulic conductivities in the bedrock. At the time that the project was carried out, there were no resources available to initiate such a study. The wide range in the pressure heads in the mid-depth piezometers may indicate a permeable layer that was not identified during the field program.

The correlation between the measured and calculated pressure heads obtained at the toe of the slope is shown in figure 4.19. The finite element simulation yielded pressure heads that were 1 meter too high near the surface and two meters too low at depth. There was a poor fit between the respective maximum and minimum pressure heads for the measured and calculated pressure heads. In both piezometers, the finite element model underestimated the range of values and produced a curve that closer approximated steady state conditions. This could be the result of boundary effects near the toe of the slope or again the effects of a heterogeneous bedrock.

The regression line that produced the best fit between calculated and measured pressure heads is shown in figure 4.20. The linear regression analysis produced a line with a slope of 0.98, an intercept of -0.029 and a correlation coefficient of 0.85. The slope and the intercept are close to the required 1.0 and 0.0 respectively, however, the correlation coefficient shows that there is some scatter about the line. Possible sources of error that could produce the scatter are: measurement errors, errors in the formulation of the finite element equations and of the equations of saturated-unsaturated flow, and scatter due to the assumptions involved in the physical model.

The results presented here must be interpreted in terms of what can be considered as acceptable limits of scatter. In the laboratory situation where there is close control of the physical situation, it is possible to obtain a good approximation of the flow system using finite element techniques. Narasimhan (1975) was able to predict flow rates in a sand box experiment almost perfectly. However, the calculated pressure heads were consistently higher than the measured. The actual error depended upon the elapsed time and the fit was better at the end of the experiment than at the beginning. Over a meter depth, the maximum error in the calculated pressure head was approximately 0.1 meters of water.

The prediction of pressure heads in the field is complicated by the lack of complete data. Lafleur and Lefebvre (1978) have shown that the prediction of the field pressure heads was reasonable only when there was good control of the permeability coefficients and the boundary conditions. In the simulations carried out by Lafleur

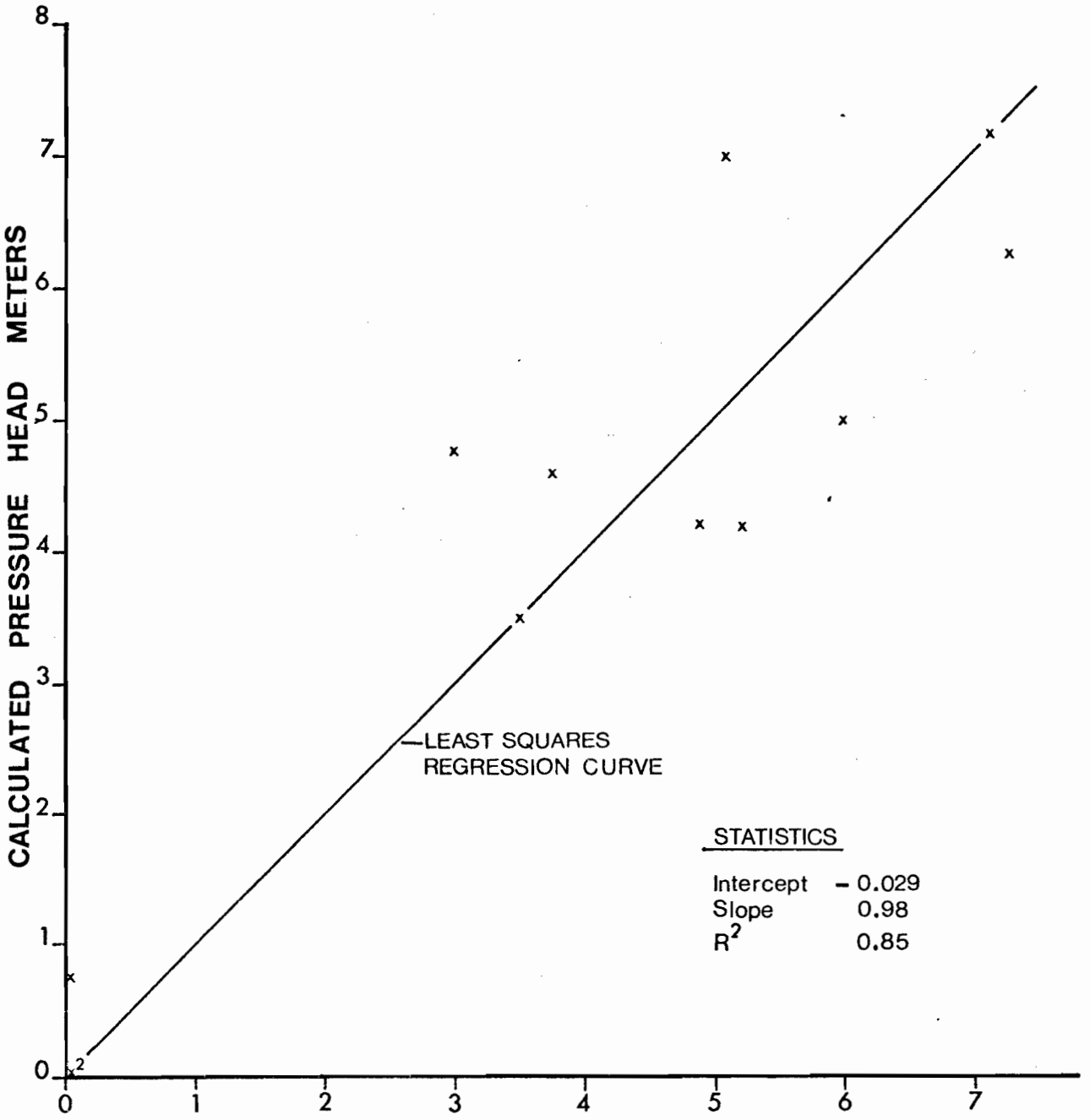

FIG 4.20 REGRESSION ANALYSIS OF CALCULATED AND MEASURED PRESSURE HEADS

and Lefebvre (1978), a steady state model was used which could account for some of the difference in the measured versus the calculated pressure heads. A five meter difference between the measured and calculated pressure heads was considered reasonable by Lafleur and Lefebvre (1978) and lends support to the two meter maximum difference that was obtained for this study.

4.6 Finite Element Modelling of Slopes

4.6a General

It has been shown that the sensitive clays are composed of at least four distinct stratigraphic units and that each of the units can be assigned a hydraulic conductivity that is a good approximation of the field values. It was also shown that the finite element method could predict reasonably accurately the pore pressure distribution in a slope composed of a number of different soil layers. The site used for verification of the finite element method can be considered unique in terms of stratigraphy, slope geometry and the bedrock sink. Therefore, it is not generally possible to extrapolate the information gained from one site to another where the physical characteristics of the site are different. Since the finite element technique appears to be applicable to flow in sensitive clay slopes, then the method can be used to approximate the pore pressure distribution in slopes of different geology.

There are an infinite number of different site geologies, each with its own pore pressure distribution. Limitations had to be placed on the number of models that would be simulated since the resources available for this

study were limited. The question arises as to which geological factors are important and as to which ones should be concentrated upon for the purpose of demonstrating the geological control of the pore pressure distribution. Obviously, slope angle and height are critical to both the stability and the groundwater flow. However, relationships between the slope angle, height and factor of safety have been published by Klugman and Chung (1976) and need not be redone here. On the basis of information obtained from the literature review and from the field mapping, the following five geological factors will be investigated: depth to bedrock; number of soil layers; nature of the surficial layer; bedrock sink; and depth of submergence. Different permutations and combinations of the five geological factors have resulted in the simulation of forty-six different models or geologic settings. A single finite element mesh was used for the simulation of all the forty-six settings. The mesh consisted of 161 nodal points and 147 elements. The configuration of the mesh and the location of the climatic boundary and the seepage face are shown in figure 4.21. The vertical sides of the model as well as the base are considered to be specified flux boundaries across which there is no flow. Table 4.5 shows the different combinations of geological factors that have been modelled. Reference to a particular model will in future discussions be made by the alphabetical code listed under the setting number. Within a certain setting group, the soil geometry remained constant and the depth of the external body of water was varied. Therefore, reference to setting A25 means setting A with a submergence to elevation of 25 meters.

The finite element model used in this study can simulate the actual climatic factors that will affect the

FIG 4.21 FINITE ELEMENT MESH

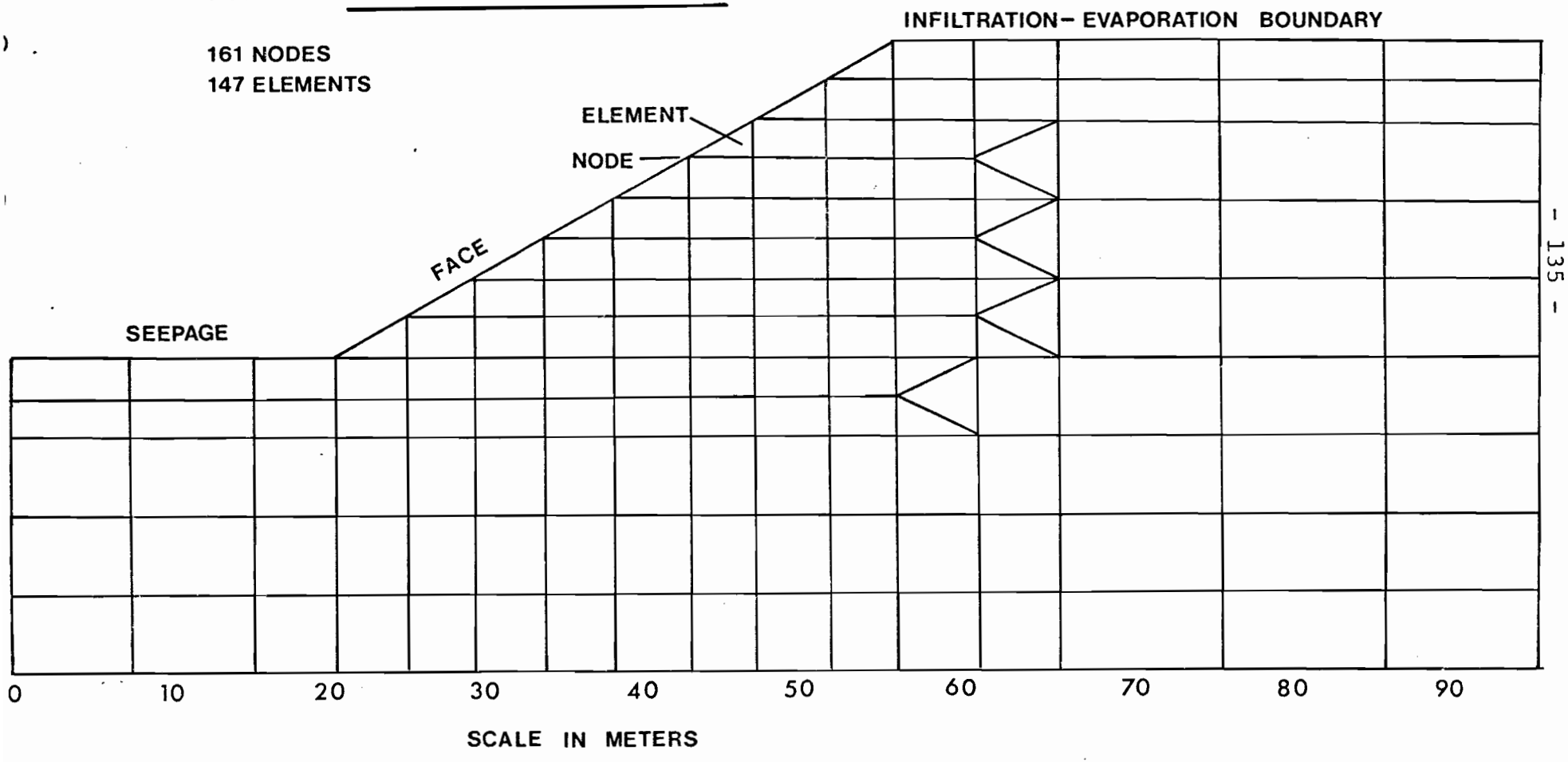

SETTING	NO. OF SOIL LAYERS	DEPTH TO BEDROCK meters	PERCENT OF SLOPE SUBMERGED 0	25	50	75
A	3	15	x	x	x	x
B	3	10	x	x	x	x
C	3	5	x	x	x	x
D	3	0	x	x	x	x
E	4	15	x	x	x	x
F	4	10	x	x	x	x
G	5	15	x	x	x	x
H	5	15	x			
I	3	15	x	x	x	
J	3	10	x	x	x	
K	3	5	x	x	x	
L	2	0	x	x	x	
M	1	na	x	x	x	

Settings A-H have a surficial layer of sand
Settings I-M have a surficial layer of clay
Setting H incorporates a bedrock sink term

TABLE 4.5 COMBINATION OF GEOLOGICAL FACTORS MODELLED

pore pressures in a slope. Therefore, the pore pressures will be constantly changing in response to the flux across the climatic boundaries. For comparison purposes, it was necessary to generate statistics that would describe the variation in the pressure head at a node over the time period simulated. For this purpose, a few modifications were made to the original program code to enable the generation of: mean total head, mean pressure head, minimum and maximum pressure heads, and the standard deviation. For the stability analyses which form the basis for the next part, the maximum pore pressures are used. The remainder of the statistics have no direct bearing on this thesis but have been included in Appendix D as supplementary information.

For each of the forty-six models, a profile was drawn on which the following information was included: the site geology; the maximum total head at each nodal point; and contours of equipotential. The refraction of the equipotentials at the soil boundaries was by judgement only and not by the law of reflection and refraction. The profiles for each of the forty-six models can be found in Appendix D. Comparison of the flow regime between the various models will be on the basis of pressure head versus depth profiles for the crest region and the toe of the slope. Since there is always more than one pressure head versus depth on the profiles, each curve is identified by a letter code that equates to the setting number shown in table 4.5.

4.6b Depth to Bedrock

Scott et al. (1976) showed diagramatically that, as the permeable bedrock outcrops in the valley bottom, any

artesian pressures which may have been present in the toe area are dissipated. To investigate this phenomenon, a series of models were tested where the bedrock was at a maximum depth of 15 meters beneath the toe (settings A, E, G, H, I) to a minimum depth of outcropping in the valley bottom (settings D, L). Intermediate depths were also chosen so as to compare the effect of bedrock at shallower depths. Other depths studied were 5 meters (settings C, K) and 10 meters (settings B, F, J). In all cases, the bedrock was assumed to be flat. From the drilling carried out as part of this study, it is apparent that the bedrock surface contains numerous scarps and valleys. The distribution of pore pressures resulting from an irregular bedrock surface is beyond the intended scope of this study but is a problem which needs to be investigated.

Profiles showing the effect of the depth to bedrock on the pressure head with depth are given in figures 4.22 to 4.25. Figures 4.22 and 4.23 are for models A to D or those with a surficial layer of sand, while figures 4.24 and 4.25 relate to models with a surficial layer of clay. From the crest profile (figure 4.22), it is evident that the downdrainage increases as the bedrock is located at shallower depths. The pressure head in the upper five meters of the section is the same for all the models reflecting the more or less constant recharge of the groundwater from the sand layer. The sharp break in the curves at depths 20, 25 and 30 for curves D, C and B respectively are due to the onset of near hydrostatic conditions in the fractured bedrock. No break in curve A was detectable. The difference in the pore pressure profiles for the toe area is not as pronounced for models A, B and C as it was at the crest. Here again, the break in the curves

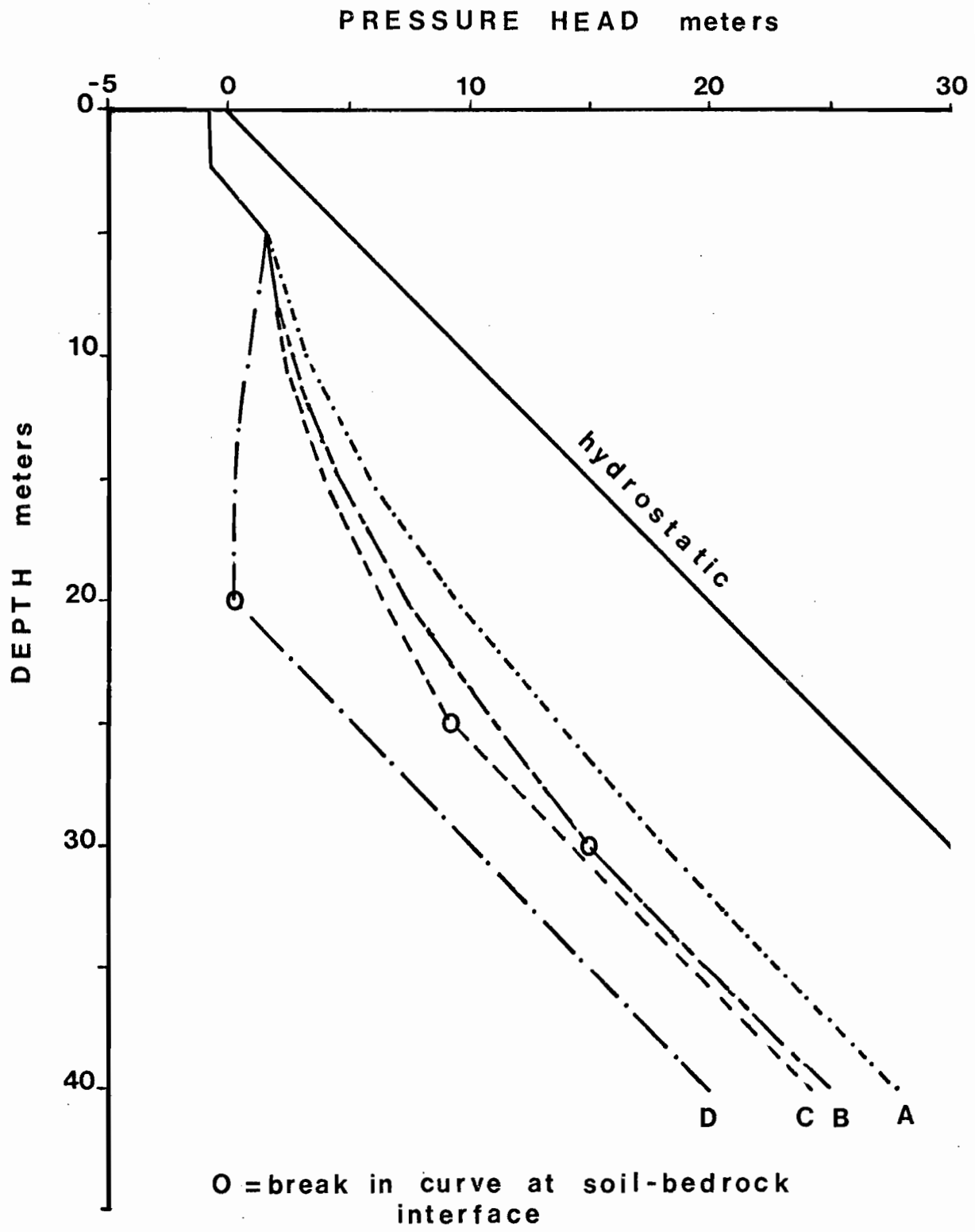

FIG 4.22 PRESSURE HEAD vs DEPTH

CREST - NO SUBMERGENCE
SAND AT SURFACE

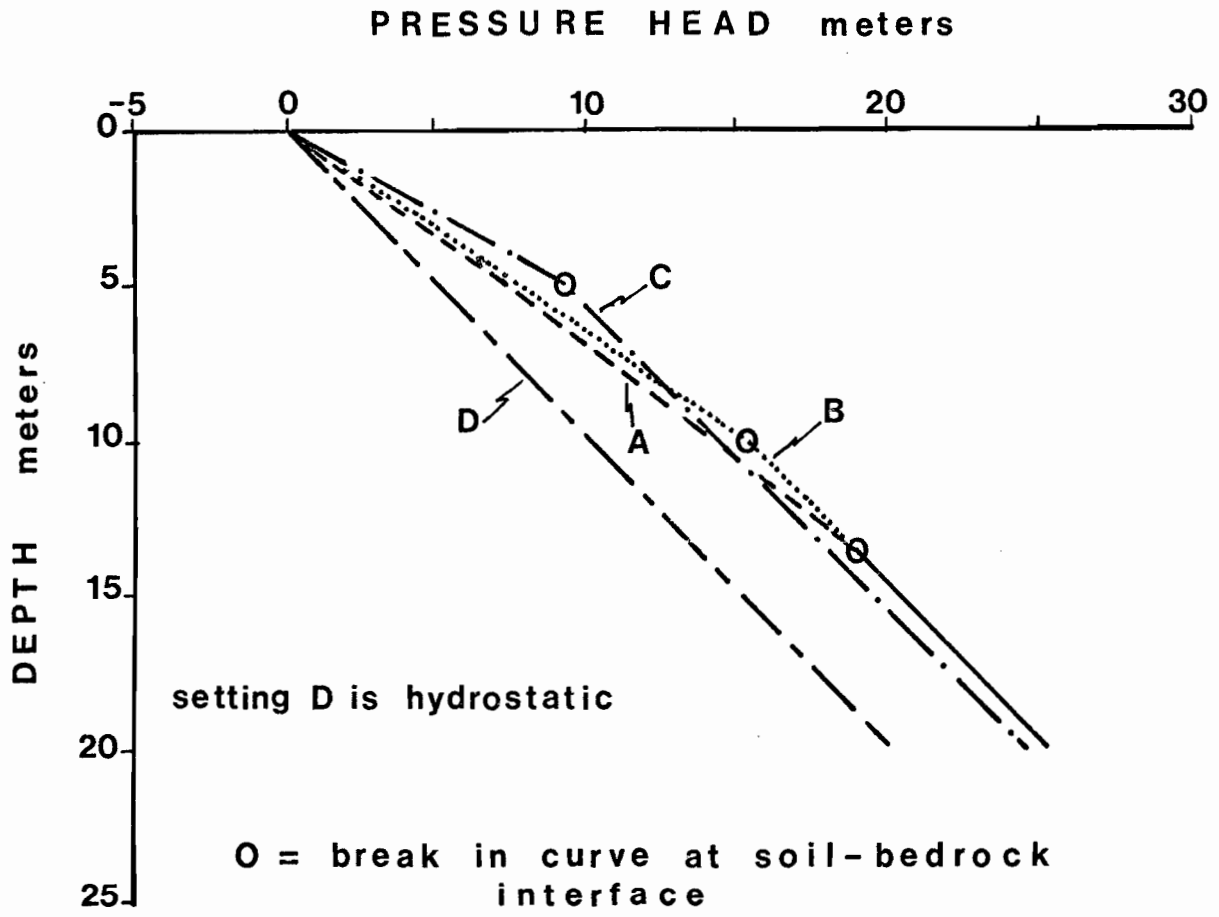

FIG 4.23 PRESSURE HEAD vs DEPTH

TOE - NO SUBMERGENCE
SAND AT SURFACE

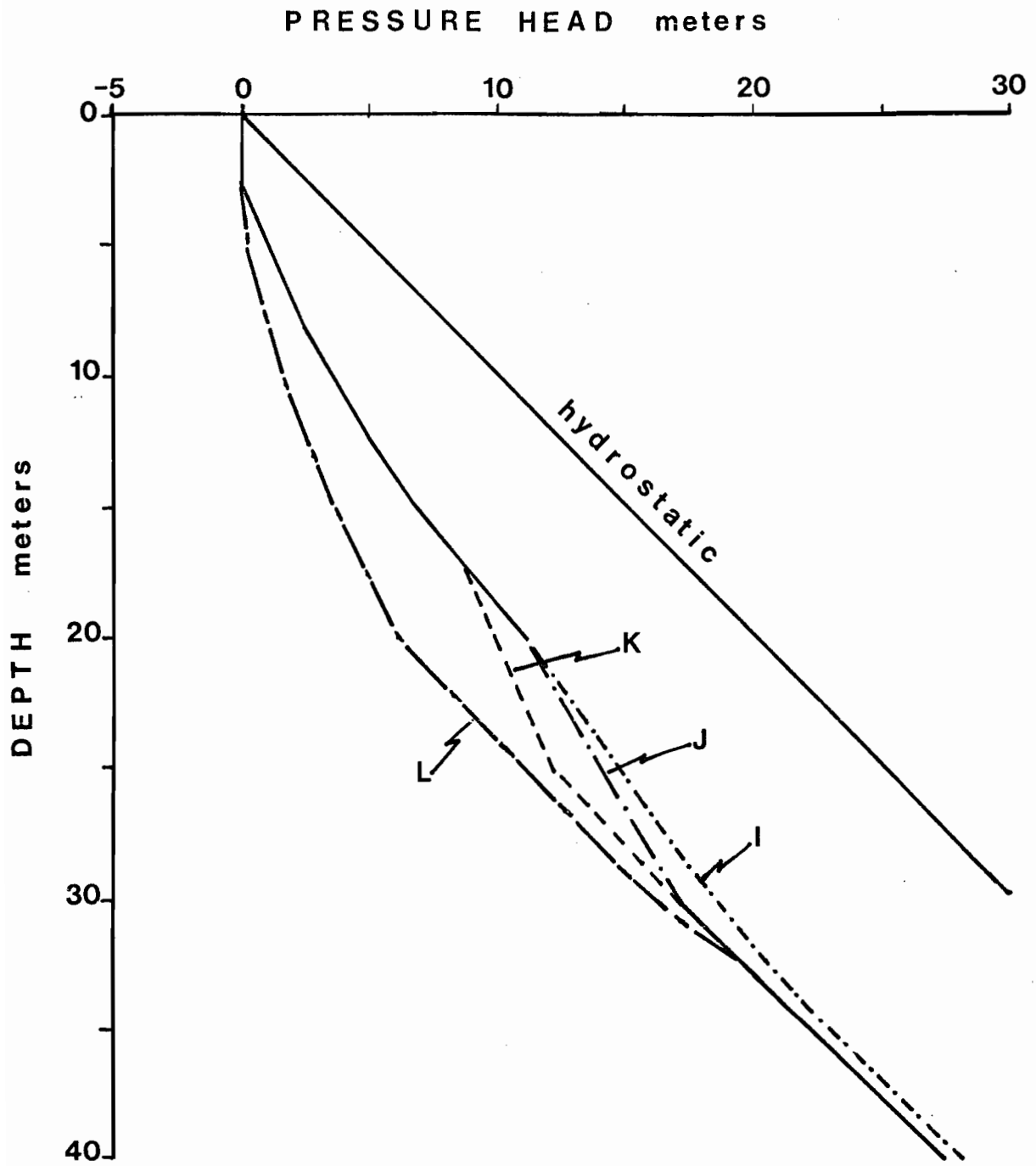

FIG 4.24 PRESSURE HEAD vs DEPTH

CREST - NO SUBMERGENCE
CLAY AT SURFACE

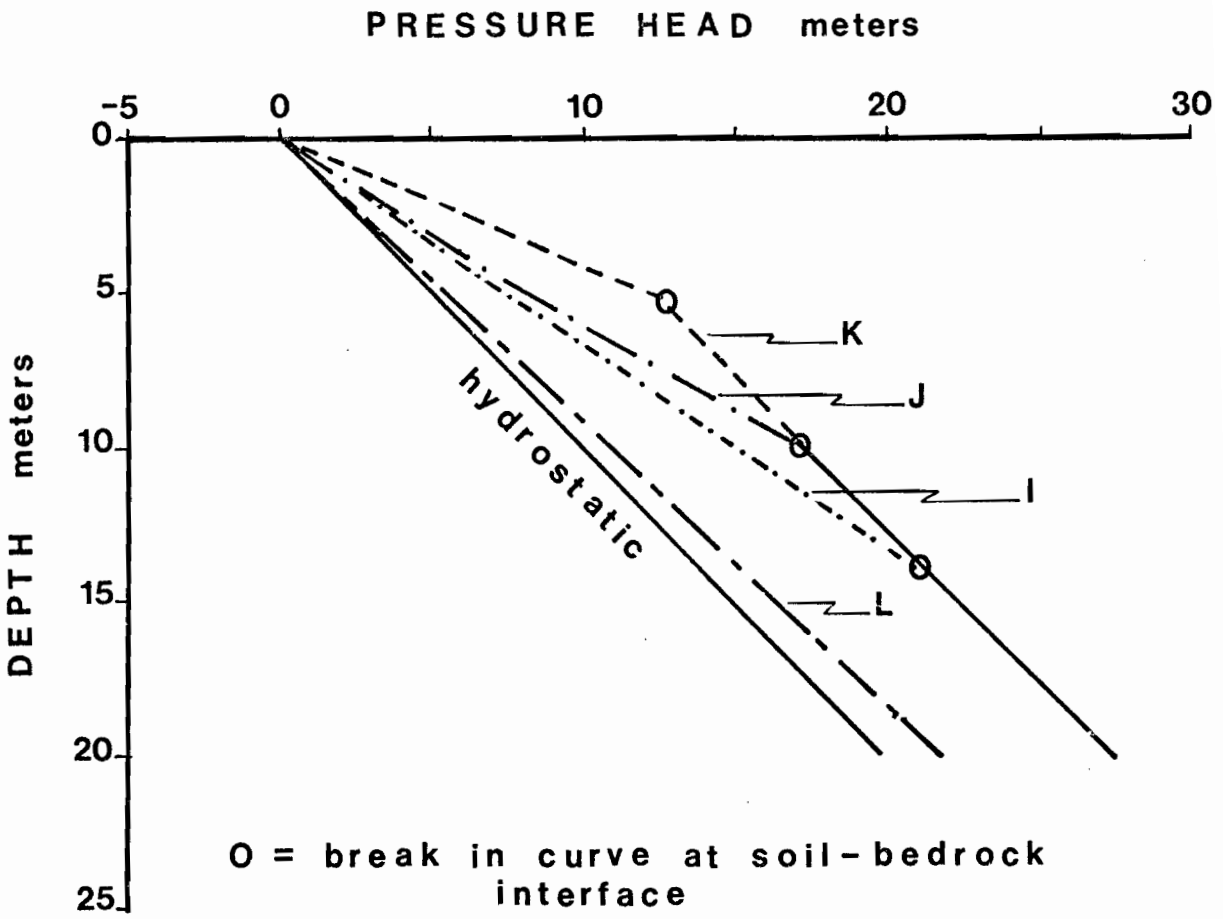

FIG 4.25 PRESSURE HEAD vs DEPTH

TOE - NO SUBMERGENCE
CLAY AT SURFACE

is at the bedrock-soil interface. The curve for model D falls along the line representing hydrostatic conditions indicating that no artesian pressures are present when the bedrock outcrops in the valley bottom.

The models which had no sand at the surface and in which the depth to bedrock was varied are I, K, J, and L. The trends in the pore pressure with depth curves are not as clear as for the models with sand at the surface. The pressure head for all the models was essentially the same at depths greater than 35 m (see figures 4.24 and 4.25). The range in pressure head versus depth between the models is bounded on the lower pressure side by the curve for setting L or the one where the bedrock outcrops in the valley bottom and, on the upper side, by the curve for setting I in which bedrock is at a depth of 15 m. All the curves meet at the top of the section and are close to joining near the bottom of the section. The lines joining the I and L curves at intermediate depths are those for the models of J and K and represent the shift in pore pressures due to the influence of the bedrock. The pressure-depth curves for the toe area are shown in figure 4.24 and are similar to those described for the region where sand overlies the clay. The main difference between the two groups of models (i.e. sand versus clay) is that the artesian pressures are greater where clay is found at the surface than where the sand is the surficial layer. Examples of the pressure head difference for comparable bedrock elevations are 25 m of water for setting A at a depth of 20 m and a pressure head of 27.5 m for setting I at the same depth.

The previous discussion of the effect of the depth to bedrock was based only on the models where there

was no external body of water submerging the slope. For the sake of brevity, the pressure-depth curves for the other degrees of submergence will not be given here. However, it should be noted that the same general trends were identified and that the depth of submergence tended to reduce the difference between the pore pressures for the different models. For example, with no submergence the difference between the pressure heads at 40 m for models A and D was 8 m of water, while for a slope submerged to 25% the difference was reduced to 3 m of water and at 50% submergence the pressure difference was 1.5 m. It may be, therefore, concluded that as the percent of the slope which is submerged increases, the effect of the depth to bedrock becomes less significant.

The results which have been presented here show that the artesian pressures which are present in the toe area are dissipated when the bedrock outcrops in the valley bottom. This is compatible with the field results which have been presented by Scott et al. (1976). Since it was necessary to use a bedrock sink term for modelling of the flow regime at site P1, it must be anticipated that the bedrock control would be affected by the piezometric level in the bedrock aquifer. Therefore, the depth to bedrock is likely to be more significant than has been shown here where the sink term has been ignored.

4.6c Number of Soil Layers

In any geologic depositional environment, there exists the possibility that not all of the soil units will be found in any given section. The finite element program used here had a limit of five different soil layers. More

could be added, but it would be necessary to alter the dimension statements in seven of the program subroutines. It was decided that it would be better to group some of the like soil layers rather than try to simulate the flow through seven or eight soils. The fractured bedrock, till and gravel were grouped into a single hydrogeologic unit. The bedrock is very permeable and so is the ice contact gravel. The till is more permeable than the overlying clay and should have a hydraulic conductivity at least an order of magnitude greater than the clay. Also the till is patchy and is generally not more than a couple of meters thick. For this and the above reasons, it was combined in with the bedrock and the gravel. The overlying clay layers were considered to be made up of three distinct units. The first was the deepwater marine clay; overlying this was a banded clay followed by interbedded silt and clay. Each of these units were modelled using the hydraulic conductivities obtained from the modelling of site P1. To be explained later, convergence problems were encountered when clay was used as the surficial layer. It was, therefore, necessary to reduce the permeability of the banded clay by two orders of magnitude in order that a solution could be obtained.

The number of soil layers investigated ranged from a minimum of one to a maximum of five. The nature and sequence of the soil layers were similar to that which was identified in the field; i.e. the more massive deepwater marine clay was found overlying the bedrock and a sand layer capped the clay layers.

For comparing the effect of the number of soil layers on the pore pressure distribution, models A, E, and G are used. Pressure head-depth curves for the crest and toe

are shown in figures 4.26 and 4.27 respectively. For the crest area, there appears to be no visible trends. Model A had three layers and has a pressure-depth curve which lies between the curves for four and five layers. At depths greater than 15 m, the difference in pressure head between the three models at any given depth is under 1 meter of water. For depths less than 15 m, the difference increases to a maximum of 2.5 meters of water at a depth of 5 m. The difference between the pressure heads at the toe was less. The maximum difference between the three models at any depth is about 0.5 m.

The indication here is that the number of soil layers has only a negligible effect on the pore pressure distribution and that there is no consistent relationship between the number of soil layers and the type of pressure head profile with depth which may be expected.

4.6d Depth of Submergence

Most of the active slides are occurring along the banks of eroding rivers. Therefore, there is almost always some water which is external to the slope. This body of water is generally thought to have a stabilizing effect on the slope. Since the portion of the slope that is submerged can vary from season to season and year to year, then it was necessary to determine the pore pressure distribution for the model slopes under three to four different degrees of submergence. For settings A to G, four degrees of submergence were evaluated. The first was a completely dry slope with no water. The degree of submergence was then increased to 25% of the slope submergence and on up to 75%. From the first few models, it was evident

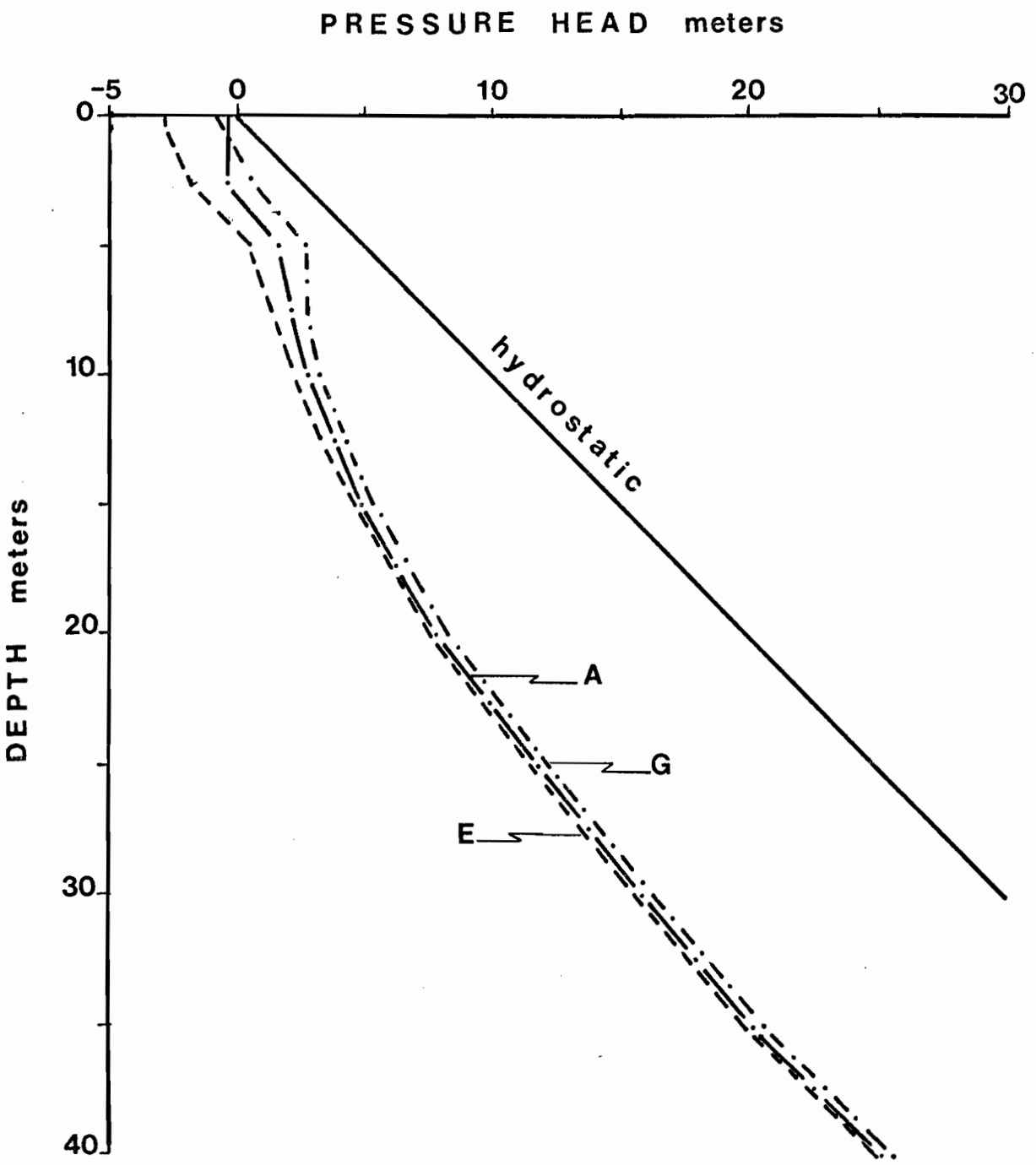

FIG 4.26 PRESSURE HEAD vs DEPTH

- CREST
- NO SUBMERGENCE
- BEDROCK ELEVATION: 5 METERS
- SAND AT SURFACE

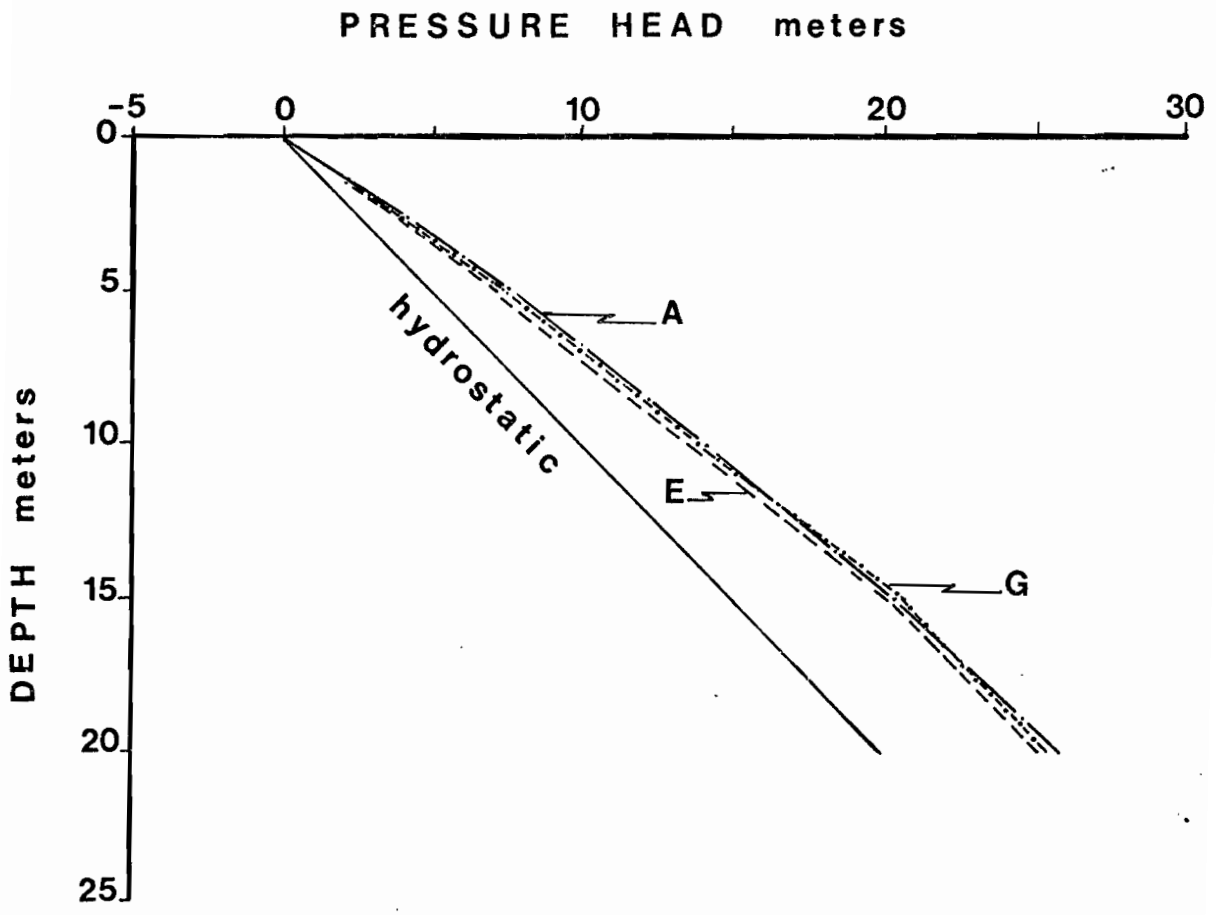

FIG 4.27 PRESSURE HEAD vs DEPTH

- TOE
- NO SUBMERGENCE
- BEDROCK ELEVATION: 5 METERS
- SAND AT SURFACE

that the flow changed very little between the different settings when the slope was 75% submerged. Therefore, the remaining settings I to M were evaluated only up to 50% submergence.

Model A is used for discussion of the effect of the depth of submergence on the distribution of pore pressures in the slopes. The results are plotted in figures 4.28 and 4.29 in a similar manner to the influencing factors previously described. The hydrostatic line (figure 4.28) represents the pressure heads that could be anticipated if the slope was 100% submerged. As the slope becomes less submerged, the drawdown increases up to the maximum recharge conditions when the slope is completely free of any external body of water. The difference in pressure head at a depth of 40 m between the hydrostatic conditions and the 0% submergence is roughly 15 meters of water. As the percentage of submergence becomes less than or equal to 75%, the curves for the pressure head versus depth join at a common depth of 5 m and diverge from this point. The control at the 5 m depth is due to the water table which is maintained in the surficial sand layer. Pressure head versus depth curves are also given for setting G for the crest region and show that not all the curves join at the depth of 5 m. This difference between the two models is due to the greater number of layers in model G (figure 4.30). Submergences of 0 and 25% join at a common point of 10 m or at the base of the silt and clay layer. At 50 and 75%, the curves join at the base of the sand layer. The reason for this change is that, as the slope becomes more submerged, the influence of the individual soil layers that are at depths lower than the elevation of the external water no longer play a significant role in the distribution of the pore pressures in the slopes.

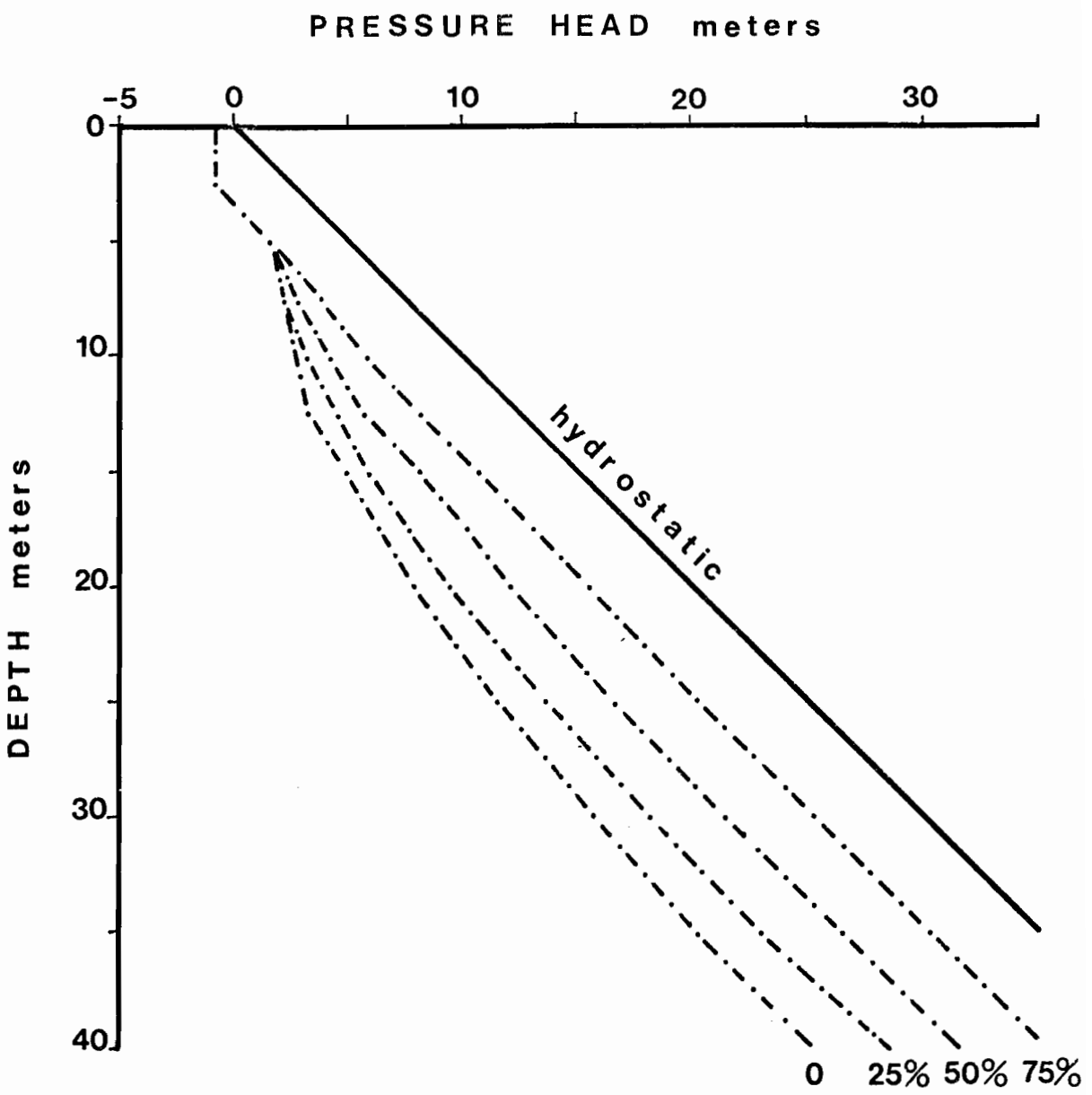

FIG 4.28 PRESSURE HEAD vs DEPTH

- CREST
- MODEL A
- BEDROCK ELEVATION : 5 METERS
- SAND AT SURFACE

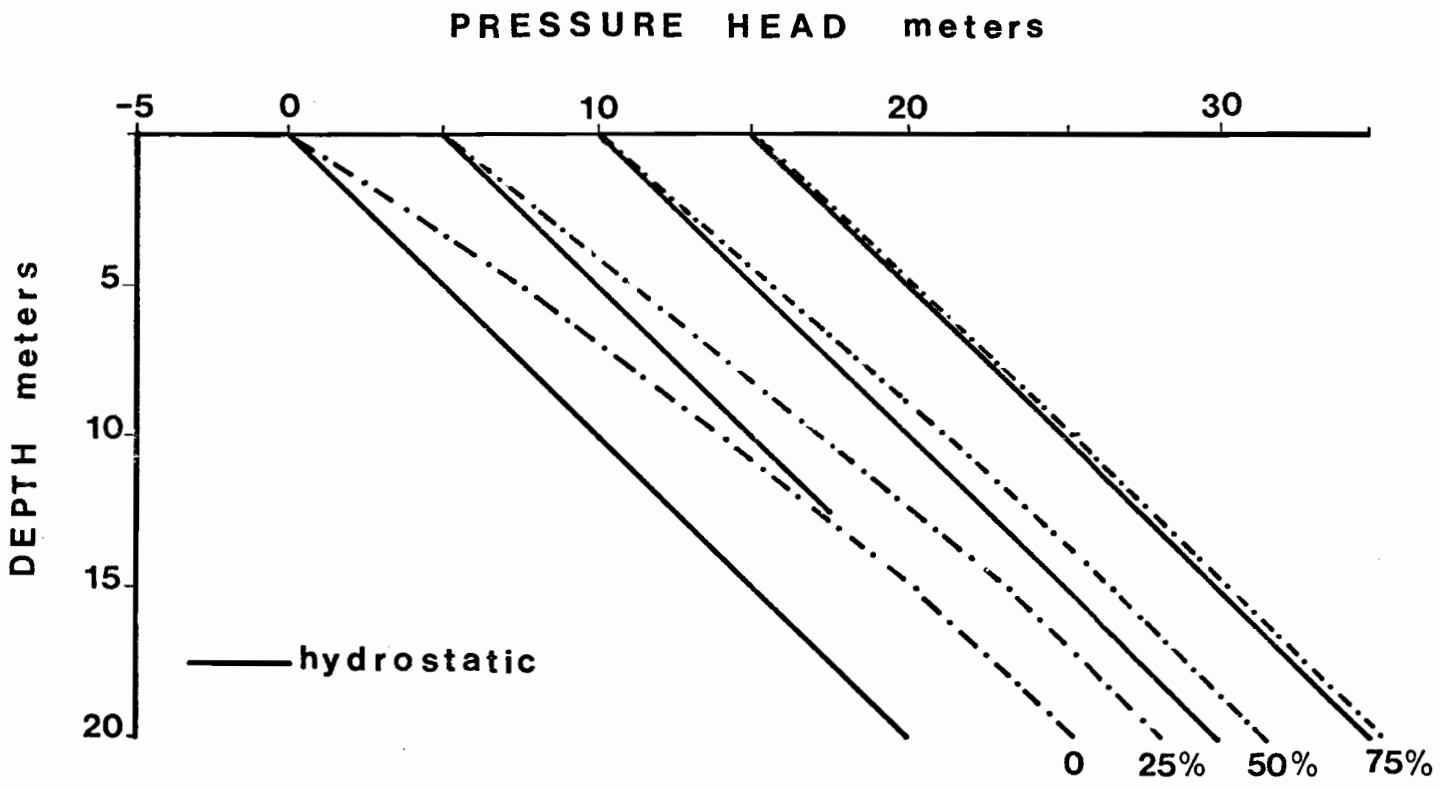

FIG 4,29 PRESSURE HEAD vs DEPTH

- TOE
- MODEL A
- BEDROCK ELEVATION : 5 METERS
- SAND AT SURFACE

Pressure head-depth curves for the toe area of the models A and G are shown in figures 4.29 and 4.31 respectively. Since the two are essentially identical in this case, only model A will be discussed. With the increasing submergence, there is a shift to higher pressure heads. However, if the hydrostatic pressure is taken into account, it is evident that, as the depth to submergence increases, the excess pressure head or the artesian pressures are greatly reduced until they are completely absent under 100% submergence. For example, the excess pressure at 0% submergence is 5.5 m of water, while at 75% submergence the excess pressure is in an order of magnitude lower or about 0.5 m of water.

It appears that the depth of submergence has a controlling influence on the recharge and discharge of the groundwater system and the distribution of the pore pressures. Not only does the external body of water change the stability by loading the toe, but it also changes the groundwater regime which, in turn, will affect the stability of natural slopes.

4.6e Bedrock Sink Term

As previously shown, it was necessary to incorporate a bedrock sink term in order that a good fit be obtained between the measured and the calculated pore pressures for site P1. Since it was not possible to apply universally the same sink term to different sites with different soil properties, it was decided that different sink terms would be applied to setting G so as to investigate the influence of the sink term on the distribution of the pore pressures. Three sink terms were used: -0.00015, -0.00050 and -0.00075. The greater the magnitude, the

the more the pore pressures were reduced in the bedrock aquifer. For the present study, the slope was assumed to be free of an external body of water. Ideally, the sink term should be used in conjunction with different depths of submergence.

The effect of the sink can be seen in figures 4.30 and 4.31. Models G and H had the same soil conditions; the only difference between the two models was that the pressure head in the bedrock was lowered for model H. The magnitude of the sink was increased until the soil immediately overlying the bedrock became partially unsaturated. For the crest region, the effect of the sink is to draw the piezometric levels below that of the 0% submergence for model G. The effect at the toe area is to reduce the artesian pressures. With a sink term of -0.00015, there is an artesian pressure of about 1 meter of water at a depth of 20 m. With an increase to -0.00050, there is a substantial reduction in the pressure head at 20 m depth to a value of 8 m of water lower than hydrostatic. Finally, with a sink of -0.00075, the pressure head is reduced to 3.5 meters of water or 16.5 meters of water below hydrostatic.

Referring back to figure 4.6, which shows the pressure head versus depth curves for site P1, it is evident that the pore pressures near the toe approximate that of hydrostatic. It is therefore concluded that a sink term of -0.00015 produces results which are compatible with those which have been identified in the field. However, the shape of the curve for the calculated pressure head versus depth curve does not approximate very well the results obtained for sites P1 and P2. This could be due to the difference in site geometry of the field sites as compared to the basic model used for the numerical simulation of the groundwater flow.

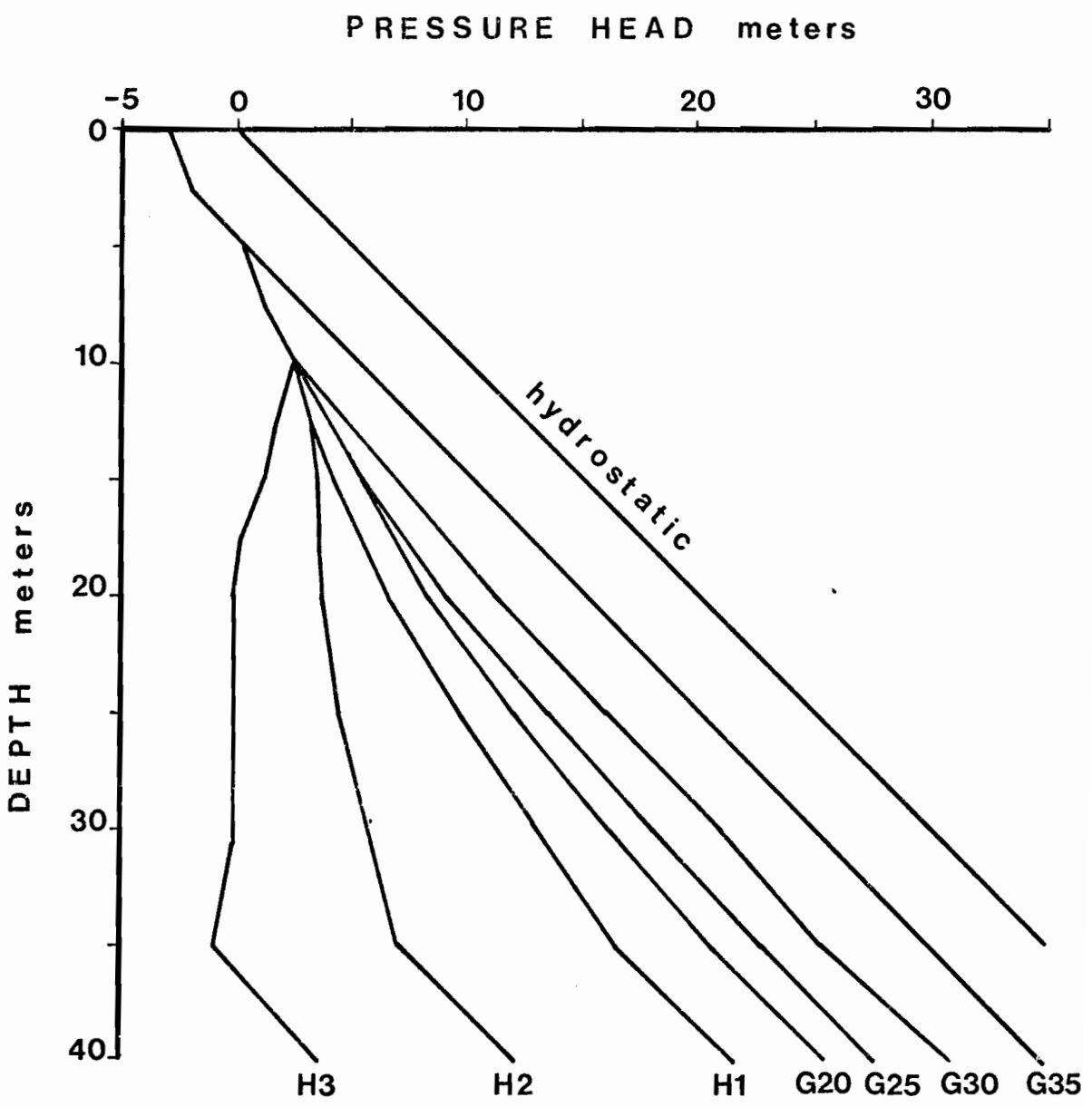

FIG 4.30 PRESSURE HEAD vs DEPTH

- CREST
- MODELS G & H
- BEDROCK ELEVATION : 5 METERS
- SAND AT SURFACE

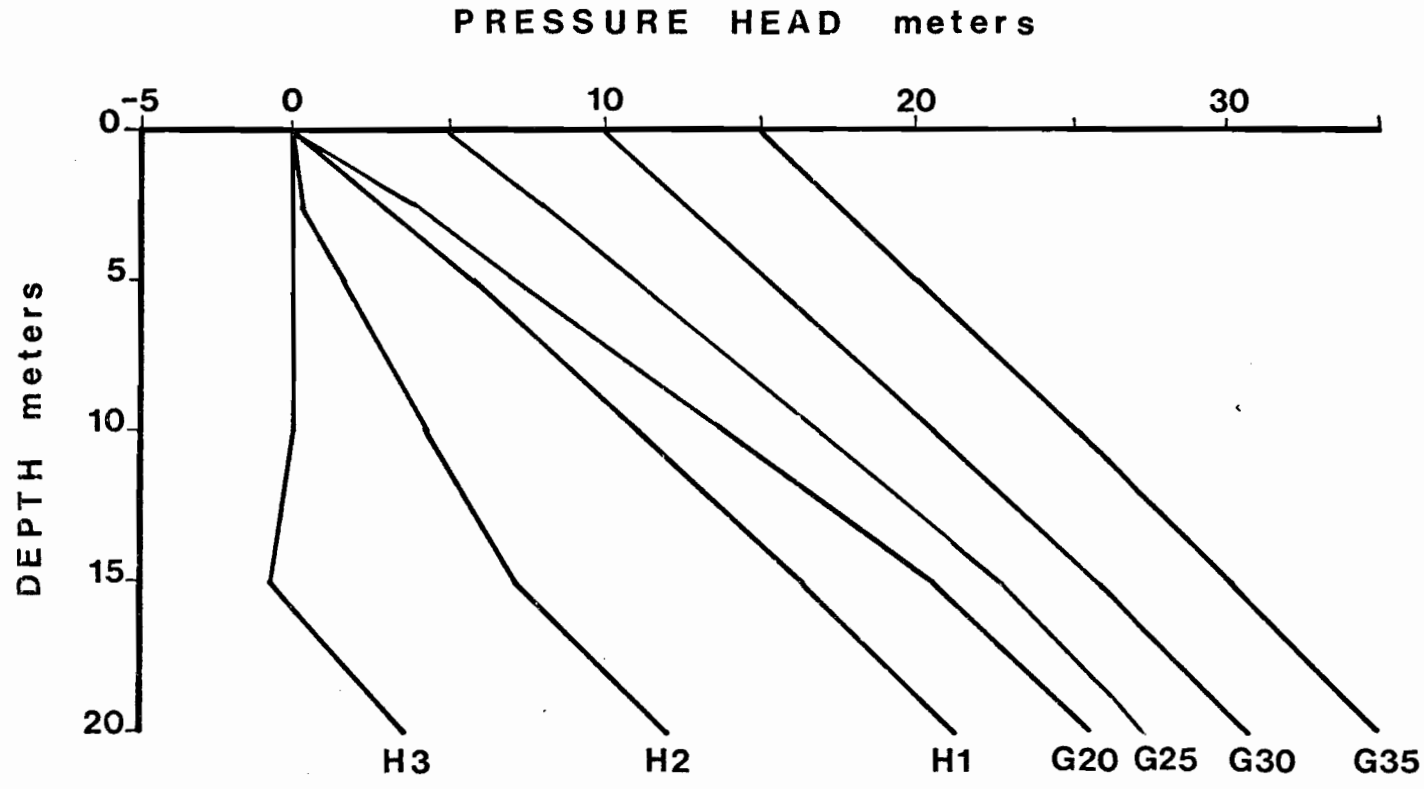

FIG 4.31 PRESSURE HEAD vs DEPTH

- TOE
- MODELS G & H
- BEDROCK ELEVATION ; 5 METERS
- SAND AT SURFACE

4.6f Nature of the Surficial Layer

The stratigraphy and geological mapping of the region have shown that there are essentially only two different soil layers on the surface: sand and clay. From airphoto analyses made during the mapping of the sensitive clay deposits, it was evident that the clay had a considerably greater drainage density than the sand. This indicates that the clay being more impervious has greater runoff than the sand. It is therefore evident that the recharge to the groundwater system would vary according to the nature of the surficial layer. In accordance with the two typical slope profiles described in the beginning of this chapter, the models were divided into two groups: those with a surficial layer of sand and those with a surficial layer of clay. Models A to H had a stratigraphy consisting of a number of clay layers overlain by a 5 m thick layer of sand. Models I to M had clay at the surface. With models I to M, convergence problems were encountered. With the highly impervious soil at the surface, the solution would not converge and the program would stop before a complete solution could be obtained. It was therefore necessary to increase the permeability of the clay by two orders of magnitude before a solution could be arrived at. This meant that the permeability contrasts were not as great between the soil layer as they were for the models with sand on the surface. Consequently, the flow nets for the clay at surface models will show that there is considerably more flow in the bedrock than would likely occur if the clay was more impermeable.

Comparison of the two groups of models, one having a surficial layer of sand, the other having a surficial

layer of clay, has been rendered difficult due to the convergence problems. The discussion which follows here is at best speculative and should be viewed in this light.

The sand acts as a groundwater storage basin and therefore influences the position of the water table. There is a spring line which develops along the slope face at the contact between the sand and the underlying clay. The result is that the water table is relatively flat even close to the slope face. The clay-only profiles have a more sloping water table and the top of the seepage face along the slope is generally 5 to 10 meters lower in elevation than where there is sand at the surface. Examples of the differences in the water table locations can be seen in Appendix E. Models A to H have a surficial layer of sand while I to M have a surficial layer of clay.

In terms of the pressure head versus depth profiles, it appears that the pressure head in the clay-only models is on the average higher than in the sand models. Comparison of the pressure head versus depth for the crest area can be seen in figures 4.22 and 4.24. For comparison purposes, it is necessary to choose two models which have the same depth to bedrock. Taking models A and I and comparing the total heads at a depth of 40 m, the total heads are 25.39 and 27.47 respectively or a difference of about 2.1 meters of water. Since the total head is nearly constant in the bedrock, the 2.1 meter difference is also found at the toe of the slopes. Therefore, there is less drawdown in the crest region for the crest area of the clay-only models and the artesian pressure is greater in the toe area. The effect of the higher pore pressures

on the stability of the clay-only slopes will be shown in the next part; however, intuitively speaking, there should be lower safety factors in the clay-only slopes.

4.7 Summary and Conclusions

The pore pressure distribution along a potential failure plane is an integral part of an effective stress analysis. It has been shown that the permeability contrasts between soil or rock layers governs the pore pressures (Hodge and Freeze, 1977). It was shown in Chapter 2 that the sensitive clay deposits can be made up of at least four units and that there can be either a surficial layer of sand or clay at the surface. Therefore there are a variety of different site geologies, each of which can be expected to have its own pore pressure distribution. To study the effects of the geology on the pore pressures in sensitive clay slopes, a field and numerical study of the groundwater regime in the Ottawa Valley has been carried out.

Three field sites were instrumented with piezometers and show the influence of the bedrock on the pore pressure profiles. Sites P1 and P2 are located east of Ottawa (see figure 4.3) and are underlain by fractured Ordavician sedimentary rocks. The bedrock is sufficiently permeable that a lower piezometric level is maintained, as can be seen in figures 4.6 and 4.7. Site P3 is located north of Ottawa and is underlain by massive Precambrian gneissic rocks. The pore pressures for site P3 are shown in figure 4.8 and indicate that artesian pressures are present at the toe. The pore pressures at site P3 closely approximate those that would be expected from the neoclassical flow theory.

A finite element simulation of the groundwater flow at site P1 was made with two objectives. The first was to obtain values of the hydraulic conductivities for the various soil and rock layers. The second objective was to determine the reliability of the finite element method in predicting the pore pressures in sensitive clay slopes of the Ottawa Valley. Table 4.4 lists the hydraulic conductivities obtained from the numerical modelling. Figures 4.17 to 4.19 show the measured and calculated pressure heads for the piezometer nests at the crest, mid-slope and toe respectively. A regression analysis was made comparing the measured and calculated pressure heads. The results of the regression analysis are shown in figure 4.20. The correlation coefficient is 0.85 which indicates that the calculated pressure heads are a reasonable approximation of the in situ pressure heads. It is interesting to note that only a poor correlation was achieved without artificially lowering the piezometric level in the bedrock; the lower piezometric level in the bedrock is likely due to river valley bottoms intersecting the permeable bedrock. The bedrock pressure head is then a function of the surface elevation of the river.

From the drilling and mapping programs, it was concluded that the sensitive clay deposits were made up of a number of distinct units. An investigation of the effects of the various site geologies on the distribution of the pore pressures in slopes was made. The results indicate that the depth to bedrock is an important factor in determining the pore pressure distribution that will be recorded in slopes. In the discussion of figures 4.22 to 4.25, it was demonstrated quantitatively that the artesian pressures at the toe of the slope are dissipated when the

bedrock outcrops in the valley bottom. The results for the depth to bedrock investigation are compatible with those reported by Scott et al. (1976). In section 4.6f on the nature of the surficial layer, it was shown that the pressure head versus depth profiles are significantly different where there is a surficial layer of sand rather than clay. The sand acts as a groundwater reservoir and maintains near hydrostatic pressures in the clay directly beneath the sand. However, on the whole, the pressure heads in the bedrock are about 2 meters higher for those models which had clay on the surface. For the clay-only models, the artesian pressure at the toe was also greater, hence the gradients were greater than for similar depth to bedrock models which had sand on the surface.

From figures 4.26 and 4.27, it is evident that the number of soil layers had the least effect on the pressure head versus depth profiles. Models A, E, and G have 3, 4, and 5 soil layers respectively and there is only a 0.5 m to 1.0 m difference in the pressure head for the different models. This would indicate that only the macrocospic stratigraphy needs to be evaluated for slope stability work. By macroscopic inspection, it is inferred that only such items as the nature and thickness of the surficial layer and the depth to bedrock need to be obtained. With the stratigraphy and an estimate of the groundwater level in the bedrock, a reasonable approximation of the pore pressures in the remainder of the slope could be obtained by numerical techniques.

External bodies of water have been shown to affect the flow of groundwater (figures 4.28 and 4.29). As the slope becomes progressively more submerged, the

hydraulic gradients are reduced and the groundwater regime approaches that of hydrostatic. It was also shown that an increase of 25% in the portion of the slope submerged produces a change in the pressure head in the bedrock of about 3 m of water. Since most of the slides are now occurring along active rivers, then the depth of submergence is an important facet of stability calculations.

Models G and H are used to demonstrate the effect of a bedrock sink term or, in other words, a lower piezometric level in the bedrock. Figures 4.30 and 4.31 are plotted to show how the lowering of the piezometric level increases the downward drainage to the bedrock. Model G35 has the highest pressure head in the bedrock, while H3 has the lowest. It is not possible to apply the same sink term to all slopes since the drawdown effect which the sink term produces depends on the configuration of the mesh and the permeability of the soils. However, it was shown by the field results that, for the two sites to the east of Ottawa, a lower bedrock piezometric level did exist. Therefore, a knowledge of the piezometric level in the bedrock is critical to accurate simulation of the groundwater flow by numerical techniques.

Although many of the differences in pore pressures and groundwater flow for the various geologic settings which were modelled are somewhat subtle, they cannot be ignored. The change in stability for the various models will be given in the following part and will demonstrate that the groundwater regime is a controlling factor in the stability of slopes.

5 - SLOPE STABILITY OF SENSITIVE CLAY SLOPES

5.1 General

The calculation of the factor of safety for a slope requires an appropriate stability model which, when supplied with the correct information on the geology, strength parameters, and the pore pressures, will predict not only the factor of safety but also the location of the failure plane. There are several different stability models available to the engineer. The methods differ in the formulation of the stability equation and the assumptions that render the problem determinate (Fredlund, 1974). For reasons that will be given later, the Bishop method is used here in all the stability calculations. A review of the theory of the method is given along with the fundamental assumptions that are required for its formulation.

The factor of safety (FOS) for forty-six slopes of different site geology has been calculated using the strength parameters described in Chapter 3 and the pore pressure distributions obtained in Chapter 4. It has, therefore, been possible to investigate the change in the factor of safety with varying site geology. One of the forty-six models approximated closely the site conditions of a documented failure. Since the predicted FOS for the model was close to one, this would indicate that the approach to slope stability that has been taken here is valid.

5.2 Slope Stability Theory

Fredlund (1974) reviewed six of the most commonly used stability models: Spencer, Morgenstern-Price, Bishop, Ordinary, and two forms of Janbu's method. It was shown

that each of the methods could be derived from the same basic equations and that the differences lay mostly in the assumptions governing the side forces. In six case histories, the difference in the factor of safety obtained from the Bishop, Morgenstern-Price and Spencer methods was approximately 1%. The Bishop simplified method was used in this study for three reasons:

1) it is one of the best approximations of the real phenomenon (Yong et al., 1977);
2) it yields factors of safety that are as accurate as the more rigourous approaches; and
3) it is one of the more inexpensive models in terms of computer costs.

The method is based on the assumption that, when failure is imminent, the quantitative estimate of the FOS is determined by "comparing the strength necessary to maintain limiting equilibrium with the available strength of the soil". The shear strength that is mobilized along the failure plane is given by equation 5.1.

$$S = \frac{1}{F}\left[c' + (\sigma_n - u)\tan \phi'\right] \qquad (5.1)$$

S = shear strength
F = factor of safety
c' = effective cohesion
ϕ' = effective angle of friction
σ_n = total normal stress
u = pore pressure

The stability analysis assumes that:

1) failure occurs along a circular or composite surface and that the soil can be divided up into slices;

2) the material behaves according to equation 5.1;
3) the factor of safety with respect to the cohesive component and the friction component of strength are the same; and
4) the FOS is the same for all slices.

Figure 5.1 shows the forces involved in the solution of a circular or composite failure. The variables in figure 5.1 are defined as follows:

E_L, E_R = resultants of the total horizontal forces on the left and right sides of the n-th slice
X_L, X_R = resultants of the vertical shear forces on the left and right sides of the n-th slice
Q_L, Q_R = resultants of the horizontal and vertical forces on the left and right sides of the n-th slice
θ_L, θ_R = angle of the Q_L and Q_R forces, respectively, from the horizontal
p = total normal stress acting on the base of the slice
p' = effective normal stress acting on the base of the slice
u = pore water pressure on the base of the slice
S_m = shear force mobilized on the base of the slice
h = height of the slice
b = breadth of the slice
ℓ = arc length along the base of the slice
α = average angle between the tangent to the base of the slice and the horizontal
x = horizontal distance of the slice from the centre of the rotation
f = perpendicular offset of the normal force from the centre of rotation
W = total weight of the slice

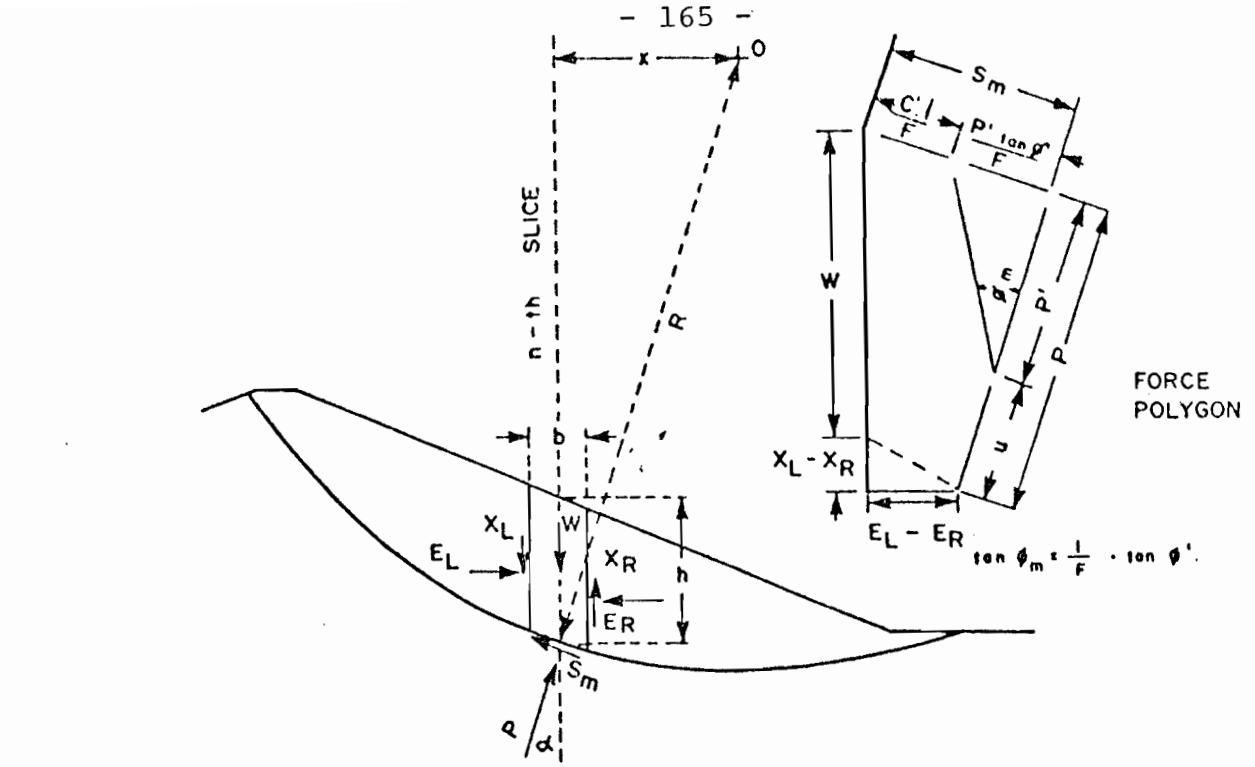

(a) CIRCULAR SLIP SURFACE

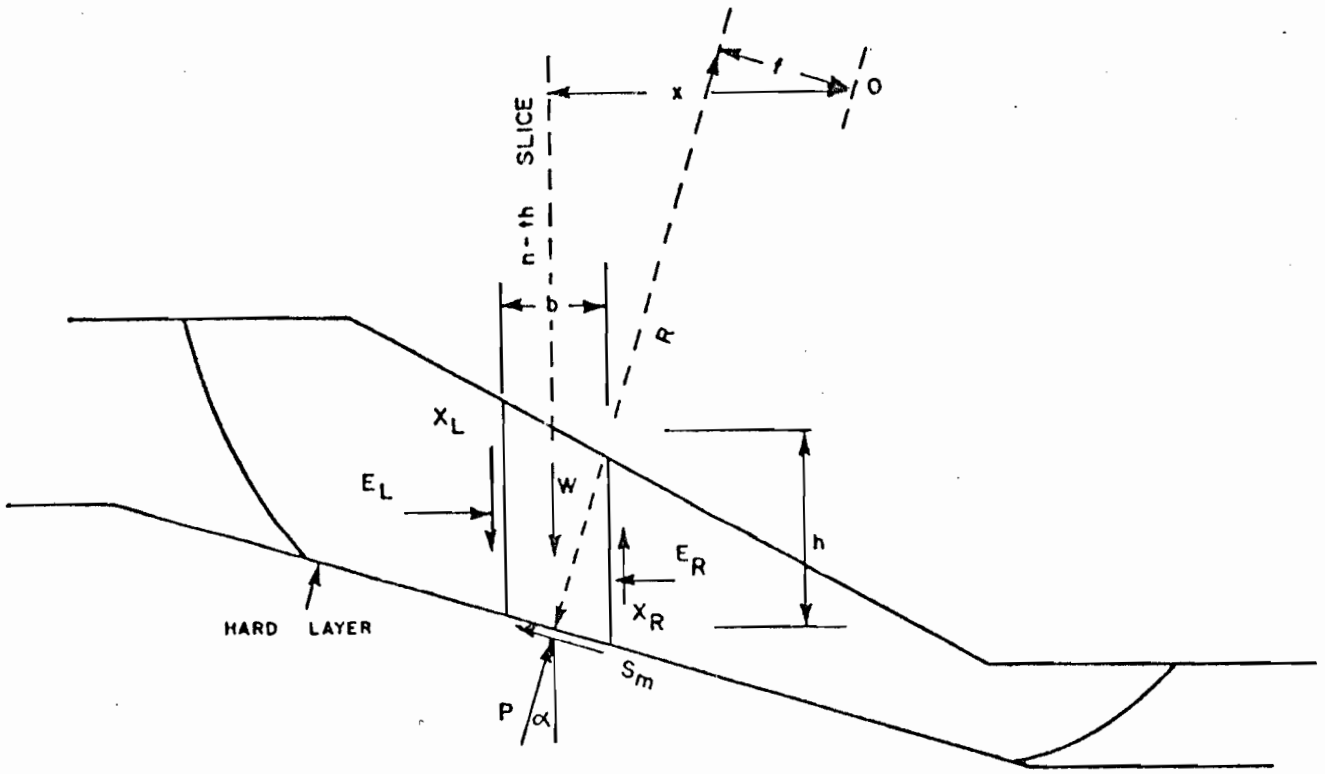

(b) COMPOSITE SLIP SURFACE

FIGURE 5.1 FORCES ACTING FOR THE METHOD OF SLICES APPLIED TO A CIRCULAR AND COMPOSITE SLIDING SURFACE
(AFTER FREDLUND, 1974)

R = radius (Note: this is a variable for the composite slip surface)

ϕ_m = angle of internal friction mobilized

c' = effective cohesion parameter

ϕ' = effective angle of internal friction parameter.

Equation 5.1 is indeterminate due to an inadequate knowledge of the normal stress distribution on the base of the slice and the normal and shear stresses on the sides of the slice. Assumptions must be made on either the side or base forces in order that the problem be determinate. The Bishop method assumes that the resultant of all the side forces on each slice acts horizontally.

The normal stress on the base of a slice is:

$$\sigma_n = p/\ell \tag{5.2}$$

It is therefore possible to rewrite equation 5.1 as

$$S = \frac{1}{F}\left[c' + \left(\frac{p}{\ell} - u\right) \tan \phi'\right] \tag{5.3}$$

By letting the shear force on the base of the slice equal to $S.\ell$ and equating the moments about the centre of the trial circle with the moments of the forces acting on the failure surface, equation 5.4 is obtained.

$$\sum W_x = \sum S\ R = \sum S\ \ell\ R \tag{5.4}$$

Substituting 5.4 into 5.3 and rearranging the terms it follows that

$$F = \frac{R}{\Sigma W_x} \cdot \sum \left[c'\ell + (p - u\ell) \tan \phi' \right] \qquad (5.5)$$

An expression for p (equation 5.6) is obtained by resolving the forces in a direction normal to the failure surface.

$$p = (W + X_n - X_{n+1}) \cos\alpha - (E_n - E_{n+1}) \sin\alpha \qquad (5.6)$$

Equation 5.5 then becomes

$$F = \frac{R}{\Sigma W_x} \cdot \sum \Big[c'\ell + \tan \phi' \ (W \cos\alpha - u\ell)$$

$$+ \tan \phi' \ \{(X_n - X_{n+1})\cos\alpha - (E_n - E_{n+1})\sin\alpha\} \Big] \qquad (5.7)$$

Since there are no external forces acting on the slope, then the sum of the vertical and horizontal side forces are zero. Furthermore, it is assumed that the term $\tan \phi' \ \{(X_n - X_{n+1})\cos\alpha - (E_n - E_{n+1})\sin\alpha\}$ in equation 5.7 can be neglected without a serious reduction in accuracy of the calculated FOS. By setting $x = R \sin\alpha$, the simplified form of equation 5.7 can be written as

$$F = \frac{1}{\Sigma W \sin\alpha} \cdot \Sigma \ \{c'\ell + \tan \phi' \ (W \cos\alpha - u\ell)\} \qquad (5.8)$$

Equation 5.8 tends to be conservative, especially where the failure is deepseated and the variation in the angle between the failure surface and the horizontal is large. It is therefore convenient to redefine the effective normal stress as:

$$p' = \frac{W + X_n - X_{n+1} - \ell(u \cos\alpha + \frac{c'}{F} \sin\alpha)}{\cos\alpha + \frac{\tan \phi' \cdot \sin\alpha}{F}} \qquad (5.9)$$

Substituting 5.9 into 5.5 and letting $\ell = b.\sec\alpha$ and $x = R.\sin\alpha$, an expression for the factor of safety is obtained.

$$F = \frac{1}{\Sigma W \sin\alpha} \cdot \sum \left(\{c'b + \tan \phi' \ (W(1 - \bar{b}) + (X_n - X_{n+1}))\} M\alpha \right) \qquad (5.10)$$

where

$$u = \bar{b} \ \frac{(W)}{b} \qquad (5.11)$$

and

$$M\alpha = \frac{\sec\alpha}{1 + \frac{\tan \phi' \tan\alpha}{F}} \qquad (5.12)$$

For a composite failure surface, where the circular arc intersects a planar hard layer (see figure 5.1) the offset of the normal force must be accounted for in the stability equation. The term $\Sigma W.\sin\alpha$ therefore becomes $\Sigma W.X - \Sigma p.f$.

In practice, a solution to equation 5.10 is obtained by assuming that $(X_n - X_{n+1}) = 0$ over the entire slope. In actual fact, there are several distributions

of $(X_n - X_{n+1})$ that will lead to equilibrium conditions. However, Fredlund and Krahn (1976) have shown that the factor of safety is relatively insensitive to the interslice force assumptions and that, for six examples, the factor of safety varied by approximately 1.0 percent for different interslice force assumptions.

5.3 Stability Calculations

It should be evident from the development of equation 5.10 that the factor of safety is dependent on the location of the centre of the failure circle and the radius. It is therefore possible to miss the critical circle if the location of the circle falls between trial centres or trial radii. In the software developed by Fredlund (1974), the trial centres are specified in the form of a grid and the radii in terms of elevations to which the radii are tangent. To assure that a minimum FOS for the slope was located, two sets of grids and radii were used. The first is a coarse grid in which the trial centres were on five-meter centres and the radius for each centre was incremented five times, therefore covering the depth from the toe of the slope to ten meters beneath the toe. Figure 5.2 shows the location of the coarse grid of trial centres and the elevations to which the radii are tangent. After the initial run, a minimum FOS was calculated and a finer grid was used to isolate the critical circle. The finer grid had trial centres on a spacing of one meter and the radius was incremented by 0.5 meters. In all, better than five hundred trial circles were used to determine the minimum FOS. It is estimated that the absolute minimum FOS is within ±0.025 of the FOS obtained from the stability calculations.

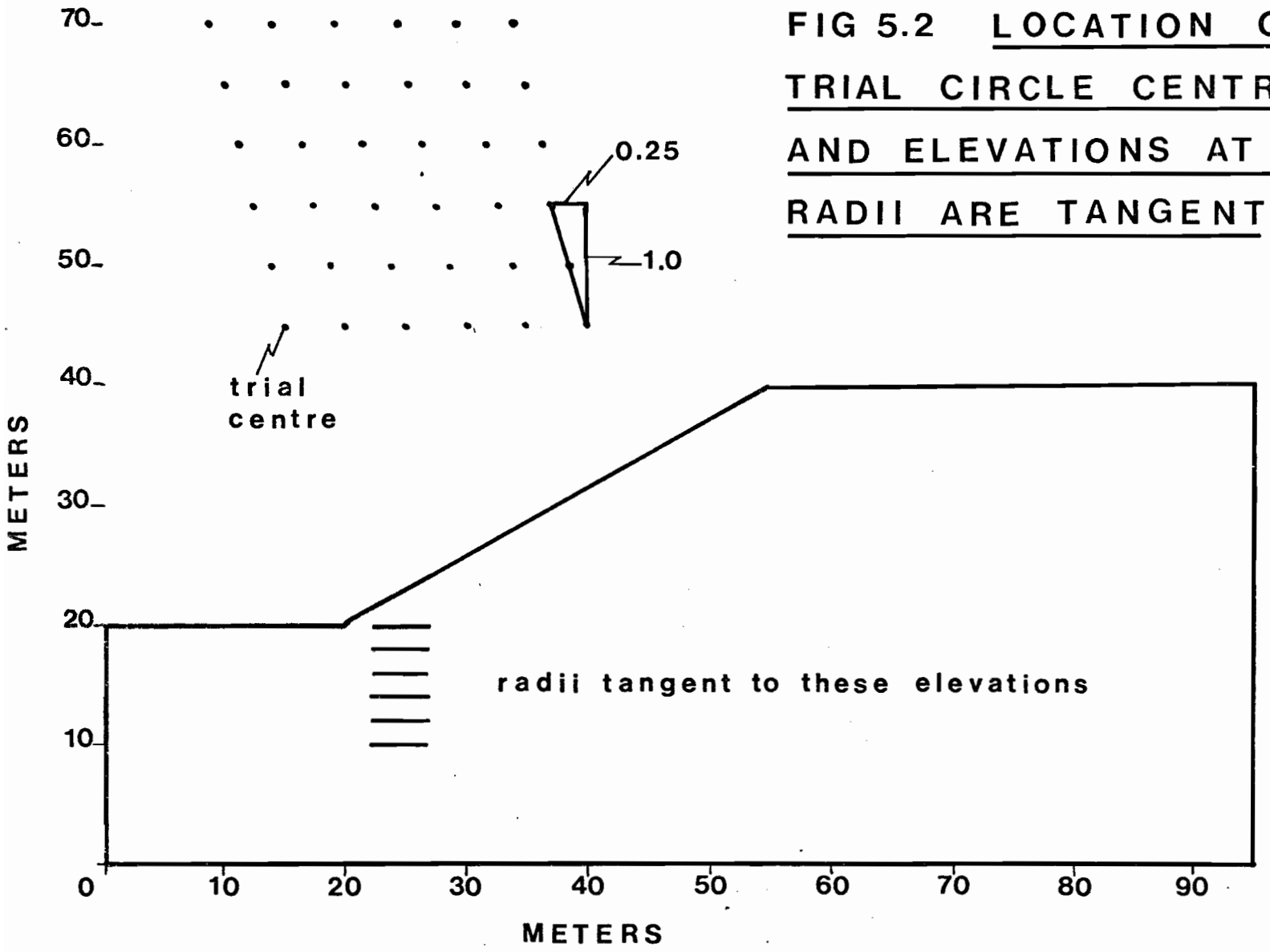

FIG 5.2 LOCATION OF TRIAL CIRCLE CENTRES AND ELEVATIONS AT WHICH RADII ARE TANGENT

It was shown in Chapter 3 that there appears to be little stratigraphic control on the mechanical behaviour of the sensitive clays. For this study, it is assumed that a single set of strength parameters will adequately define the stability of natural slopes without introducing serious error. However, the question arises as to what values of effective cohesion and friction angle best describe the in situ behaviour. The test results presented in Chapter 3 did not yield effective stress parameters that could be readily applied to stability analyses. It is therefore necessary to rely on values obtained from the literature. The problem of obtaining relevant strength parameters is complicated by the fact that there appears to be little consensus on: whether peak strengths or residual strengths are representative; whether the triaxial tests should be isotropically or anisotropically consolidated; and the confining pressure at which the tests are performed. Mitchell (1970), and Klugman and Chung (1976) suggest using a c' of about 9.58 kPa and a Ø' of 33 degrees. Since there appears to be relatively wide acceptance of these strength values, it was decided that they would be used here. However, it is acknowledged that further research still needs to be carried out on the regional variability of the strength parameters.

For the purpose of completing the parameters required for the stability calculations, the following parameters were assumed: bulk density for the clay - 15.70 kN/m^3; c' (sand) - 0.0 kPa; Ø' (sand) - 34 degrees; and bulk density (sand) - 18.9 kN/m^3. No tension crack was assumed and the failure circle extended continuously from the crest of the slope to the toe.

An advantage of the software developed by Fredlund (1974) is the provision to enter the pore pressures in the form of a network of points. It was therefore possible to take the nodal point coordinates and the maximum pore pressures from the finite element analysis and use them directly in the stability analyses. The pore pressure at the base of any slice was then calculated by a weighted average of the closest point in each of the four quadrants about the base of the slice. In this way, it was possible to represent the rather complex pore pressure distributions for the different geological settings that were given in Chapter 4.

5.4 Results of Stability Analyses

5.4a General

The results of the stability analyses on slopes of different geology are presented in this section. The objective here is to show quantitatively the influence of: slope submergence; depth to bedrock; nature of the surficial layer; number of soil layers; and the strength of a bedrock sink on the calculated factor of safety (FOS). The critical circle, circle coordinates, radius, and factor of safety have been plotted on the site profiles described previously in Chapter 4 and are given in Appendix E. The location of the critical circle needs to be considered so as to determine if the mode of failure for the different site geologies is consistent with field observations. A summary of the FOS for the forty-six different models or settings is given in table 5.1.

SETTING NUMBER	% OF SLOPE SUBMERGED			
	0	25	50	75
A	1.031	1.046	1.144	1.525
B	1.043	1.006	1.146	1.527
C	1.128	1.123	1.218	1.482
D	1.550	1.224	1.137	1.255
E	1.080	1.131	1.200	1.542
F	1.032	1.046	1.204	1.606
G	1.017	1.043	1.258	1.615
H1	1.303			
H2	1.487			
H3	1.640			
I	0.913	1.066	1.163	
J	0.870	0.987	1.180	
K	0.841	0.991	1.195	
L	1.521	1.281	1.351	
M	1.090	1.062	1.194	

TABLE 5.1 SUMMARY OF FACTORS OF SAFETY FOR DIFFERENT GEOLOGICAL SETTINGS

5.4b Depth of Submergence

Settings A, D, G, and I are used here to show the change in the FOS with the percent of the slope that is submerged by an external body of water. These settings were chosen since they represent a cross section of the relative extremes in site geologies that were investigated. For example: settings A, D, and G have a surficial layer of sand, while I has clay at the surface. Settings I, A and D have three soil layers while G has five soil layers. In essence, it is not possible to isolate the influence of the depth of submergence on the FOS without considering other geological factors at the same time. While the theme of this section is on the depth of submergence, other geological factors will be previewed here and discussed in detail in later sections. Curves showing the relationships between the depth of submergence and the FOS are plotted on figure 5.3.

Setting I shows a more or less linear increase in the FOS from 0.91 at 0% submergence to 1.16 at 50% submergence. From figures E-33 to E-35 in Appendix E, it can be seen that the critical circle changes from a deepseated failure at 0% submergence to a toe failure at 50% submergence.

Settings A and G have an exponential type of increase in the FOS as the slope becomes more submerged. Since the trends in both settings are essentially the same, reference will be made to setting A only. As the submergence increases from 0% to 25%, the FOS increases only marginally from 1.03 to 1.05 respectively. Although the increase in the FOS is slight, there is a distinct change in the mode of failure. At 0% submergence, the failure is deepseated and is tangent to an elevation of 7 meters beneath the toe of the slope. However, at 25% submergence, the failure is through the toe of the slope and daylights at an elevation

FIG 5.3 FACTOR OF SAFETY - VS - % OF SLOPE SUBMERGED

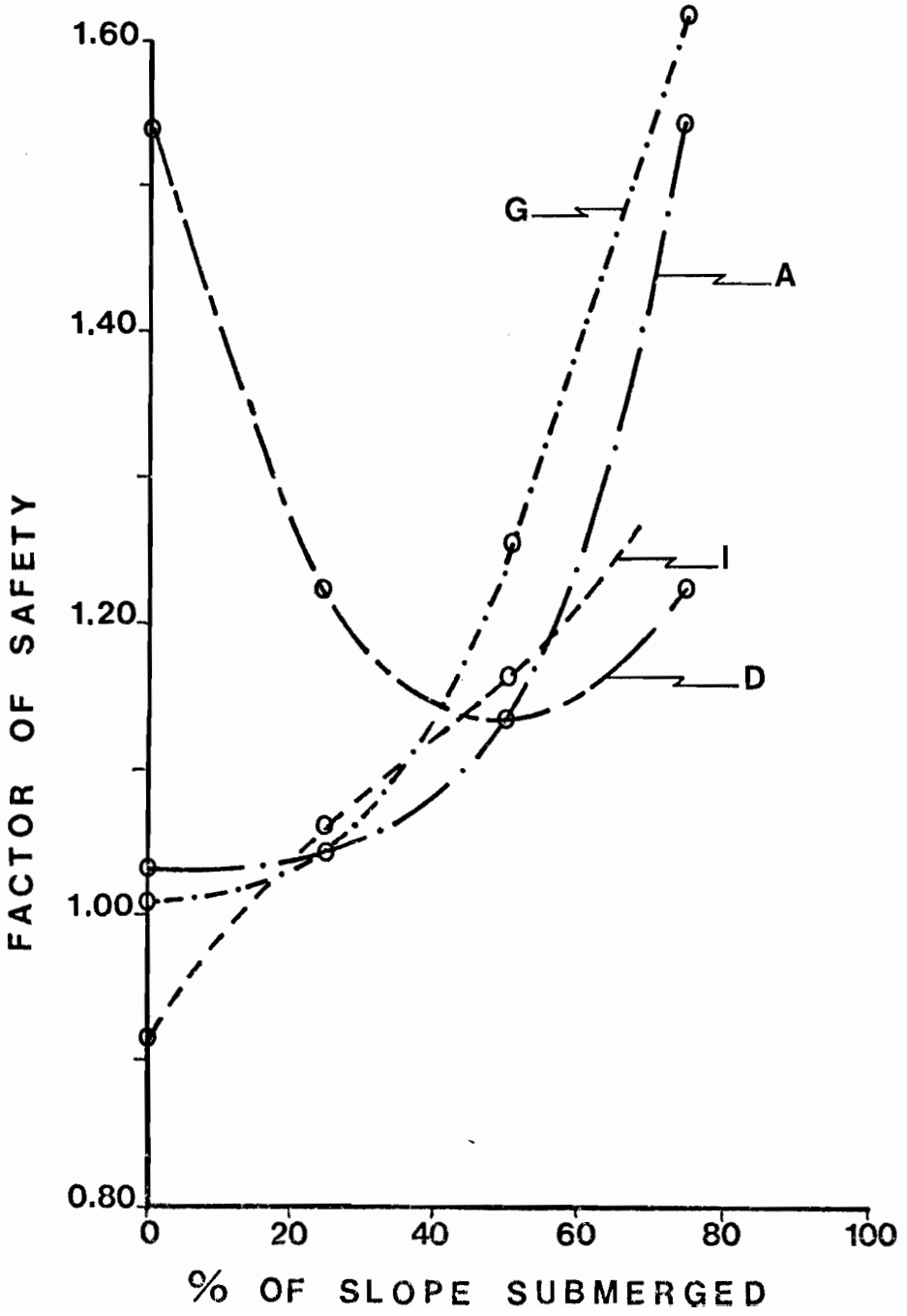

of about 1 to 2 meters lower than the crest (see figure A3). For depths of submergences greater than 25%, the factor of safety increases rapidly up to 1.52 for a slope submerged to 75% of its height. At 75% submergence, the critical circle reverts back to being deepseated.

Setting D is a good example that the FOS does not always increase as the slope is submerged. The FOS shows a decrease from 1.55 at 0% submergence to 1.14 at 50% submergence and then increases to 1.26 at 75% submergence. In all of the four settings, the failure plane was composite and did not appear to be sensitive to the depth of submergence (see figures E14 to E17).

The significance of the FOS versus % of slope submergence (figure 5.3) is that an increase in the elevation of the external body of water will vary the FOS of a slope differently, depending on the site geology. In certain cases, a submergence of up to 25% does not produce an increase in the FOS but, instead, changes the mode of failure from deepseated to a toe failure. Since modern failures are occurring along the banks of rivers, the depth of submergence cannot be neglected in a slope stability analysis. Alonso (1976) and Yong et al. (1977) have developed probabilistic models for slope stability but have neglected the external body of water in the formulation of the probabilistic equations. Since river levels fluctuate in response to runoff and precipitation, then the factor of safety along a given water course can be expected to vary considerably during the course of the year.

5.4c Depth to Bedrock

For the purpose of showing the influence of the depth to bedrock on the FOS, two groups of settings are used. The first group includes settings A to D which have a surficial layer of sand, while the second group (I to M) has a surficial layer of clay. Here again it is not possible to isolate one geological factor and study it independently of the others. For this reason, curves showing the variation in the FOS with the depth to bedrock have been plotted for different depths of submergence (figures 5.4 and 5.5).

Where the slopes have a surficial layer of sand and are submerged to 25% or less of their height, the FOS decreases as the depth to bedrock increases from zero to ten meters and remains constant at about 1.00 for depths to bedrock greater than 10 meters. For discussion purposes on the bedrock control of the critical circle for slopes capped by a layer of sand, settings E, F, and G are included. When the slope is free of all external water, the critical circle is deepseated and is tangent to depths between 2 to 12 meters. Composite failures occur only for settings D and F. D is a composite failure due to the presence of bedrock in the valley bottom, while F is a composite failure due to the depth of the critical circle. Where the slope is submerged to 25% of the slope height, the critical circle passes through the toe and appears to be independent of the bedrock elevation for all settings except D.

Where a sand capped slope is submerged to 50%, the FOS is relatively insensitive to the depth to bedrock and varies between 1.14 and 1.22. For submergences of 75%,

FIG 5.4 FACTOR OF SAFETY - VS - DEPTH TO BEDROCK

for different depths of submergence
sand at surface

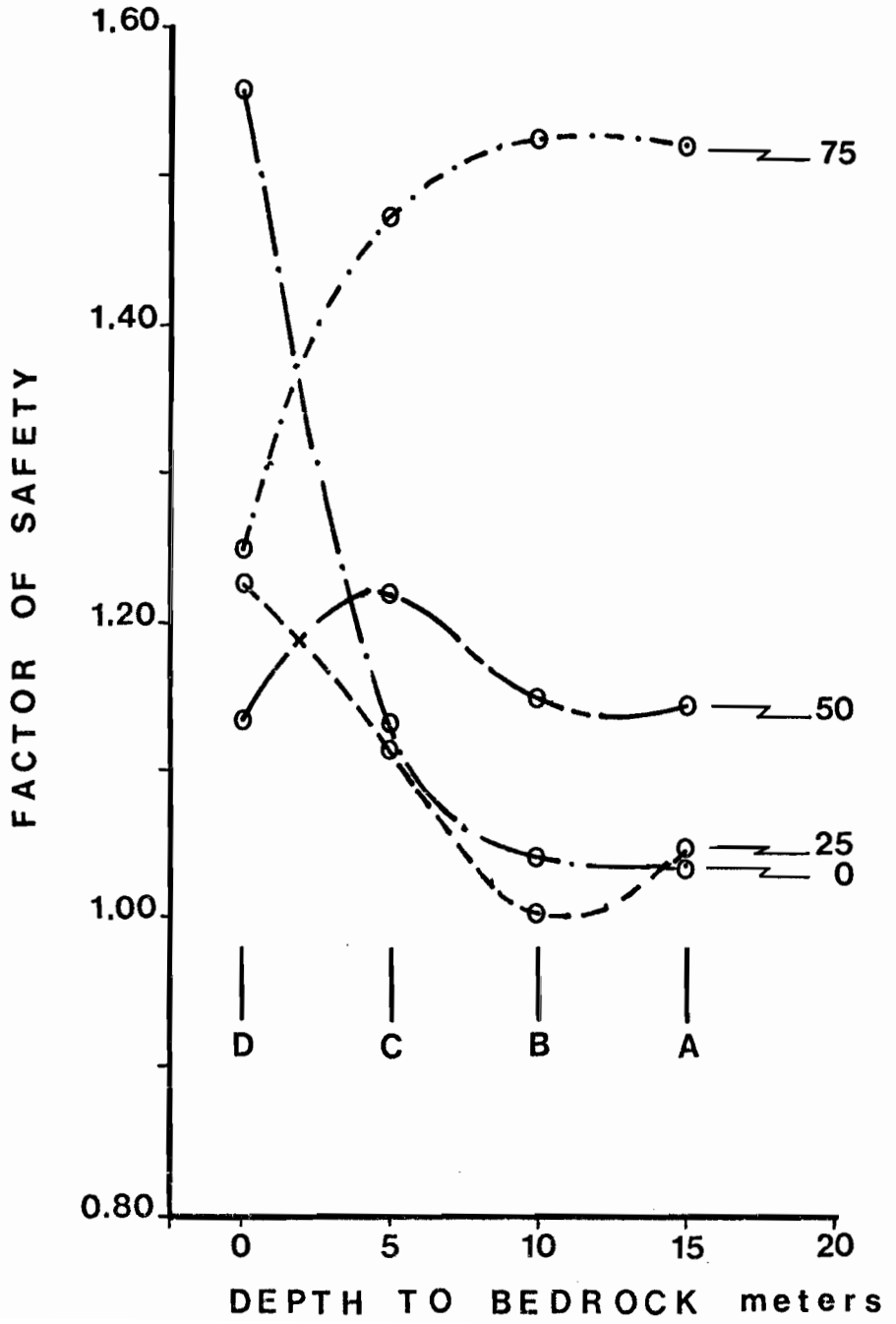

FIG 5.5 FACTOR OF SAFETY
- vs -
DEPTH TO BEDROCK

for different depths of submergence
clay at surface

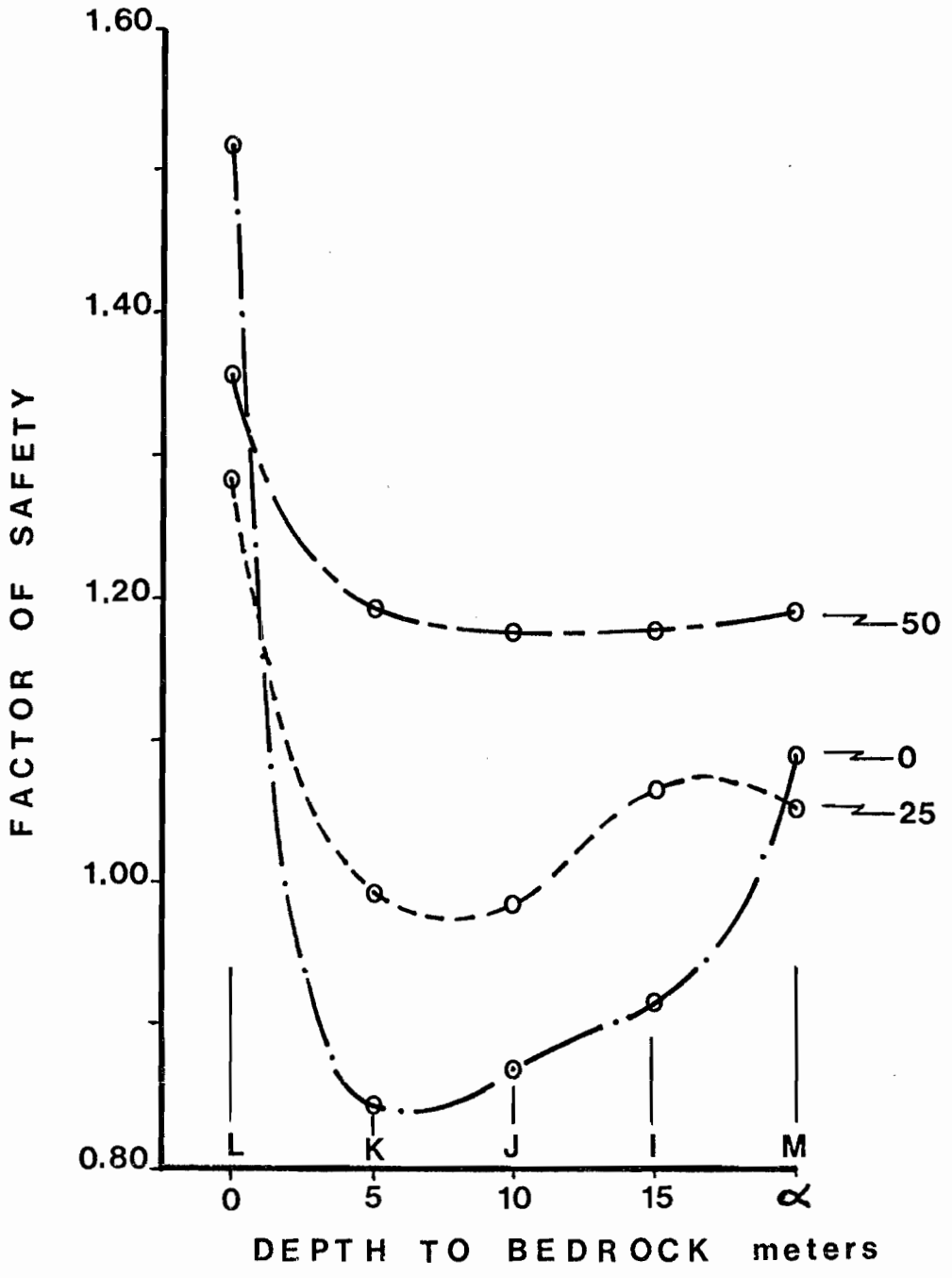

the FOS increases from a minimum of 1.26 for bedrock in the valley bottom to a maximum of 1.53 for depths to bedrock greater than 10 meters. At 50% submergence, all of the critical circles are tangent to a depth of 6 meters beneath the toe for settings A, B, F, and G and are through the toe for settings C, D, and E. C and D have critical circles that are bedrock controlled, whereas for setting E there was an error in the pore pressure data that likely changed the location of the critical circle.

Figure 5.5 shows the variation in the FOS versus the depth to bedrock and submergence for those settings having a surficial layer of clay. Where the slope is not submerged, the FOS decreases from 1.52 for zero depth to bedrock to a minimum of 0.84 for bedrock at 5 meters and then increases to 1.09 when the bedrock is impermeable and at a depth of 20 meters. The location of the critical circles for settings I to M are shown in figures E33 to E47 in Appendix E, and indicate that there is more variation in the location of the critical circle for a surficial layer of clay than for sand at the surface. As expected, setting L is a composite failure due to the outcropping of the bedrock in the valley bottom. The remainder of the critical circles are deepseated; however, the failure circle for settings J, K, and M does not encompass the entire slope height and daylights at elevations below the crest of the slope. Setting K has a failure surface that is deep enough to intersect the bedrock and form a composite failure.

Similar trends in the FOS versus depth to bedrock are noted for submergences of 25 and 50% as have been given above. The FOS decreases with increasing depth

to bedrock and, in the case of 25% submergence, the FOS increases at depths to bedrock greater than 10 meters. At 50% submergence, the FOS is relatively constant (1.16 to 1.20) for depths to bedrock of 5 meters and greater. Composite failures occur for setting L at 25% and 50% submergence and for setting K at 50% submergence. Both toe and deepseated type failures are obtained for the remaining settings and there does not appear to be any relationship between the location of the critical circle and the site geology.

From the foregoing results, it is evident that the effects of one geological factor on the FOS cannot be isolated and studied independently of the other factors. For the discussion on the influence of the depth to bedrock on the FOS, it is necessary to consider both the depth of submergence and the nature of the surficial layer. Generally speaking, the FOS is a minimum when the bedrock is located at a depth of 5 to 10 meters beneath the toe of the slope and the slope is free of any external body of water. When the slope is 50% submerged, the FOS is virtually independent of the depth to bedrock. However, a 75% sand covered slope shows an increase in the FOS as the depth to bedrock increases.

The location of the critical circle and the mode of failure are in part dependent on the depth to bedrock. For settings D and L which have bedrock outcropping in the valley bottom, the critical circle intersects the bedrock in all cases regardless of the depth of submergence. In some of the other settings, a composite failure does occur; however, most of the critical circles are tangent to elevations less than 5 meters beneath the toe. Therefore, only in the

case of settings C, D, K, and L is the bedrock at shallow enough depths that composite failures would generally develop. Where the slope is 25% submerged, it has been shown in the previous section that the critical circle will almost always pass through the toe when there is a surficial layer of sand. This was not the general case for settings with clay at the surface and a submergence of 25%. Here the failures were all deepseated with the exception of setting M which does not have a permeable bedrock basal layer. For setting M, the critical circle was through the toe.

5.4d Number of Soil Layers

In the groundwater section, it was shown that the number of soil layers appeared to have little effect on the pore pressure distribution in the model slope. Since the strength parameters are the same for all of the clay layers, it is anticipated that the FOS should be relatively insensitive to the number of soil layers. This is in fact the case as can be seen from figure 5.6. Although there is a certain amount of variability in the FOS for each depth of submergence, there are few visible trends in the data. At depths of submergences less than 50%, the FOS versus the number of soil layers has a sinusoidal shape. At submergences of 50% and 75%, the FOS versus number of soil layer curves indicate that a minimum FOS is obtained for slopes with three soil layers.

In all cases, the difference in the FOS for varying number of soil layers at the same depth of submergence is in the order of 0.1 and is therefore not as significant as some of the previously mentioned factors.

FIG 5.6 FACTOR OF SAFETY - VS - NO. OF SOIL LAYERS

for different depths of submergence

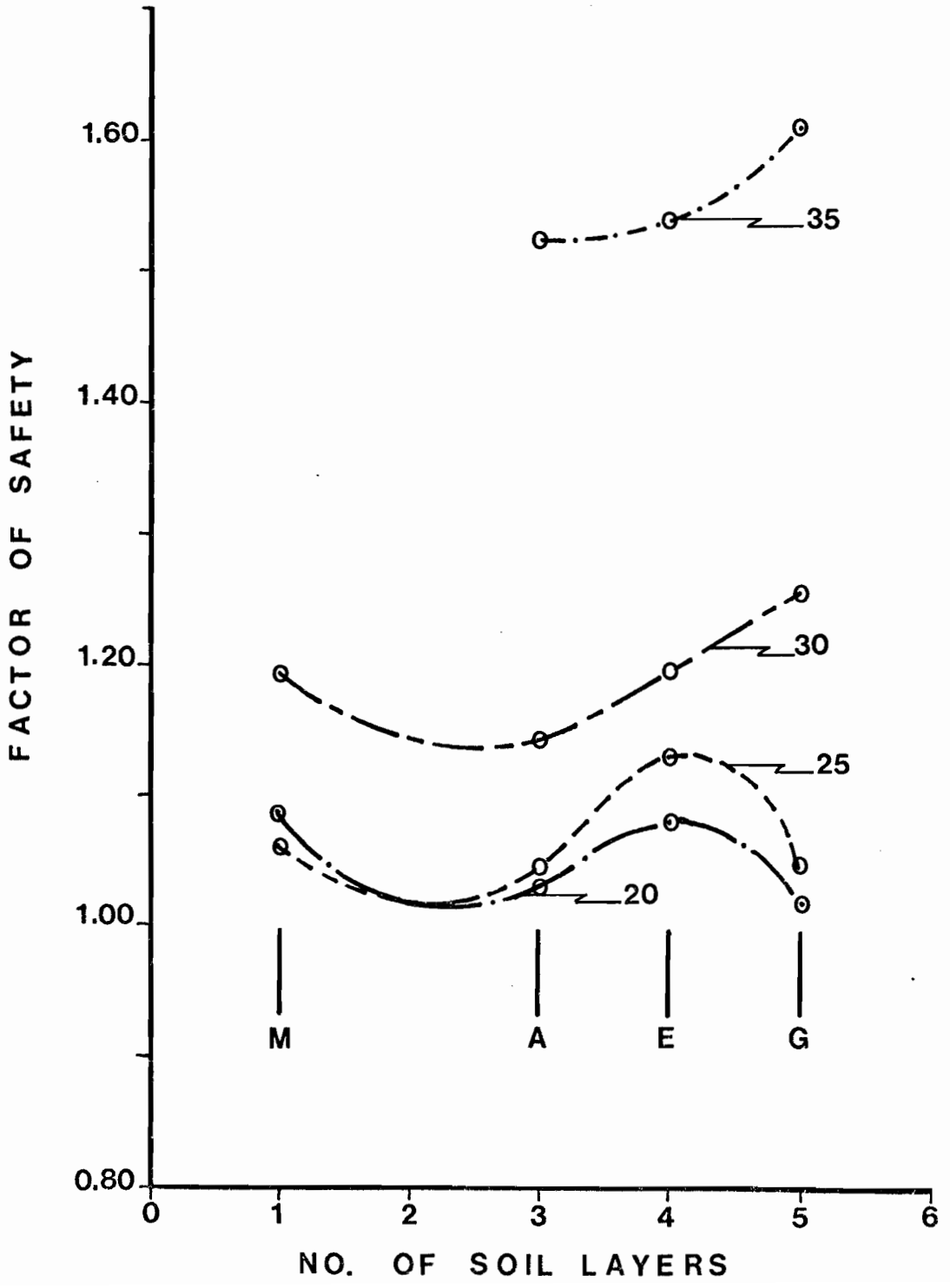

5.4e Bedrock Sink Term

It has been established that there is indeed a lower piezometric level in the bedrock for some areas in the Ottawa Valley. This sink or lower piezometric level is caused by the control of rivers and streams which have eroded down to the bedrock surface. The effect that a sink term has on the pore pressure distribution was shown in a previous part, and, in this section, the control of the sink on the stability of slopes will be given. Only models G and H are used here, although the trends should be more or less the same for all models if a sink term was incorporated in the finite element analyses. The curve showing the change in the factor of safety with the depth of submergence and the sink term is given in figure 5.7. The curve has been plotted with the degree to which the slope is subjected to downdrainage along the horizontal axis. For example, setting G with a submergence of 75% has the least amount of downdrainage at the crest, while setting H with a sink term of -0.00075 has the strongest downward gradients. At 0% submergence, the sink term is also 0; therefore, the two models have identical safety factors at this point.

It has already been shown that, for those settings where the bedrock is located at some depth, the factor of safety increases as the slope becomes more submerged. In the case of setting G, the FOS increases from 1.02 to 1.62 as the slope is submerged from 0% to 75%. It can be seen from figure 5.7 that the FOS increases considerably from the minimum of 1.02 when a sink term is applied to the bedrock. For a sink term of magnitude -0.00015, which lowers the pressure head by less than

FIG 5.7 FACTOR OF SAFETY

- vs -

% OF SLOPE SUBMERGED
and
BEDROCK SINK TERM

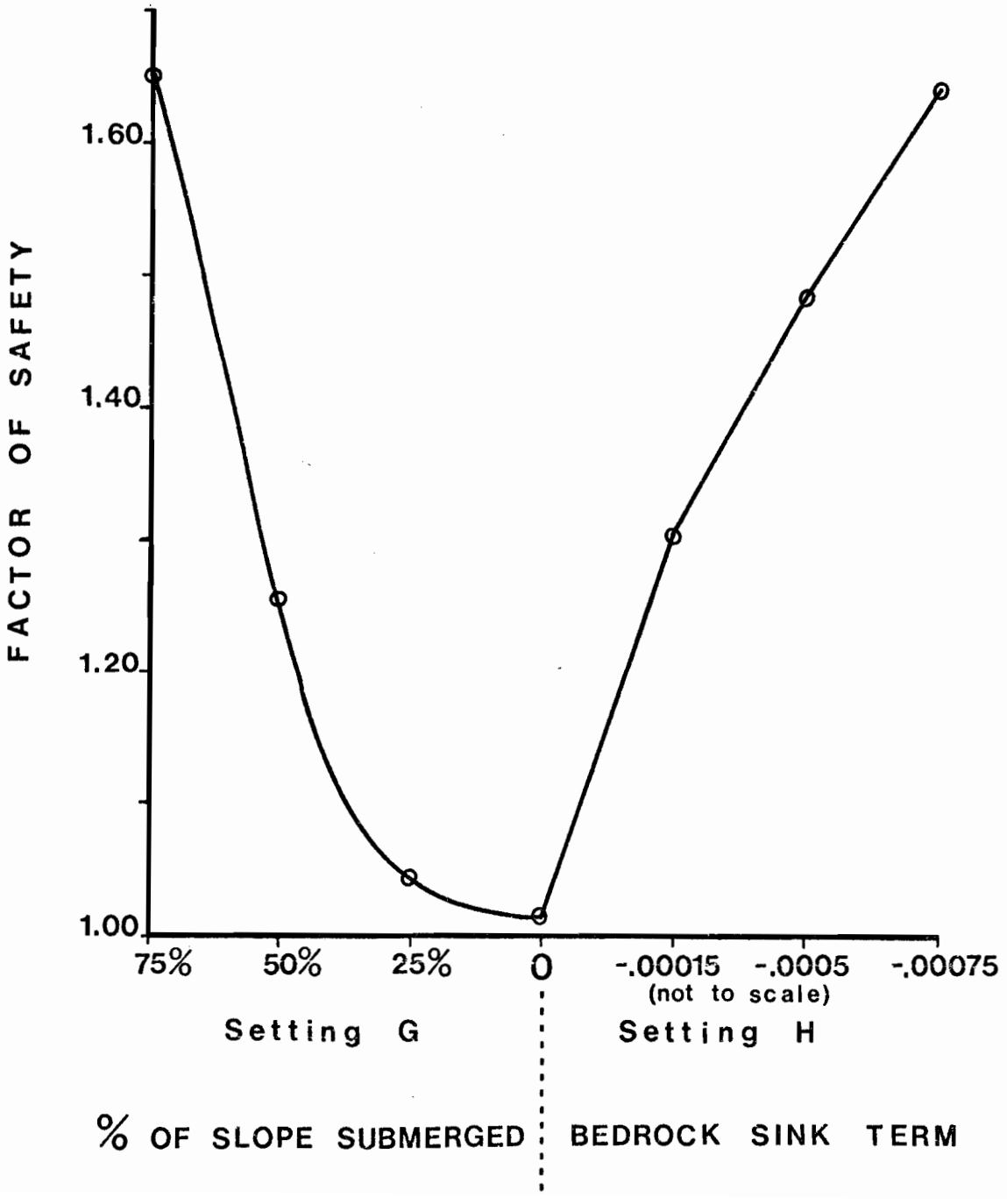

5 meters in the bedrock, the FOS increases from 1.02 to 1.30. By increasing the sink to -0.00075, thereby lowering the pressure head by about 20 meters in the bedrock, the FOS becomes 1.64.

The location of the critical circles is also dependent on the strength of the sink term. For setting G with no submergence, the critical circle is deepseated and is tangent to a depth of 7 meters beneath the toe. With the lowering of the piezometric level in the bedrock, the critical circle is tangent to a depth of 3 meters for a sink term of -0.00015 and is through the toe for sinks of -0.00050 and -0.00075.

Although only one setting has been used to illustrate the significance of the bedrock sink term, it is evident that a lower piezometric level of only 5 meters can increase the FOS by 30%. Since other factors such as the depth to submergence and the depth to bedrock can be readily determined through a limited field survey, a piezometer should be placed in the bedrock to evaluate the rock type, permeability, pressure head, and depth to bedrock. With this information, finite element simulations of the groundwater flow can be made and realistic FOS determined.

5.4f Nature of the Surficial Layer

This aspect of the geological controls on the FOS has already been partially discussed in the sections on the depth of submergence and the depth to bedrock and will only be summarized in this section. Where the slopes are not submerged, the FOS is lower for a clay at surface slope than for an equivalent sand at surface slope. For example,

setting A has sand at the surface, bedrock at a depth of 15 meters, and a FOS of 1.03. Setting I has a similar depth to bedrock but with clay at the surface and the FOS is 0.913. Therefore, for slopes of similar height and slope angle, the clay-only slope would likely fail, while the sand capped slope would be marginally stable. The exception to the rule are settings D and L which have a FOS of 1.55 and 1.52 respectively, thereby indicating that the bedrock appears to override the influence of the surficial layer. For submergences of 25% and more, the FOS is roughly the same regardless of the nature of the surficial layer.

The location of the critical circle varies depending on the surficial layer. Except for those settings that have a composite failure (C, D, K, and L), the critical circles are: deepseated for non-submerged slopes; toe failures for sand capped slopes 25% submerged; and deepseated for clay slopes 25% submerged. At submergences of 50% and more, the critical circles can be either deepseated or toe failures.

5.4g Proposed Stability Mapping Method

It is evident from figures 5.3 to 5.7 that the local site conditions do govern the factor of safety. For this study, a slope height of 20 meters and a slope angle of 30° were used. Hence, there is not a unique relationship between the factor of safety and the slope geometry. This fact is more adequately shown in figure 5.8. The lack of a suitable line separating the failed from the unfailed slopes shows that other factors (eg. geology, groundwater, strength parameters) must be accounted for in the stability analysis. For regional mapping of the stability of natural slopes, each slope must be considered on an individual basis

FIG 5.8 FAILED VS UNFAILED SLOPES IN RELATION TO A FACTOR OF SAFETY OF 1.0 (AFTER KLUGMAN & CHUNG, 1976)

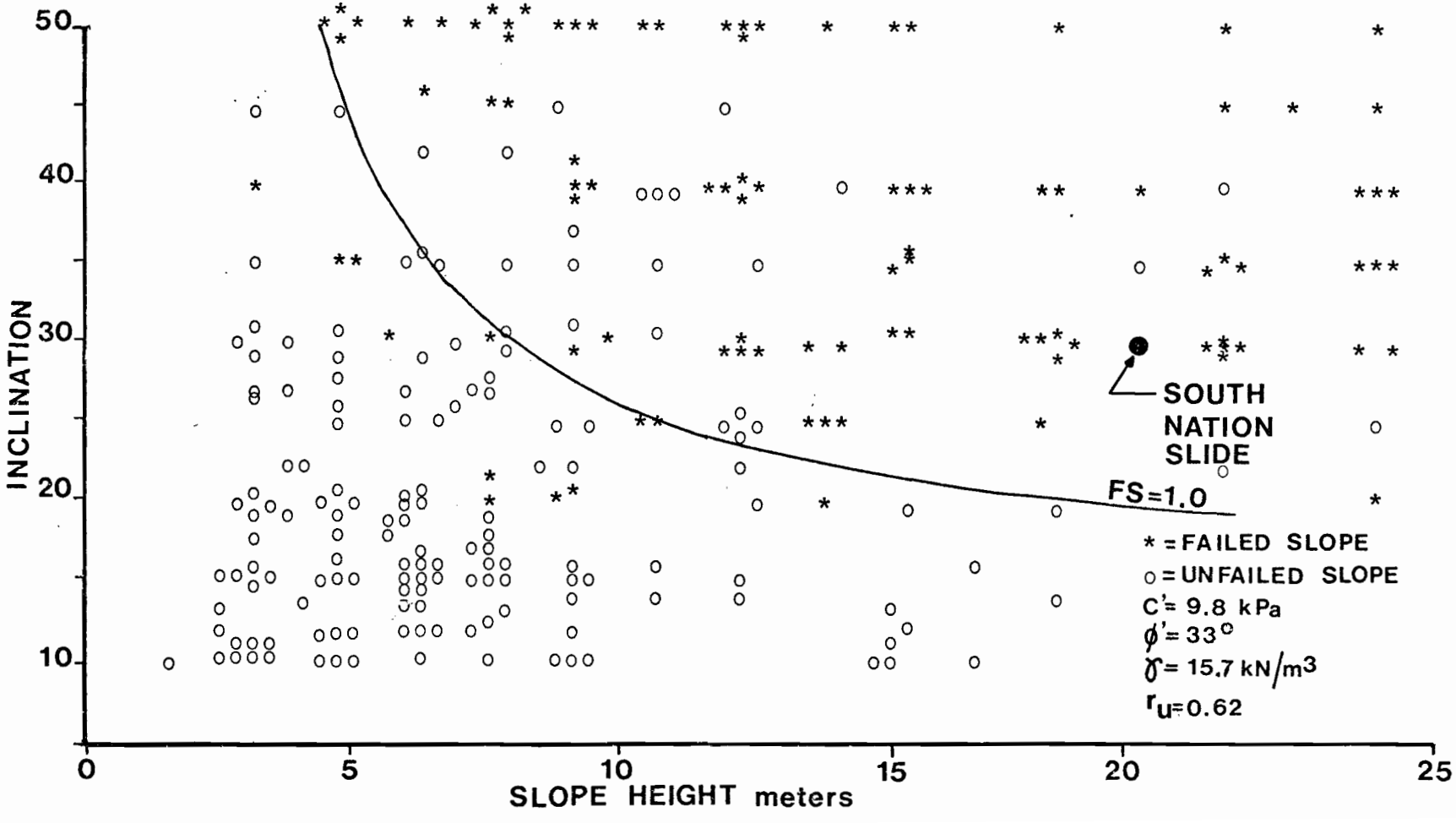

and in the absence of suitable strength and groundwater data, a factor of safety can be arrived at by using graphs such as figures 5.3 to 5.7.

Since this thesis dealt only with one slope angle, slope height and set of strength parameters, further research should be carried out towards providing a complete set of graphs that would span the entire range of possible site conditions.

Figures 5.3 to 5.7 are not meant to replace detailed slope stability investigations; however, they are intended to provide a preliminary assessment of the factor of safety. From a reconnaissance field survey of a given set of slopes, it should be possible to delineate those slopes where a definite potential for instability exists from those where the probability of failure is low. The follow-up study would then be able to concentrate on the potentially unstable zones, thereby maximizing the efficiency of the slope stability investigation.

5.5 Verification of Stability Mapping Method

This section will compare the method proposed for stability mapping described in the previous section with a documented failure. It will therefore be possible to verify the reliability of the method and its potential application to stability mapping of slopes in the Ottawa Valley. The South Nation River landslide provided a unique opportunity to compare the results of this study with a known failure. The pre-slide geometry closely approximates that of the slope height-slope angle model used in this study. The South Nation River slide has been described in detail by Eden et al. (1971) and by Lo and Lee (1974).

The description that follows here has been paraphrased from the above mentioned two works. The South Nation River landslide occurred during the night of May 16 to 17, 1971. The slide was a retrogressive type failure and the final crater covered an area of nearly 28 ha. The general profile of the pre-slide topography and stratigraphy is shown in figure 5.9. The stratigraphy is somewhat of an approximation, probably based on a few holes placed back of the headwall of the slide. Borings 74-1, 74-4, and 76-1 are in the same general geologic setting as the slide and a visual inspection of the headwall and the debris apron indicated that the stratigraphy was similar to that of the above mentioned borings and to the general stratigraphic column described in Chapter 2.

From figure 5.9, it can be seen that the sensitive clay is overlain by a layer of sand. Furthermore, the bedrock does not outcrop in the valley bottom. Therefore, as a first analysis, models A, B, C, E, F, G, and H can be considered as approximating the pre-slide geology.

The slide occurred after an unseasonal spring melt and during a heavy thunderstorm. There was a record snow fall during the winter of 1970-71 and the melting was gradual. It would appear that the assumptions regarding the infiltration rate for the finite element analysis would therefore be applicable in this case. For the finite element simulation, the snow was considered to melt at a uniform rate throughout the month of April, thereby yielding maximum pore pressures during the month of May. It is reported by Eden et al. (1971) that there was standing water in the fields at the time of the landslide. A similar situation is present during most spring thaws, the reason being that

FIG 5.9 PROFILE OF SOUTH NATION RIVER

(After Eden et al., 1971)

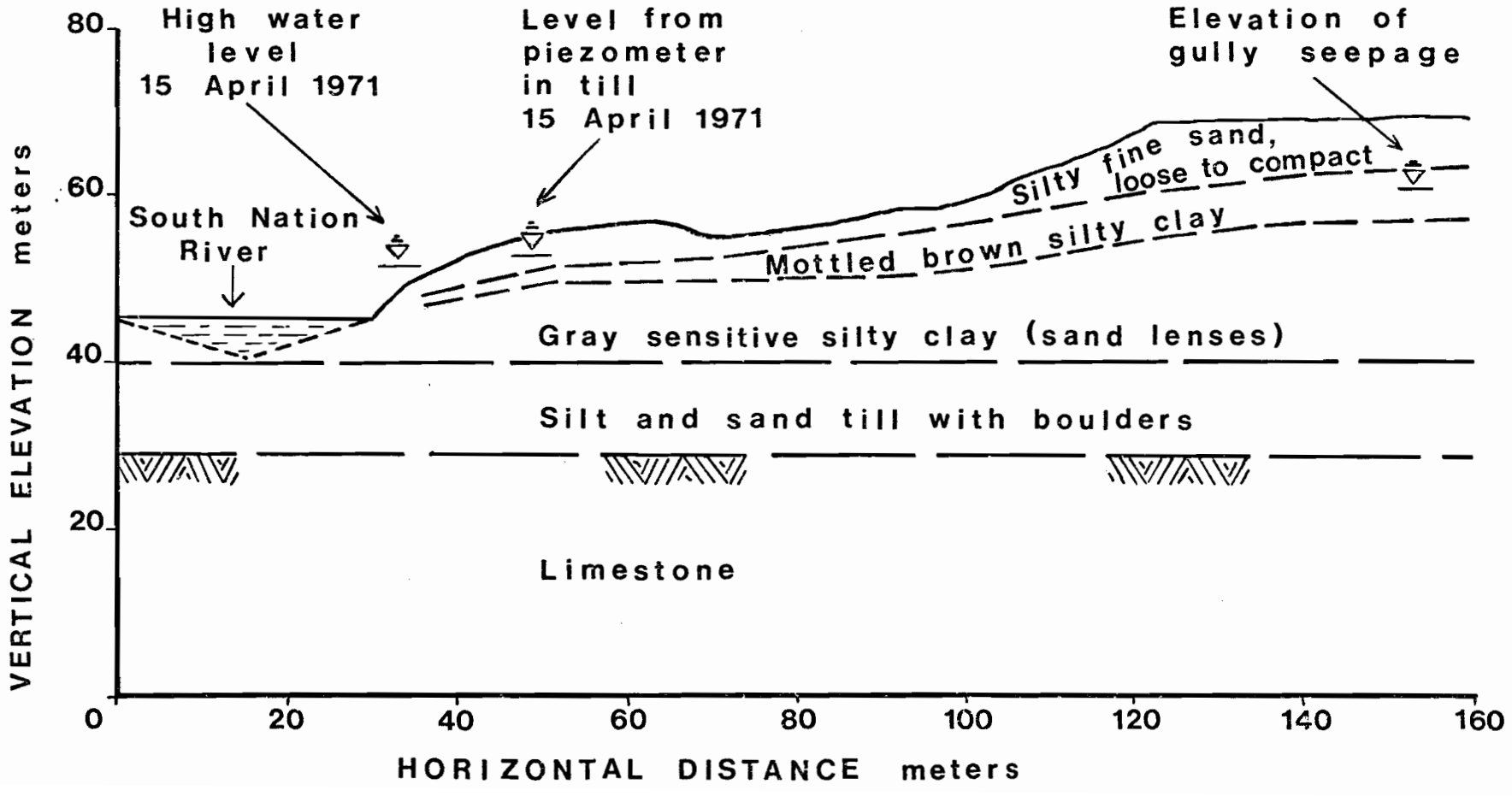

the permeable sand overlying the impermeable clay stores the water from the snow melt. Since the melt infiltrates slowly down through the clay or evaporates, it tends to pond in shallow depressions on the surface. It is also reported by Eden et al. that water was observed to be seeping from the bottom of gullies flanking the slide (ibid.). The elevation of the seepage is also shown in figure 5.9 and corresponds closely to the interface between the sand cover and the underlying clay. A seepage line should normally develop at this point where a permeable sand overlies an impermeable clay. Piezometers had been installed in a nearby slope and showed that the piezometric levels rose as the river levels rose, but that the groundwater levels remained high even after the river dropped in elevation. The piezometers were installed in the till; however, the authors did not report on the position of the piezometers with respect to the slope. It does seem apparent that there was no lower piezometric level in the bedrock prior to the slide and that pore pressures were close to their maximum. Model H need not be considered here since it deals with a lower piezometric level in the bedrock.

It was shown in figure 5.6 that the factor of safety is virtually independent of the number of soil layers. Also, at the time of failure, the slope was about 25% submerged. Therefore, the model(s) that best approximate(s) the pre-slide conditions will depend on the depth to bedrock. The depth to bedrock requires some judgement, since about 10 meters of till overlie the bedrock. If it is assumed that the hydraulic conductivity of the till is close to the clay's conductivity, then the depth to bedrock is about 10 meters. However, should the hydraulic conductivity be close to that of the bedrock, then the

equivalent depth to bedrock is about 5 meters. From table 4.5, it can be seen that models A25, C25, E25 and G25 could be considered as reasonable approximations of the pre-slide geology. Table 5.1 lists the factors of safety for models A25, C25, E25, and G25 as being 1.046, 1.123, 1.131 and 1.043 respectively.

Table 5.2 shows the recommended minimum factors of safety for slopes. In the case of a slope similar to the South Nation River landslide, it must assumed that the uncertainty in the strength and groundwater measurements are large and a factor of safety of 1.5 must be considered as a minimum. The factors of safety given for the four models mentioned above indicate that the pre-slide slope was only marginally stable.

Factors of safety were calculated for model G25 using an ru parameter instead of the pore pressure grid, the object being to establish an equivalent ru value for the groundwater conditions obtained from the finite element analysis. Figure 5.10 shows the relationship between the factor of safety and the ru parameters, thus for a factor of safety of 1.043 the equivalent ru is 0.44. Assuming, as Klugman and Chung (1976) have done, that the ru value is 0.62 underestimates the factor of safety by about 0.30. It is obvious that the assumption of 0.62 for ru may not always yield factors of safety that are applicable for regional slope stability mapping. However, the method presented here yields factors of safety close to 1.0 for an actual failure and must therefore be considered a more rational approach to stability mapping in the Ottawa Valley.

COST AND CONSEQUENCES OF SLOPE FAILURE	UNCERTAINTY OF STRENGTH MEASUREMENTS SMALL[1]	LARGE[2]
Cost of repair comparable to the cost of construction. No danger to human life or other property if slope fails.	1.25	1.50
Cost of repair much greater than cost of construction, or danger to human life or other valuable property if slope fails.	1.50	2.0+

1 The uncertainty of the strength measurements is smallest when the soil conditions are uniform and high quality strength test data provide a consistent, complete and logical picture of the strength characteristics.

2 The uncertainty of the strength measurements is greatest when the soil conditions are complex and when the available strength data do not provide a consistent, complete or logical picture of the strength characteristics.

TABLE 5.2 RECOMMENDED MINIMUM VALUES OF STATIC FACTOR OF SAFETY
(after Duncan and Buchignani, 1975)

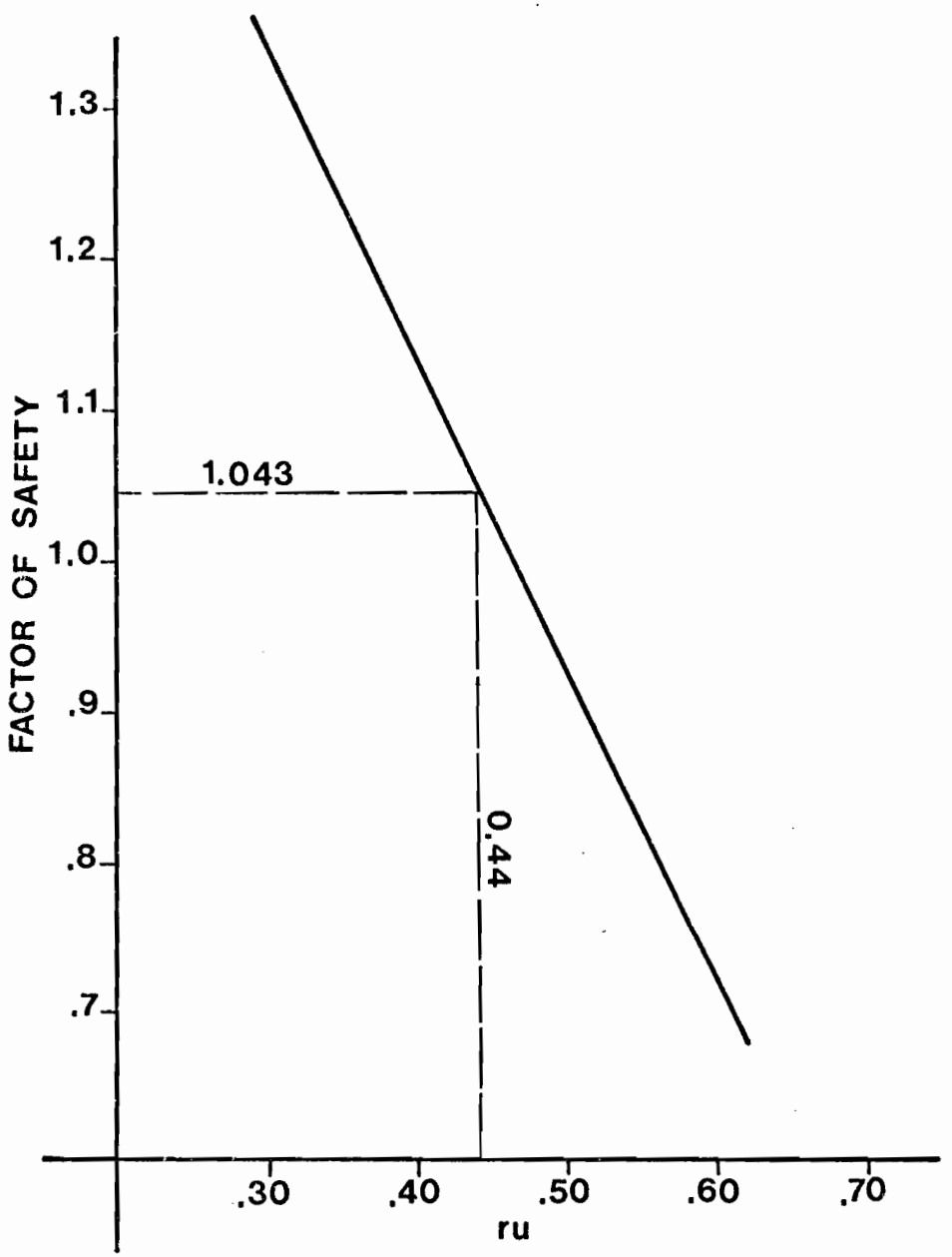

FIG 5.10 FACTOR OF SAFETY VS ru PARAMETER

5.6 Summary

For the model slope, it has been shown that the depth of submergence, depth to bedrock, and bedrock sink have the greatest influence on the FOS. The nature of the surficial layer and the number of soil layers may in certain cases influence the factor of safety but are not as significant as the other three.

Generally, the FOS of a slope will increase as a slope is submerged. However, when bedrock outcrops in the valley bottom near the toe of a slope, the FOS decreases with submergence up to 50% and then increases as the slope is submerged to 75%. The location of the critical circle is highly dependent on the depth of submergence. For unsubmerged sand capped slopes, the critical circle is deepseated. However, at 25% submergence, the critical circle passes through the toe, but the FOS remains essentially the same as for no submergence. Field evidence would indicate that most landslides initiate as a toe failure (Eden and Mitchell, 1970). Since most of the slides are occurring along the banks of rivers, hence the slopes are partially submerged, it appears that the toe failures associated with partial submergence would be the mode of failure.

Where the slope is submerged to less than 25% of its height, the depth to bedrock is fundamental to the slope stability. A minimum FOS is obtained where the depth to bedrock is less than 10 meters. The reason for this reduction in the FOS is due to the presence of artesian pressures at the toe. As the depth to bedrock increases, the artesian pressures are dissipated over a greater portion

of soil and the pore pressures are less in the zone through which the critical circle passes.

It has been established that a lower piezometric level can be found in the bedrock. The net result of the lower piezometric level is to increase the stability of the slopes by lowering the pore pressure. A decrease in the pressure head by 5 meters results in an increase in the FOS by about 30%. It is therefore essential that the pressure head in the bedrock be established before any stability calculations or finite element groundwater simulations are made.

The number of soil layers appears to have little or no effect on the FOS. Since it was also shown in the chapter on the groundwater that the pressure head appeared to be independent of the number of soil layers, it seems likely that the stratigraphy need only be evaluated in general terms for the purpose of stability of sensitive clays.

The FOS is less for those slopes that have clay at the surface than sand only when the depth of submergence is less than 25%. At submergences greater than 25%, the difference in the FOS between the sand capped slopes and the clay-only slopes is marginal.

Figures 5.4 to 5.7 show graphically the dependence of the factor of safety on the local site conditions. By providing similar graphs for different slope geometries, it will be possible to estimate in the field the factor of safety for a given slope based solely on a knowledge of the

site geology. The basic site geology can be obtained from surficial maps, while a simple hammer seismic survey can estimate the depth to bedrock if necessary.

A comparison of the method presented here with a documented failure has shown that this approach to stability mapping will yield factors of safety close to one for an actual slide. This would indicate that methods employed here are valid and could serve as a useful tool for slope stability mapping.

6 - SUMMARY AND CONCLUSIONS

6.1 General

The overall objective of this thesis is to provide the geotechnical engineer with a simple field method for stability mapping of sensitive clay slopes in the Ottawa Valley. It was shown in Chapter 1 that a slope stability analysis requires a combined geological, geotechnical and groundwater investigation and that the regional variation and interrelationships of these factors are needed for regional stability mapping. To achieve the above mentioned objective, a four-part research program was initiated. The parts are: 1) a review of regional geology and stratigraphy; 2) a field and laboratory investigation of the mechanical behaviour; 3) a field and numerical study of the groundwater regime; and 4) an investigation into some of the geological controls of sensitive clay slope stability.

Presented in Chapter 5 are graphs that show how the factor of safety of a slope varies with the local geology. These graphs are the basis for the stability mapping method and demonstrate that the factor of safety can vary as much as 60% depending on the local geology. Therefore, it is evident that any regional approach to stability mapping must consider the geological and groundwater controls.

A review of the four parts of the research program follows here and will show which aspects of the geology are important to the problem of sensitive clay slope stability.

6.2 Geology and Stratigraphy

In Chapter 2, a review of the geology and stratigraphy of the sensitive clay deposits of the Ottawa Valley was given. The surficial distribution of the sensitive clays and associated landslides was presented and shows that a large portion of the Ottawa Valley is covered with a layer of sensitive clay. Landslides, some of which are up to 5 km in length, have occurred along the banks of both modern and ancient river channels. Most of the large slides have developed in the central part of the Ottawa Valley and Gatineau River Valley, and it appears that the potential for slope instability decreases in the north-western sections of the Ottawa Valley.

It was also shown in Chapter 2 that the sensitive clay deposits could be subdivided into four distinct stratigraphic units. The four units are: varved clay facies; deepwater marine clay facies; prograding delta facies; and shoaling prograding delta facies. Photographs and a description of each of the units have been given and demonstrate that the sensitive clays are for the most part anisotropic.

The subdivision of the sensitive clay deposits into stratigraphic units has allowed for: the investigation of the mechanical properties of each unit; and the influence of the stratigraphy on the pore pressure distribution in sensitive clay slopes. The results of these aspects of the research are given in subsequent sections.

6.3 Mechanical Behaviour

A field and laboratory investigation was carried out to determine if the undrained shear strength, consolidation

behaviour, effective stress parameters, and porewater chemistry were dependent on the stratigraphic unit. Two borings were made at a site 50 km east of Ottawa. At each of the borings, field vane tests were made and five good quality Osterberg samples were obtained. The undrained shear strength does not appear to be related to the stratigraphic unit and is likely a function of the effective overburden stress.

Consolidation tests were performed on each of the ten Osterberg tube samples and show that while the shape of the strain-log pressure curve may be influenced by the stratigraphic unit, the preconsolidation pressure appears to be dependent only on the effective overburden stress.

Thirty-eight consolidated undrained triaxial tests with pore pressure measurements were performed. While the results are not conclusive, they do indicate that the peak strength and mohr envelope are governed by the preconsolidation pressure and the confining pressure at which the sample was tested.

The porewater chemistry analyses indicate that the cation concentration is relatively low over the entire profile. The lowest concentrations were recorded in the prodelta clay at a depth of 15 meters. The variation in the salt content could be due to either leaching or changes in the depositional environments at the time of formation of the clay units. There does not appear to be any trends to suggest that the mechanical behaviour of the clay is related to the porewater chemistry. However, the possibility exists that the fissuring is due to changes in the chemistry.

6.4 Groundwater Investigations

A field and numerical investigation of the groundwater regime in sensitive clay slopes was carried out. For the purpose of simplifying this study, sensitive clay slopes were grouped according to the nature of the surficial layer. There are essentially only two groups, those which have sand on the surface and those which have a desiccated clay layer. The infiltration capacity of the clay soil is considerably less than the sand, hence the recharge to the groundwater regime must also be different for the two groups. The classification of the slopes enabled the remainder of the study to proceed in a systematic manner. Piezometers were installed in three slopes, two were in the sand at surface group of slopes, while the third was in the clay at surface group. Monitoring of the piezometers was done over the period from May to August 1976 and should have recorded the spring maximum pressures and the summer minimum pore pressures. The significant difference between the pore pressure distribution in the two groups of slopes is the existence of a perched water table in the sand cover. Although a lower piezometric level was identified for the bedrock in the sand covered regions and not for the clay, a review of the literature showed that a lower bedrock piezometric level can be anticipated where the bedrock is composed of fracture Carboniferous age rocks. The conclusion drawn here is that the bedrock is in fact the main control of the pore pressure distribution in the slopes.

Results of the field groundwater investigations were extrapolated to other geologic settings by means of a finite element simulation. The model was first verified

using field data from site P1. A reasonable correlation was obtained between the measured and calculated pressure heads. The results were, however, only marginally good without the use of a bedrock sink term, which in this case represented the bedrock control of the groundwater flow. It was postulated that the control of the pressure head in the bedrock is regional in nature and is actually due to the intersection of local rivers or streams and the fractured bedrock surface. The pressure head is, therefore, controlled by the surface elevation of the river, which, in turn, means that the pressure head in the bedrock is subject to the annual variations in river levels. As the river surface elevation rises in response to increased runoff, so does the pressure head in the bedrock.

In all, forty-six different site configurations were used to investigate the role of geology in the distribution of the pressure heads in slopes. To completely cover the entire spectrum of geologic controls, it is estimated that at least 300 models would have to be analysed. Therefore, it was necessary to limit the geologic factors that would be studied. Those of interest were: the depth of slope submergence; the number of soil layers; the nature of the surficial layer; the depth to bedrock; and the influence of the bedrock sink term. The changes in the pore pressures in the different models were made by considering the equivalent of two strings of piezometers, one at the crest and the other at the toe.

Submergence of a slope modified the groundwater flow by reducing the hydraulic gradients. At full submergence, a condition of no flow exists, while maximum hydraulic

gradients and flow develop at no submergence. It was also noted that the toe of the slope is a groundwater discharge zone even when the slope is submerged to 75%.

The results of the models which analyse the effect of the depth to bedrock show that the artesian pressures present in the toe area are dissipated when the bedrock outcrops in the valley bottom. This result is in agreement with field data reported upon in the literature and shows that the finite element method can predict with some degree of success the actual flow patterns that would be anticipated in the field.

The nature of the surficial layer does have an effect on the pore pressure distribution. It was shown that the pressure head is generally greater in the bedrock for those settings which have a clay layer on the surface. Therefore, the artesian pressures at the toe are greater and the downdrainage at the crest is less for the clay at surface slopes than similar sand at surface slopes.

The bedrock sink term increased the downward gradients as the magnitude of the term increased. In a regional sense, a prerequisite to numerical modelling of pore pressures is the knowledge of the: bedrock type, permeability, morphology and pressure head.

The factor which had the least influence on the flow regime was the number of soil layers. There was little difference in the pressure head versus depth curves for profiles with three, four, or five soil layers. This would

indicate that, for regional groundwater studies, it is not too critical if the stratigraphic profile is not obtained in detail. A general stratigraphic column should be made at each site, but only such items as the nature and thickness of the surficial layer and the depth and topography of the bedrock surface as well as the type of bedrock need be obtained.

6.5 Stability Calculations

Stability calculations were performed on each of the forty-six models. Maximum pore pressures obtained by the finite element analysis were used as input into the stability model. In all, more than 500 different trial centres and radii were used to isolate the critical circle. It was observed that the calculated safety factor is dependent on the grid of points which are used as trial centres. Hence, it is virtually impossible to completely remove any doubt that the minimum factor of safety has been obtained by using a reasonable number of trial centres. It is estimated that the accuracy of the calculated factor of safety should be at least ± 0.02.

The same geologic factors which were investigated as part of the groundwater investigation were also used here to determine what geological controls on the stability of natural slopes existed.

The depth of submergence is shown to have a strong effect on both the factor of safety and the location of the critical circle. For models which have a surficial layer of sand, the factor of safety increased only marginally from 0% submergence up to 25% submergence. However, the

location of the critical circle changes from one of a deepseated failure for a non-submerged slope to that of a toe failure for a partially submerged slope. Reports in the literature suggest that the actual failure surfaces do pass through the toe. Since most of these failures are occurring along active rivers which are partially submerging the slopes, it would then appear that the pore pressures which have been generated by the finite element method result in factors of safety and failure surface locations that are compatible with field observations. It is also of interest to examine the response of slopes which have bedrock outcropping in the river valley to an increase in the depth of submergence. As the depth of the external body of water increases, the factor of safety decreases. At submergences greater than 50%, the factor of safety increases. This suggests that the general rule which states that, as the slope becomes more submerged the factor of safety increases, should be applied with a certain amount of caution. This fact has considerable consequences for slopes which may be submerged as the result of the ponding of water behind a dam. Submergence over a wide area may, in certain cases, initiate instability instead of preventing it.

In terms of slope stability, it was noted that the factors of safety were generally lower where there was a surficial layer of clay as compared to a surficial layer of sand, for depths of submergence less than 25% of the slope height. As the slope is submerged to depths greater than 25%, the differences in the FOS for a comparable sand on surface slope and a clay at surface are marginal.

It was previously stated that the number of soil layers had little effect on the pore pressure distribution, hence there was also little change in the factor of safety according to the number of soil layers. Perhaps, an investigation of different thicknesses of soil layers, different slope heights and angles may show that there is some relationship between the number of layers and the stability, but, for the slope investigated here, there are no apparent trends.

The last item to be investigated was that of the bedrock sink term. It was shown that the sink term greatly increases the factor of safety. The sink term also governs the location of the critical circle. By applying a sink term to a non-submerged slope, the critical circle changes from one of being deepseated to a toe type failure for slopes which have a lower piezometric level in the bedrock.

By using the surficial maps and stratigraphy described in Chapter 2 and the factor of safety versus different site geologies from Chapter 5, it is now possible to obtain a reasonable estimate of the factor of safety for a given slope in the field. A check of the proposed stability mapping method with the South Nation River landslide yielded a factor of safety close to 1.0, thus showing the validity of an approach to regional stability mapping that is based on an understanding of the geology and groundwater.

6.6 Recommendations for Further Research

Although this thesis has presented some of the geologic controls of natural slope stability in the sensitive

clays of the Ottawa Valley, more research needs to be carried out before a full field stability mapping method is available. Since only one slope geometry was used here, several more pairs of slope height-slope angle need to be analysed to cover the full range of slope geometries that may be encountered in the field. The bedrock surface was considered flat and horizontal: what would be the effects of an irregular bedrock surface on the stability of a slope? Finally, the limits of strength variations for the sensitive clays should be established.

Ideally, any stability mapping method should include a probability of failure. The finite element method is an approximation of the pore pressure distribution and, hence, may introduce a certain error into the calculation of the factor of safety. By recognizing that variations in the site geology, strength parameters and groundwater conditions exist, future research should be to evaluate the magnitude of those variations and their effects on the stability of sensitive clay slopes.

REFERENCES

Alonso, E.E.
1976: Risk analysis of slopes and its application to slopes in Canadian sensitive clays; Geotechnique, vol. 26, no. 3, pp. 453 to 472.

Antevs, E.
1925: Retreat of the last ice sheet in eastern Canada; Geol. Surv. Can. Memoir 146, 142 pages.

Attewell, P.B., and Farmer, I.W.
1976: Principles of Engineering Geology; John Wiley and Sons, New York, 1045 pages.

Berner, R.A.
1974: "Iron sulfides in Pleistocene deep Black Sea sediments and their paleo-oceanographic significance", in The Black Sea - Geology, Chemistry and Biology. Edited by E.T. Dagens and D.A. Ross. A.A.P.G., Tulsa, Oklahoma, p. 524.

Bishop, A.W.
1955: The use of the slip circle in the stability analysis of slopes; Geotechnique, vol. 4, no. 1, page 148.

Bjerrum, L.
1954: Geotechnical properties of Norwegian marine clays; Geotechnique, vol. 4, pages 49 to 69.

Bozozuk, M.
1972: Gloucester test fill; PhD thesis, Perdue University, School of Civil Eng., 184 pages.

Bozozuk, M.
1977: Evaluating strength tests from foundation failures; Proc. 9th I.C.S.M.F.E., Tokyo, Vol. I, pages 55 to 59.

Braester, C., Dagan, G., Neuman, S.P., and Zaslavasky, D.
1971: "A survey of the equations and solutions of unsaturated flow in porous media"; 1st annual report, Project no. A10-SWC-77, Hydraulic Engineering Lab., Technion, Haifa, Israel, 176 pages.

Brooker, E.W., and Ireland, H.O.
1965: Earth pressures at rest related to stress history; Can. Geotech. J. Vol. II, No. 1, pages 1 to 15.

Brooker, E.W., Scott, J.S., and Ali, P.
1968: Transducer piezometer for clay shales; Can. Geotech. J., Vol. V, No. 4, pages 256 to 264.

Chagnon, Jean Y.
1975: Stabilisation de glissement à Hull, Province de Québec; Proc. 28th Can. Geotech. Conf., Montreal, Quebec, pages 264-277.

Charron, J.E.
1974: A study of groundwater flow in Russell County, Ontario; Scientific Series No. 40, Inland Waters Directorate, Department of the Environment, Ottawa, Canada, 26pp.

Childs, E.C.
1969: The physical basis of soil water phenomena; John Wiley and Sons, New York, 493 pages.

Childs, E.C., and Collis-George, N.
1950: The permeability of porous materials; Proc. Royal Soc., Vol. 201A, pages 392 to 405.

Crawford, C.B., and Eden, W.J.
1967: Stability of natural slopes in sensitive clay; A.S.C.E., J.S.M.F.E., vol. 93, SM4, pages 326 to 333.

Duncan, J.M., and Buchignani, A.L.
1975: An engineering manual for slope stability studies; Dept. of Civil Eng., Institute of Transportation and Traffic Eng., University of California, Berkeley, 83 pages.

Eden, W.J., Fletcher, E.B., and Mitchell, R.J.
1971: South Nation River landslide, 16 May 1971; Can. Geotech. J., vol. 8, no. 3, pages 446 to 451.

Eden, W.J., and Mitchell, R.J.
1970: The mechanics of landslides in Leda Clays; Can. Geotech. J., vol. 7, pages 285 to 296.

Fransham, P.B., Gadd, N.R., and Carr, P.A.
1976: Distribution of sensitive clay deposits and associated landslides in Ottawa Valley; Geol. Surv. Can. Open File 352, 17 maps.

Fransham, P.B., and Gadd, N.R.
1976: Geological and geomorphological controls of slope stability in Ottawa Valley; Can. Geotech. J., vol. 14, no. 4, pages 531 to 539.

Fredlund, D.G.
1974: Slope stability analysis; Trans and Geotech Group, Publ. CD-4, Department of Civil Eng., University of Saskatoon, Saskatoon, Saskatchewan, 101 pages.

Fredlund, D.G., and Krahn, J.
1976: Comparison of slope stability methods of analysis; Proc. 29th Can. Geotech. Conf. Vancouver, B.C., pages VIII-56 to VIII-74.

Gadd, N.R.
1963: Surficial geology of Ottawa and area Ontario and Quebec; Geol. Surv. Can. Paper 62-16, 4 pages.

Gadd, N.R.
1964: Surficial geology, Beauceville map area, Quebec; Geol. Surv. Can. Paper 64-12, 4 pages.

Gadd, N.R.
1975: Surficial geology and landslides of the Thurso-Russel map area; Geol. Surv. Can. Paper 75-35, 7 pp.

Gadd, N.R.
1977: Offlap sedimentary sequence in Champlain Sea, Ontario and Quebec; In Report of Activities, Part A, Geol. Surv. Can. Paper 77-1A, pages 379 to 380.

Gale, J.E.
1975: A numerical, field, and laboratory study of flow in rocks with deformable fractures; PhD thesis Department of Civil Eng., University of California-Berkeley, 255 pages.

Harr, M.E.
1962: Groundwater and seepage; McGraw-Hill Book Co., New York, 315 pages.

Haynes, Janet E., and Quigley, Robert M.
1976: Mineralogy and physico-chemistry, Leda Clay from deep bore holes, Hawkesbury, Ontario; Ontario Division of Mines OFR5214, 131 pages.

Hodge, R.A., and Freeze, R.A.
1977: Groundwater flow systems and slope stability; Can. Geotech. J., vol. 14, no. 4, pages 466 to 475.

Hvorslev, M. Juul.
1951: Time lag and soil permeability in groundwater observation; Bull No. 35, Waterways Experimental Station, U.S. Army Corps of Eng., Vicksburg, Miss., 50 pages.

Jarrett, P.M., and Eden, W.J.
1970: Groundwater flow in Eastern Ottawa; Can. Geotech. J., vol. 7, pages 326 to 333.

Johnston, W.A.
1916: Pleistocene and recent deposits in the vicinity of Ottawa, with a description of the soils; Geol. Surv. Can. Memoir 101, 69 pages.

Klugman, M.A., and Chung, P.
1976: Slope stability study of the regional municipality of Ottawa-Carleton; Ont. Geol. Surv. Misc. Paper MP68, 13 pages.

Lafleur, J., and Lefebvre, G.
1978: Groundwater regime associated with slope stability in Champlain clay deposits; 31st Can. Geotech. Conf., Winnipeg, Manitoba, pages 7.1.1 to 7.1.14.

Lambe, T.W., and Whitman, R.V.
1969: Soil mechanics; John Wiley and Sons, New York, 553 pp.

La Rochelle, P.
1975: Causes and mechanisms of landslides in sensitive clay with special reference to the Quebec Province area; Proc. 4th Guelph Symposium of Geomorphology, Department of Geography, University of Guelph, Guelph, Ontario, pages 174 to 182.

Lindberg, Denis Arnold
1965: Comparative aspects of five piezometer designs; MSc thesis, Department of Civil Eng., University of Alberta, Edmonton, Alberta, 102 pages.

Lo, K.Y., and Lee, C.F.
1974: An evaluation of the stability of natural slopes in plastic Champlain Sea Clays; Can. Geotech. J., vol. 11, no. 3, pages 165 to 181.

Lo, K.Y., and Morin, J.P.
1972: Strength anisotropy and time effects of two sensitive clays; Can. Geotech. J., vol. 9, no. 3, pages 251 to 277.

Marshall, T.J..
1958: A relation between permeability and size distribution of pores; J. Soil Sci., vol. 9, pages 1 to 8.

McEniry, G.P.
1978: The estimation of the effective shear strength parameters of Leda Clay; MSc thesis, Department of Civil Engineering, University of Ottawa, Ottawa, Ont., 316 pages.

Mitchell, R.J.
1970: On the yielding and mechanical behavior of Leda Clay; Can. Geotech. J., vol. 7, pages 297 to 312.

Mitchell, R.J., and Markell, A.R.
1974: Flowslides in sensitive clays; Can. Geotech. J., vol. 11, no. 1, pages 11 to 31.

Narasimhan, T.N.
1975: A unified numerical model for saturated-unsaturated groundwater flow; Ph.D. Thesis, Dept. of Civil Eng., University of California, Berkeley, 243 pages.

Neuman, S.P., Feddes, R.A., and Bresler, E.
1974: Finite element simulation of flow in saturated-unsaturated soils considering the uptake of water by plants; Third Annual Report, Project A10-SWC-77, Hydraulic Eng. Lab. Technion, Haifa, Israel, 104 pages.

Patton, F.D., and Hendron, J.R.
1973: General Report on "Mass Movements"; Proc. 2nd Int. Cong. of Int. Assoc. of Eng. Geol., vol. 2, pages 1 to 57.

Peck, R.B.
1975: Landslides and their prevention; 4th Guelph Symposium on Geomorphology, Dept. of Geography, University of Guelph, Guelph, Ontario, pages 133 to 136.

Prest, V.
1970: Quaternary Geology; in Geology and Economic Minerals of Canada, Geol. Surv. Can. Economic Geology Report No. 1, pages 675 to 764.

Raymond, G.P., Townsend, D.L., and Lojkucek, M.J.
1971: The effects of sampling on the undrained soil properties of Leda soil; Can. Geotech. J., vol. 8, no. 4, pages 546 to 557.

Rosenqvist, I. Th.
1946: Om leires Kvikkakfighet (On the sensitivity of clays); Meddelelsor Fra Vegdirecktoren, no. 3, page 24.

Sangrey, D.A., and Paul, M.J.
1971: A regional study of landsliding near Ottawa; Can. Geotech. J., vol. 8, pages 315 to 335.

Scott, J.D., Shields, D.H., and Bauer, G.E.
1976: Champlain Sea clay in the Ottawa-Hull region; Proc. 29th Can. Geotech. Conf., Vancouver, B.C., pages XI-24 to XI-36.

Seekings, D.R.
1974: A geochemical-geotechnical analysis of a borehole from the site of the South Nation River Landslide; M.A. Thesis, Department of Geography, Carleton University, Ottawa, 75 pages.

Sheeran, D.E., Fattah, I., Fransham, P.B., and Dalton, C.J.
1977: Insitu response of muskeg to dynamic loading; Proc. 17th Muskeg Research Conf., Saskatoon, Saskatchewan, pages 11 to 24.

Thornthwaite, C.W.
1945: An approach towards a rational classification of climate; Geographical Review, vol. 38, pages 55 to 94.

Thurston, A.E.
1976: Compiled bibliography on sensitive clays; Ministry of Natural Resources, Eastern Region, Kemptville, Ontario, 73 pages.

Torrance, J. Kenneth
1975: Leaching, weathering and origin of Leda Clay in the Ottawa Valley; Proc. 4th Guelph Symp. on Geomorphology, Dept. of Geography, University of Guelph, Guelph, Ontario, pages 105 to 116.

Twenhofel, W.H.
1950: Principles of sedimentation; McGraw-Hill Book Co., New York, 673 pages.

Wilson, A.E.
1941: Geology of the Ottawa-St. Lawrence lowlands, Ontario; Geol. Surv. Can. Memoir 241, 65 pages.

Witherspoon, P.A., and Neuman, S.P.
1973: Finite elements in hydrogeology; Bulletin du Bureau de Recherches Géologiques et Minières, Deuxième Série, no. 4, Paris, France, 104 pages.

Wong, G.C.Y.
1975: Stability of reservoir slopes in marine clay; 1975 Geotechnical Seminar, Acres Consulting Limited, Niagara Falls, Ontario, 35 pages.

Yong, R.N.
1975: Dynamic behavior of sensitive clays; Geotech. Research Centre Report No. SC-GS-413, Department of Civil Eng., McGill University, Montreal, 185 pp.

Yong, R.N., Alonso, E.E., Tabba, M.M., and Fransham, P.B.
1977: Application of risk analysis to the prediction of slope instability; Can. Geotech. J., vol. 14, pages 540 to 553.

Yong, R.N., and Warkentin, B.P.
1966: Introduction to soil behavior; Macmillan Company, New York, 451 pages.

Zienkiewicz, O.C.
1971: The finite element method in engineering science; McGraw-Hill Book Company, London, 521 pages.